

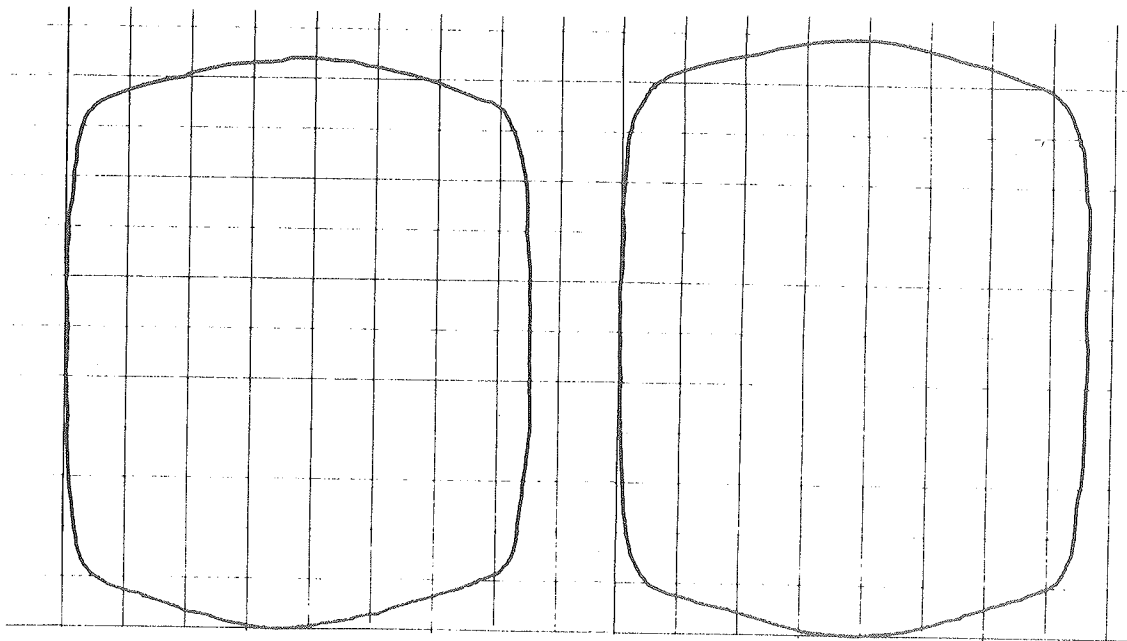
FHW A-RD-89-123 Pavement Testing Facility--Effects of Tire Pressure

Pavement Testing Facility--

Effects of Tire Pressure on Flexible Pavement Response and Performance

Publication No. FHWA-RD-89-123

August 1989



U.S. Department of Transportation
Federal Highway Administration

Research, Development, and Technology
Turner-Fairbank Highway Research Center
6300 Georgetown Pike
McLean, Virginia 22101-2296

EXECUTIVE CORRESPONDENCE

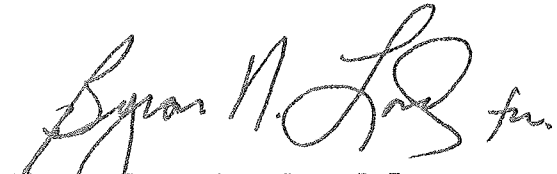
FOREWORD

In 1986, the Federal Highway Administration established the Pavement Testing Facility (PTF) at the Turner-Fairbank Highway Research Center in McLean, Virginia. The facility consists of the Accelerated Loading Facility (ALF) testing machine and eight instrumented asphalt concrete test sections. The PTF provides the capability to quickly evaluate problem areas of high national concern.

The first phase of research at the PTF was directed at establishing equivalency factors that relate the ALF loading to actual truck traffic. This research included a limited evaluation of the effects of tire pressure on flexible pavement response and performance.

This report documents the tire pressure evaluation. It will be of interest to pavement and materials engineers dealing with flexible pavements.

Sufficient copies of this report are being distributed by FHWA memorandum to provide one copy to each FHWA Region and Division and one copy to each State highway agency. Direct distribution is being made to the division offices. Additional copies for the public are available from the National Technical Information Service (NTIS), U.S. Department of Commerce, 5285 Port Royal Road, Springfield, Virginia 22161.



Thomas J. Pasko, Jr., P.E.
Director, Office of Engineering
and Highway Operations
Research and Development

NOTICE

This document is disseminated under the sponsorship of the Department of Transportation in the interest of information exchange. The United States Government assumes no liability for its contents or use thereof. The contents of this report reflect the views of the authors, who are responsible for the accuracy of the data presented herein. The contents do not necessarily reflect the official policy of the Department of Transportation. This report does not constitute a standard, specification, or regulation.

The United States Government does not endorse products or manufacturers. Trade or manufacturers' names appear herein only because they are considered essential to the object of this document.

**DO NOT WRITE ON THIS COVER AS IT IS INTENDED FOR RE-USE
RETURN IT WITH THE FILE COPIES TO ORIGINATING OFFICE**

1. Report No. FHWA-RD-89-123		2. Government Accession No.		3. Recipient's Catalog No.	
4. Title and Subtitle PAVEMENT TESTING FACILITY--EFFECTS OF TIRE PRESSURE ON FLEXIBLE PAVEMENT RESPONSE AND PERFORMANCE				5. Report Date August 1989	
				6. Performing Organization Code	
7. Author(s) R. Bonaquist, R. Surdahl, W. Mogawer				8. Performing Organization Report No.	
9. Performing Organization Name and Address Office of Engineering and Highway Operations R&D Federal Highway Administration 6300 Georgetown Pike McLean, Virginia 22101-2296				10. Work Unit No. (TRAIS) NCP 3C3c-1012	
				11. Contract or Grant No.	
12. Sponsoring Agency Name and Address Office of Engineering and Highway Operations R&D Federal Highway Administration 6300 Georgetown Pike McLean, Virginia 22101-2296				13. Type of Report and Period Covered Interim Report July 1987 - August 1988	
				14. Sponsoring Agency Code	
15. Supplementary Notes					
16. Abstract <p>The effects of tire pressure on flexible pavement response and performance were evaluated using data from the first phase of research at the Federal Highway Administration's Pavement Testing Facility. The Accelerated Loading Facility testing machine was used to simulate traffic loading.</p> <p>The evaluation consisted of three components. First, deflections and strains for various combinations of load and tire pressure were measured and compared. Second, rutting and cracking for two test sections trafficked with the same load but different tire pressures were evaluated. Finally, changes in the pavement materials resulting from traffic were compared for the two sections trafficked with different tire pressures.</p> <p>These three evaluations showed tire pressure to be a second order effect. The effect of tire pressure on flexible pavement response and performance was less significant the effects of load and temperature. During the response experiment, when load and temperature were constant, the effects of tire pressure could be observed. However, in the performance and materials evaluations, the effects of increased tire pressure were masked by differences in temperature.</p>					
17. Key Words Pavements, pavement testing, tire pressure, Accelerated Loading Facility, pavement performance, pavement response			18. Distribution Statement No restrictions. This document is available to the public through the National Technical Information Service, Springfield, Virginia, 22161		
19. Security Classif. (of this report) Unclassified		20. Security Classif. (of this page) Unclassified		21. No. of Pages 102	22. Price

SI* (MODERN METRIC) CONVERSION FACTORS

APPROXIMATE CONVERSIONS TO SI UNITS

Symbol	When You Know	Multiply By	To Find	Symbol
--------	---------------	-------------	---------	--------

LENGTH

in	inches	25.4	millimetres	mm
ft	feet	0.305	metres	m
yd	yards	0.914	metres	m
mi	miles	1.61	kilometres	km

AREA

in ²	square inches	645.2	millimetres squared	mm ²
ft ²	square feet	0.093	metres squared	m ²
yd ²	square yards	0.836	metres squared	m ²
ac	acres	0.405	hectares	ha
mi ²	square miles	2.59	kilometres squared	km ²

VOLUME

fl oz	fluid ounces	29.57	millilitres	mL
gal	gallons	3.785	litres	L
ft ³	cubic feet	0.028	metres cubed	m ³
yd ³	cubic yards	0.765	metres cubed	m ³

NOTE: Volumes greater than 1000 L shall be shown in m³.

MASS

oz	ounces	28.35	grams	g
lb	pounds	0.454	kilograms	kg
T	short tons (2000 lb)	0.907	megagrams	Mg

TEMPERATURE (exact)

°F	Fahrenheit temperature	$5(F-32)/9$	Celsius temperature	°C
----	------------------------	-------------	---------------------	----

APPROXIMATE CONVERSIONS FROM SI UNITS

Symbol	When You Know	Multiply By	To Find	Symbol
--------	---------------	-------------	---------	--------

LENGTH

mm	millimetres	0.039	inches	in
m	metres	3.28	feet	ft
m	metres	1.09	yards	yd
km	kilometres	0.621	miles	mi

AREA

mm ²	millimetres squared	0.0016	square inches	in ²
m ²	metres squared	10.764	square feet	ft ²
ha	hectares	2.47	acres	ac
km ²	kilometres squared	0.386	square miles	mi ²

VOLUME

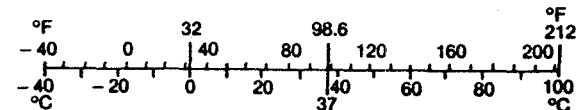
mL	millilitres	0.034	fluid ounces	fl oz
L	litres	0.264	gallons	gal
m ³	metres cubed	35.315	cubic feet	ft ³
m ³	metres cubed	1.308	cubic yards	yd ³

MASS

g	grams	0.035	ounces	oz
kg	kilograms	2.205	pounds	lb
Mg	megagrams	1.102	short tons (2000 lb)	T

TEMPERATURE (exact)

°C	Celsius temperature	$1.8C + 32$	Fahrenheit temperature	°F
----	---------------------	-------------	------------------------	----



* SI is the symbol for the International System of Measurement

(Revised April 1989)

TABLE OF CONTENTS

I. INTRODUCTION.....	1
BACKGROUND.....	1
PURPOSE AND SCOPE.....	4
REPORT ORGANIZATION.....	6
II. PAVEMENT RESPONSE EVALUATION.....	7
INTRODUCTION.....	7
EXPERIMENTAL DESIGN.....	7
PAVEMENT RESPONSE MEASUREMENTS.....	11
Surface Deflection.....	11
Surface Strain.....	14
Strain at the Bottom of the Asphalt Layer.....	16
Pavement Temperatures.....	16
TIRES.....	18
LOADING.....	21
RESULTS AND COMPARISONS.....	23
Layered Elastic Analysis.....	23
Surface Deflection.....	23
Surface Strain.....	27
Strain at the Bottom of the Asphalt Layer.....	32
EVALUATION.....	36
III. PAVEMENT PERFORMANCE EVALUATION.....	44
INTRODUCTION.....	44
TEST CONDITIONS.....	44
Environment.....	44
Construction Variability.....	46
RUTTING.....	48
CRACKING.....	50
EVALUATION.....	51
IV. MATERIALS EVALUATION.....	61
INTRODUCTION.....	61
PROFILES.....	61
ASPHALT CONCRETE.....	61
CRUSHED AGGREGATE BASE.....	69
SUBGRADE.....	71
V. SUMMARY AND CONCLUSIONS.....	76
VI. REFERENCES.....	78
APPENDIXES	
A. Tire Data.....	80
B. Pavement Response Data.....	82
C. Materials Test Data.....	94

LIST OF FIGURES

<u>Figure</u>	<u>Page</u>
1. The PTF site plan.....	2
2. Test lane cross sections.....	3
3. The ALF testing machine.....	5
4. Subgrade moisture contents from moisture cells.....	10
5. Location of the pavement instrumentation for Lane 1.....	12
6. Location of the pavement instrumentation for Lane 2.....	13
7. Photograph of the deflection beams.....	15
8. Photograph of surface strain gauge installation.....	15
9. Photograph of a strain gauge installed at the bottom of the binder.....	17
10. Thermocouple depths.....	17
11. Typical contact areas for radial and bias ply tires.....	19
12. Comparison of calculated and measured contact areas.....	20
13. ALF dual tire trolley assembly.....	21
14. Typical ALF loading.....	22
15. Typical response curve for the parallel deflection beam.....	25
16. Typical response curve for the cantilever deflection beam.....	26
17. Effects of load and tire pressure on surface deflection for Lane 1.....	28
18. Effects of load and tire pressure on surface deflection for Lane 2.....	29
19. Typical response curve for longitudinal surface strain.....	30
20. Typical response curve for transverse surface strain.....	31
21. Effects of load and tire pressure on surface strain for Lane 1....	33
22. Effects of load and tire pressure on surface strain for Lane 2....	34
23. Typical response curve for longitudinal strain at the bottom of the asphalt layer.....	35
24. Effects of load and tire pressure on strain at the bottom of the asphalt layer for Lane 1.....	37
25. Effects of load and tire pressure on strain at the bottom of the asphalt layer for Lane 2.....	38
26. Comparison of strain at the bottom of the asphalt layer for original and repeat tests.....	39

LIST OF FIGURES (Continued)

<u>Figure</u>		<u>Page</u>
27.	Equivalency between load and tire pressure based on measured strains.....	43
28.	Daily average air temperatures.....	45
29.	ALF dynamic loading at 19,000 lbs, 100 and 140 psi tire pressures.	52
30.	Comparison of average rutting for Tests 2-2 and 2-3.....	54
31.	Comparison of average cracking for Tests 2-2 and 2-3.....	55
32.	Resilient modulus versus temperature relationship for the PTF asphalt concrete.....	57
33.	Vertical compressive strains at the top of the crushed aggregate base based on ELSYM5.....	58
34.	Predicted fatigue damage.....	60
35.	Photograph of postmortem trenching.....	62
36.	Transverse profile for Test 2-2.....	63
37.	Transverse profile for Test 2-3.....	64
38.	Core locations for Test 2-2.....	66
39.	Core locations for Test 2-3.....	67
40.	Effects of temperature and tire pressure on vertical compressive stresses based on ELSYM5.....	70

LIST OF TABLES

<u>Table</u>	<u>Page</u>
1. Experimental design for the response evaluation.....	8
2. Test sequences used in the response evaluation.....	9
3. Layered elastic representation of the PTF pavements.....	24
4. Fatigue equivalency factors.....	42
5. Average pavement thicknesses.....	46
6. Average layer densities.....	47
7. Average composite moduli.....	48
8. Rut depths for Test 2-2.....	49
9. Rut depths for Test 2-3.....	49
10. Cracking for Test 2-2.....	50
11. Cracking for Test 2-3.....	51
12. Laboratory tests for postmortem evaluations.....	53
13. Marshall mix design parameters for the PTF asphalt concrete.....	65
14. Average air void contents and resilient moduli for cores from Tests 2-2 and 2-3.....	69
15. As-constructed crushed aggregate base course density.....	72
16. Crushed aggregate base course density from postmortem testing.....	72
17. Gradation of crushed aggregate base course before and after trafficking.....	73
18. As-constructed subgrade density.....	74
19. Subgrade density from postmortem testing.....	74
20. Gradation of subgrade before and after trafficking.....	75
21. Manufacturer tire data.....	80
22. Tire contact areas.....	81
23. Calculated pavement responses at the instrument locations for Lane 1 with the wheels in the -14.75-in offset position.....	82
24. Calculated pavement responses at the instrument locations for Lane 1 with the wheels in the 0-in offset position.....	83
25. Calculated pavement responses at the instrument locations for Lane 1 with the wheels in the +14.75-in offset position.....	84
26. Calculated pavement responses at the instrument locations for Lane 2 with the wheels in the -14.75-in offset position.....	85
27. Calculated pavement responses at the instrument locations for Lane 2 with the wheels in the 0-in offset position.....	86

LIST OF TABLES (Continued)

<u>Table</u>		<u>Page</u>
28.	Calculated pavement responses at the instrument locations for Lane 2 with the wheels in the +14.75-in offset position.....	87
29.	Measured pavement responses for Lane 1 with the wheels in the -14.75-in offset position.....	88
30.	Measured pavement responses for Lane 1 with the wheels in the 0-in offset position.....	89
31.	Measured pavement responses for Lane 1 with the wheels in the +14.75-in offset position.....	90
32.	Measured pavement responses for Lane 2 with the wheels in the -14.75-in offset position.....	91
33.	Measured pavement responses for Lane 2 with the wheels in the 0-in offset position.....	92
34.	Measured pavement responses for Lane 2 with the wheels in the +14.75-in offset position.....	93
35.	Air void contents and resilient moduli for cores from Test 2-2.....	94
36.	Air void contents and resilient moduli for cores from Test 2-3.....	95

I. INTRODUCTION

BACKGROUND

In recent years, the effects of increased truck tire pressures on flexible pavement performance have become a subject of great concern. Various researchers have used analytical methods to attribute decreased fatigue life, increased rutting, and accelerated serviceability loss to the effects of increased tire pressure.^(1,2,3) This report presents an analysis of the effects of tire pressure on flexible pavement response and performance based on data collected during the first phase of research at the Federal Highway Administration's (FHWA) Pavement Testing Facility (PTF).

The PTF is an outdoor, full-scale pavement testing laboratory located at the Turner-Fairbank Highway Research Center in McLean, Virginia. The purpose of the PTF is to quantify the performance of full-scale test pavements trafficked under accelerated loading. The facility consists of two 200-ft-long instrumented asphalt concrete test pavements, the Accelerated Loading Facility (ALF) testing machine, and a computer-controlled data acquisition system.

The site plan for the PTF is shown in figure 1. Each test lane is divided into four sections for a total of eight test sections. Cross sections for the two lanes are shown in figure 2. Construction of the test pavements was performed by a local highway contractor in accordance with the Virginia Department of Highways and Transportation specifications.⁽⁴⁾ The wearing and binder courses consist of crushed aggregate and AC-20 asphalt. The crushed aggregate base is dense graded, and contains a high amount of fines, approximately 50 percent passing the No. 8 sieve. The subgrade classifies as an AASHTO A-4(0) soil. Details concerning the design and construction of the test pavements were presented in a previous report.⁽⁵⁾

2

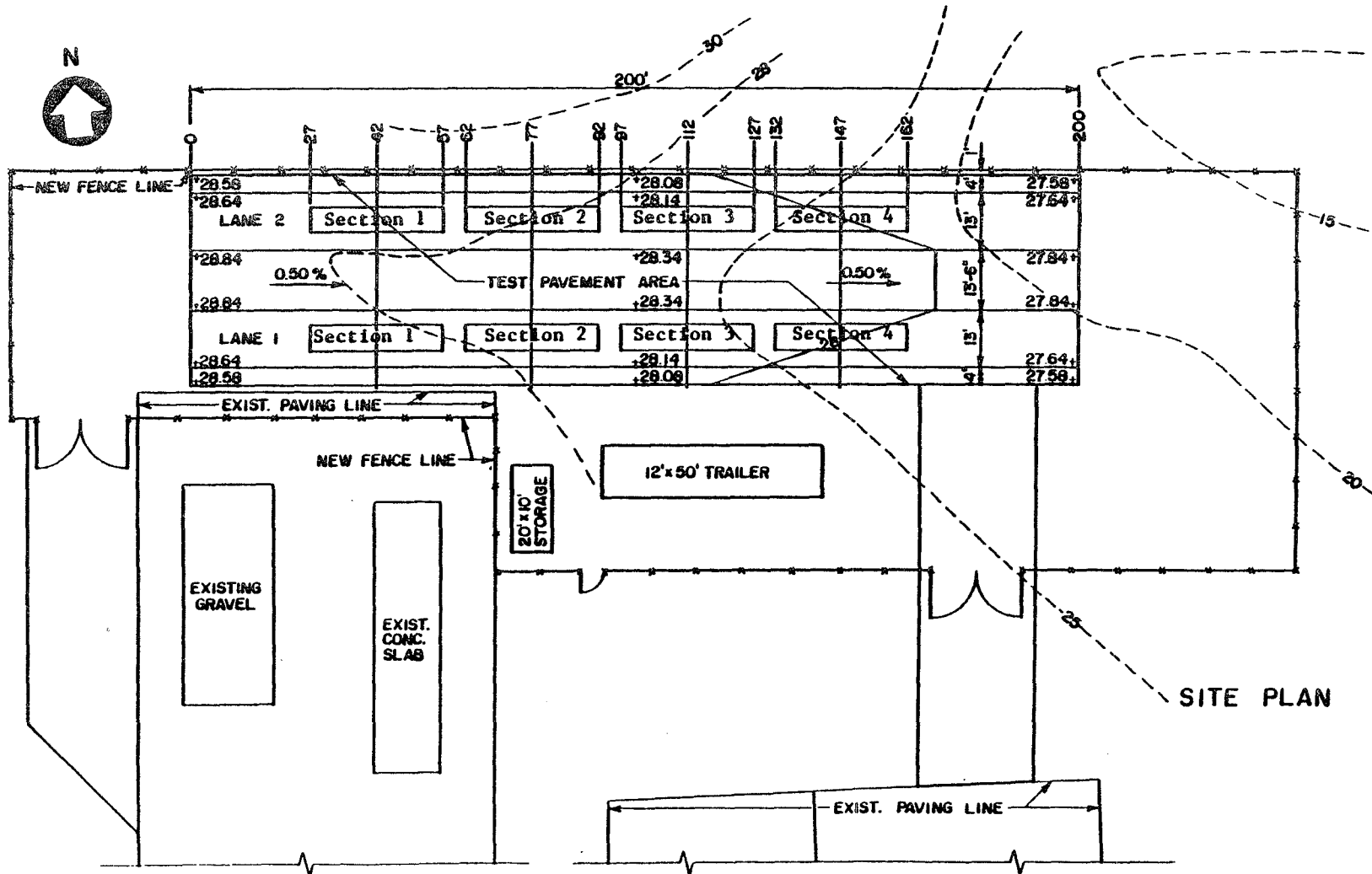


Figure 1. The PTF site plan.

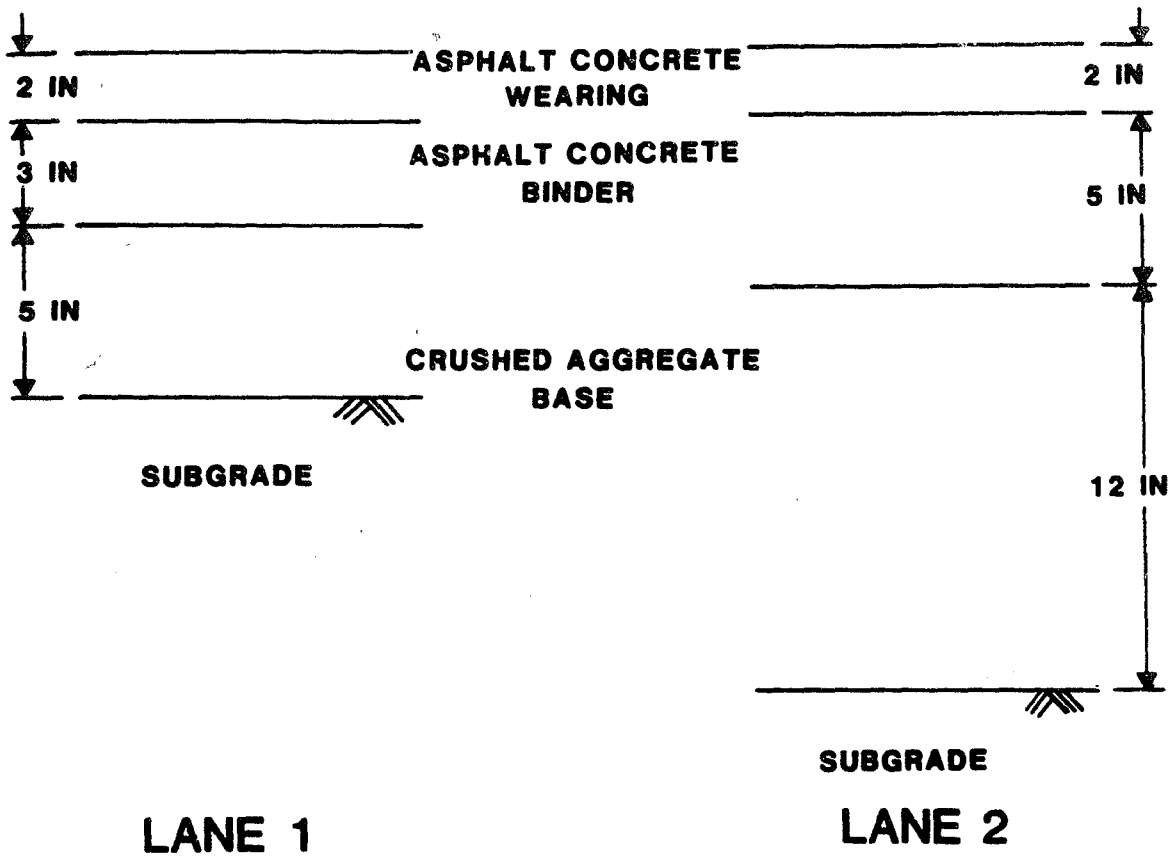


Figure 2. Test lane cross sections.

The ALF, shown in figure 3, simulates one-half of a dual-tire, single axle with loads ranging from 9,400 lb to 22,500 lb. The test wheel assembly travels at 12 mi/h over 40 ft of pavement. To simulate highway traffic, the loads are applied in one direction and are normally distributed about a 48-in wheelpath. The ALF requires very little power to operate because gravity is used to accelerate and decelerate the test wheel assembly. Other features include all-weather, computer-controlled operation, and transportability for field testing. Information concerning the fabrication and operation of the ALF was presented in a separate report.⁽⁶⁾

The pavement instrumentation and data acquisition system form an integral part of the PTF. The pavement instrumentation includes thermocouples and moisture cells at various depths in the pavement, strain gauges at the bottom of the asphalt binder, and a linear variable differential transformer (LVDT) for surface deflection. In addition, rut depth and slope variance are obtained with a semiautomatic profiling device. Signals from the various pavement instruments and the profiler are directed through signal conditioning equipment to an analog-to-digital converter mounted in a personal microcomputer. Software was developed to collect environmental, and pavement response and performance data as part of the routine operation of the PTF. The pavement instrumentation and data acquisition system were described in detail in a previous report.⁽⁷⁾

PURPOSE AND SCOPE

The first phase of research at the PTF began in October 1986. During this phase, the eight pavement sections were trafficked using a range of loads and tire pressures. Specific objectives of the first phase of research were to:

1. Establish load equivalency factors for the ALF testing machine.
2. Compare calculated and measured pavement responses.
3. Assess the American Association of State Highway and Transportation Officials (AASHTO) design procedure using the ALF loading.

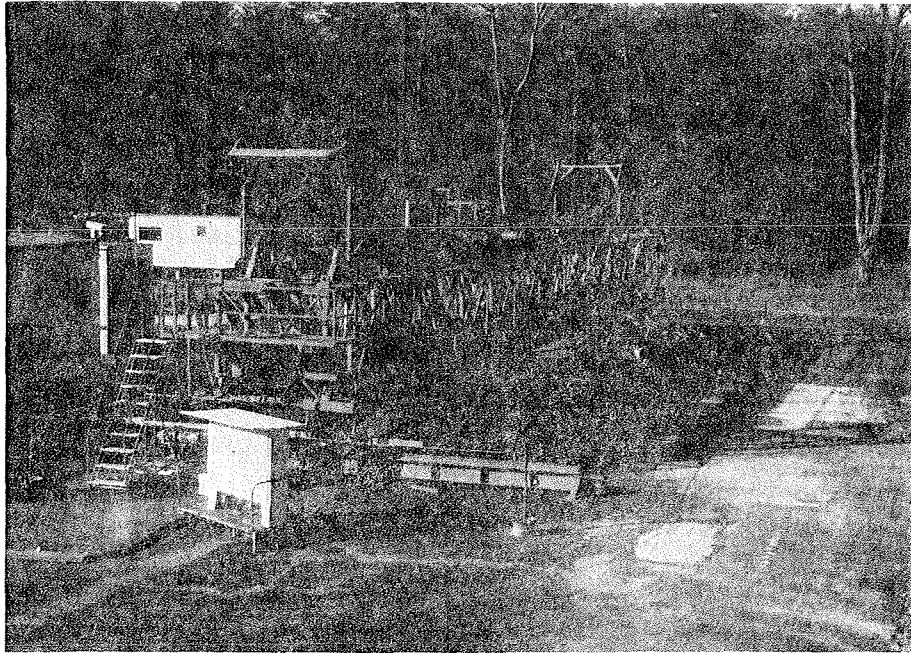


Figure 3. The ALF testing machine.

4. Evaluate the effect of tire pressure on pavement response and performance.
5. Establish a computer-based PTF Information Management System.

The research described in this report addresses the fourth objective outlined above. The scope of work included evaluating the effects of tire pressure in three ways. First, pavement responses, strain and deflection, for various combinations of load and tire pressure were measured and compared. Second, pavement performance, rutting, and cracking, for two test sections trafficked with the same load but different tire pressures were analyzed. Finally, changes in the pavement material characteristics for the two sections trafficked with different tire pressures were evaluated.

REPORT ORGANIZATION

Each chapter of this report discusses one of these three evaluations. The response evaluation is presented in chapter II, the performance evaluation in chapter III, and the materials evaluation in chapter IV. Chapter V contains conclusions concerning the effects of tire pressure on flexible pavements based on these three evaluations.

II. PAVEMENT RESPONSE EVALUATION

INTRODUCTION

This chapter describes an experiment which used the PTF to measure the effects of load, tire pressure, and tire type on the response of two flexible pavement cross sections. The pavement responses measured were surface deflection, surface strain, and strain at the bottom of the asphalt layer.

EXPERIMENTAL DESIGN

The objective of the pavement response experiment was to measure pavement responses for various combinations of load and tire pressure for two types of tires. The experiment was designed as a complete factorial with load, tire pressure, and tire type as the controlled variables. Three load levels, three tire pressures, and two tire types were used in the experiment. Table 1 summarizes the experimental design. For each experimental cell, the following data were collected:

1. Surface deflection.
2. Surface strain.
3. Strain at the bottom of the asphalt layer.
4. Pavement temperature.

The experiment was conducted on Lane 2 of the PTF in July 1987 and Lane 1 in December 1987.

Ideally, the experimental combinations should have been tested randomly with temperature and moisture conditions constant. The amount of work, and downtime required to change tires and loads, however, prohibited complete randomization. Since tire pressure was easy to vary, and loads could be changed quicker than tires, the test sequences outlined in table 2 were used. The radial tire tests using the 14,100-lb load for Lane 1 and the 19,000-lb load for Lane 2 were repeated to assess the effect of accumulated damage during the experiment.

Table 1. Experimental design for the response evaluation.

Load (lb)	Radial			Bias Ply		
	76 (psi)	108 (psi)	140 (psi)	76 (psi)	108 (psi)	140 (psi)
9,400	X	X	X	X	X	X
14,100	X	X	X	X	X	X
19,000	X	X	X	X	X	X

Pavement temperature and moisture conditions can not be controlled at the PTF. The tests were conducted, however, at times which minimized temperature fluctuations, and pavement temperatures were measured for each test to provide data for temperature adjustments. The tests on Lane 1 were conducted during normal working hours. The temperature of the asphalt layer averaged 39.7 °F with a standard deviation of 1.2. The tests on Lane 2 were conducted at night. The temperature of the asphalt layer averaged 83.1 °F with a standard deviation of 3.8. For the test sequences used, temperature variations between tire pressures at a given load level were much smaller than the temperature variations between load levels.

During the first phase of research at the PTF, the moisture content of the subgrade was monitored weekly using resistance-type moisture cells. Data from these moisture cells are shown in figure 4. The first moisture cell readings were taken in late December 1986; construction of the pavement sections was completed in September 1986. Apparently, the moisture content of the subgrade increased from the as constructed value of 10.5 percent ultimately reaching equilibrium at approximately 18 percent. The subgrade moisture content remained relatively constant since December 1986. This was supported by back-calculated moduli from periodic falling weight deflectometer tests, and oven-dried samples obtained during post-failure analyses.⁽⁷⁾

Table 2. Test sequences used in the response evaluation.

LANE 1, DECEMBER 1987

Load (lb)	Radial			Bias Ply		
	76 (psi)	108 (psi)	140 (psi)	76 (psi)	108 (psi)	140 (psi)
9,400	6	5	4	18	17	16
14,100	3	2	1	15	14	13
19,000	9	8	7	12	11	10
14,100	21	20	19			

LANE 2, JULY 1987

Load (lb)	Radial			Bias Ply		
	76 (psi)	108 (psi)	140 (psi)	76 (psi)	108 (psi)	140 (psi)
9,400	1	3	2	18	17	16
14,100	4	6	5	13	15	14
19,000	9	7	8	11	12	10
19,000	21	19	20			

Note: Numbers in table represent sequence of testing.

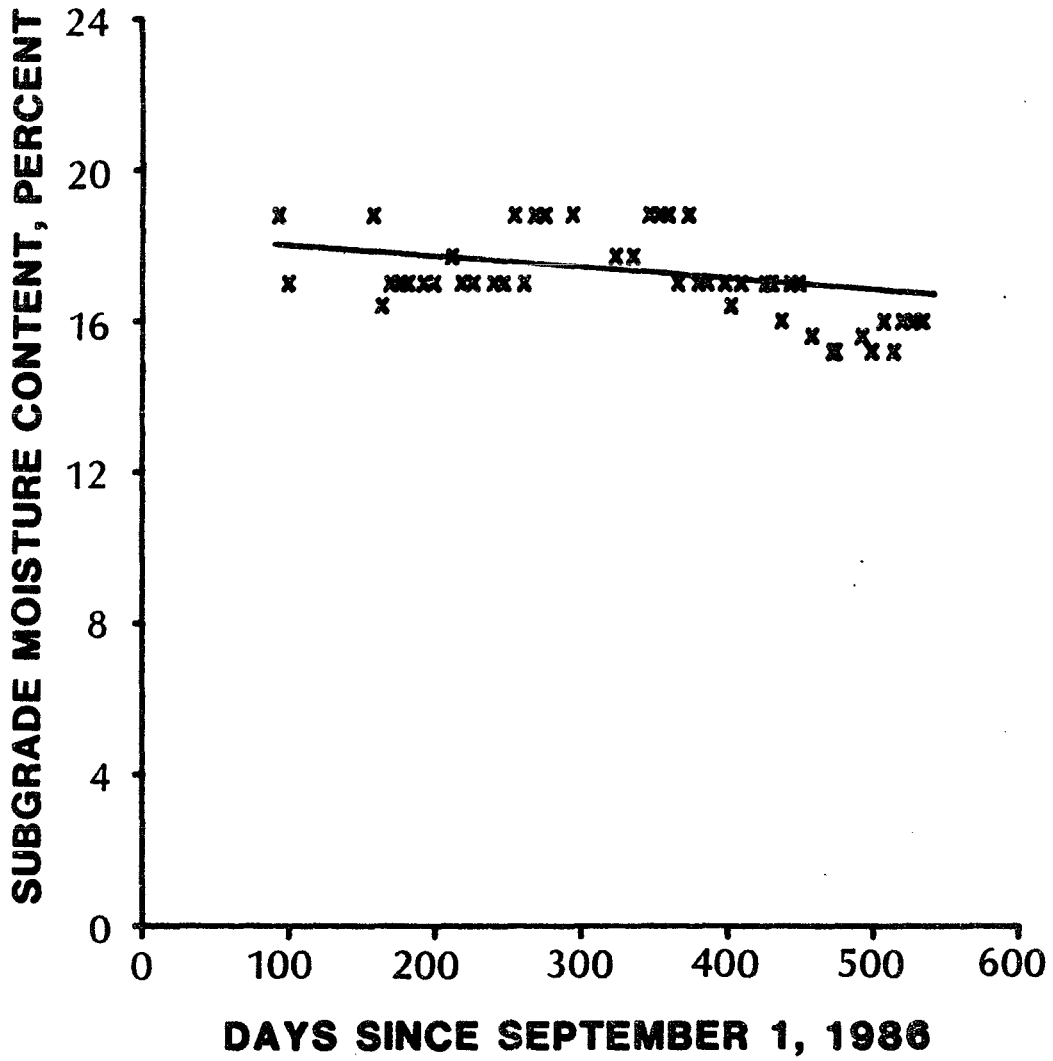


Figure 4. Subgrade moisture contents from moisture cells.

The response evaluation experiments were conducted early in the life of each pavement section. The pavements were subjected to several thousand load applications before the experiments were conducted. Based on the AASHTO load equivalency factors, Lane 1 was subjected to 9,300 18-kip equivalent single axle loads (ESAL) and Lane 2 was subjected to 33,200 ESAL prior to testing. Lanes 1 and 2 were designed for 250,000 and 3,500,000 ESAL, respectively. Cracking was first observed at 177,000 and 3,470,000 ESAL for Lanes 1 and 2, respectively.

PAVEMENT RESPONSE MEASUREMENTS

The pavement responses measured were surface deflection, surface strain, and strain at the bottom of the asphalt layer. Response curves were obtained for each of the measurements by using the computer data acquisition system to monitor the pavement instruments as the ALF wheel assembly traversed the pavement at 12 mi/h.

Figures 5 and 6 show the location of the pavement instrumentation relative to the centerline of the test section for Lanes 1 and 2, respectively. Pavement response measurements were made with the centerline of the ALF dual wheel assembly at three locations relative to the centerline of the test section. These three locations correspond to offsets of 0, +14.75, and -14.75 in.

Surface Deflection

Two devices were used to measure surface deflections. The first device consisted of a LVDT mounted at the midpoint of a 15-ft long reference beam. The beam was placed parallel to the direction of travel of the ALF wheels approximately 27 in from the center of the dual wheels when the trolley was in the +14.75-in offset position. The supports for this device were within the deflection basin produced by the ALF wheels; therefore, the second device was developed. It consisted of a LVDT mounted at the end of a 9-ft long

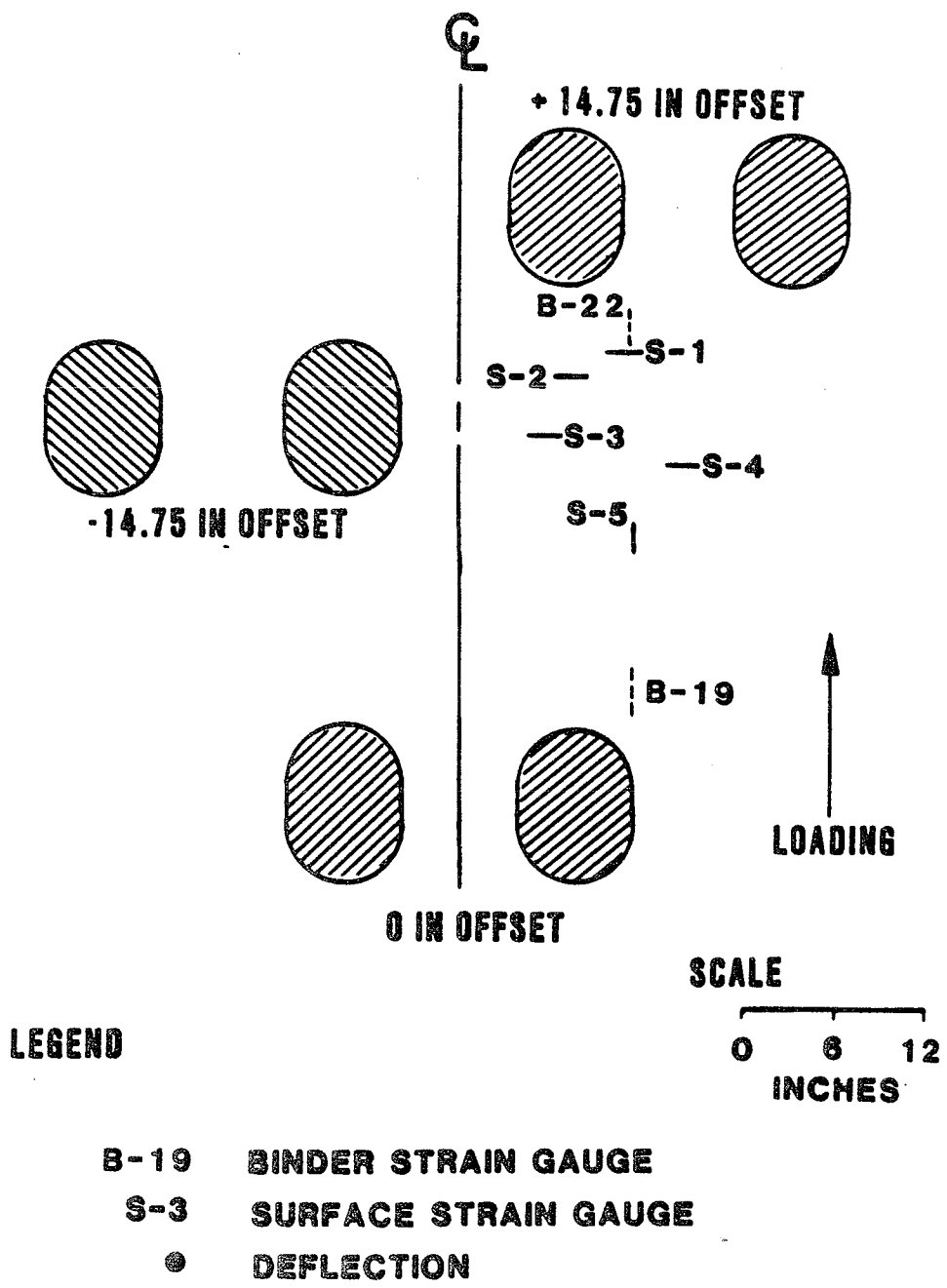


Figure 5. Location of the pavement instrumentation for Lane 1.

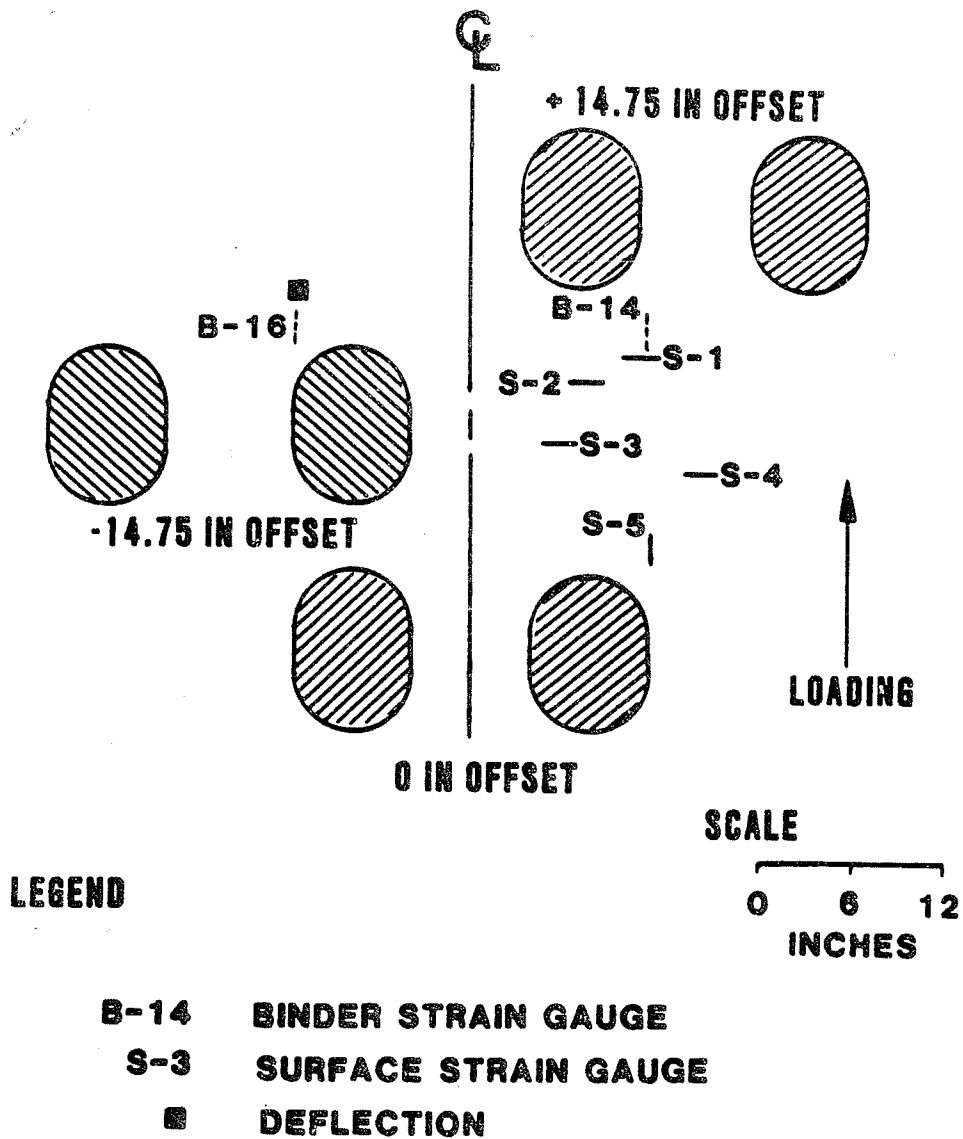


Figure 6. Location of the pavement instrumentation for Lane 2.

cantilever beam placed perpendicular to the direction of travel. Again, the beam was positioned such that the LVDT was 27 in from the center of the dual wheels when the trolley was in the +14.75-in offset position.

Only the parallel beam was used during testing on Lane 2, and deflections were measured only for the +14.75-in offset position. Both beams were used during testing on Lane 1, and deflections were measured for all three offset positions. Figure 7 shows the two deflection beams in place during testing on Lane 1.

Surface Strain

Surface strains were measured with 2-in gauge length bonded foil resistance strain gauges (Micromeritics EA-06-20CBW-120). The gauges were installed in 1/8-in deep slots at the locations shown in figures 5 and 6. A photograph of the installation is shown in figure 8. Each strain gauge was connected in a quarter bridge configuration with one of the channels of the data acquisition system. No temperature compensating gauges were installed because the strains were measured under moving wheel loads where temperature changes between strained and unstrained conditions were negligible. Although coverings were applied to protect the gauges and leadwires from moisture and mechanical damage, some of the gauges became inoperative during the testing. The failures were usually caused by broken leadwires or loose aggregate tearing the foil grid. Failed gauges were repaired or reinstalled only when the ALF was shut down for tire changes.

The surface strain gauge locations were selected to provide strain measurements outside the contact area as well as under the sidewall and center of the tire. As shown in figures 5 and 6, surface strains were measured at five locations for each offset position.

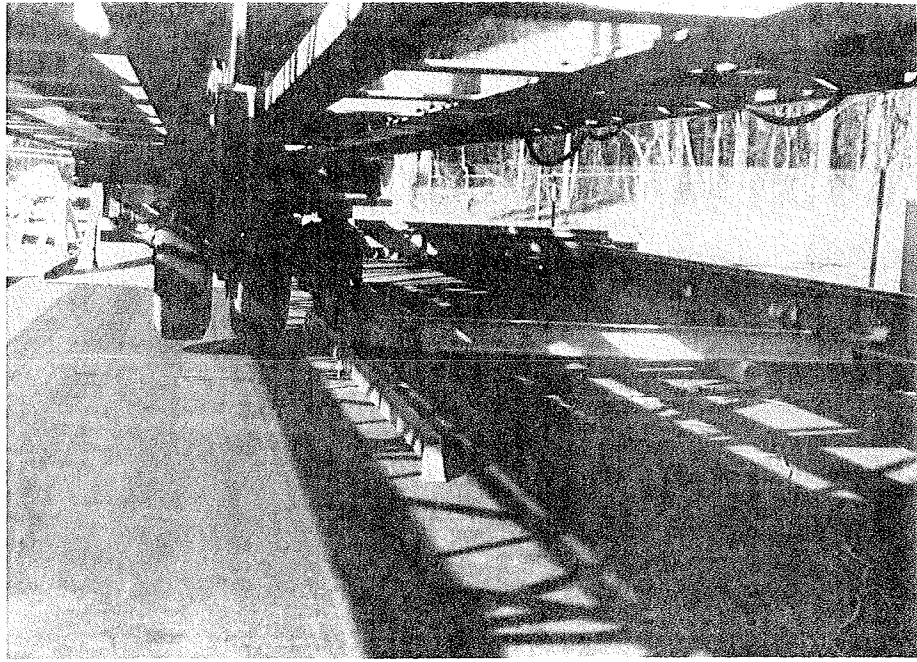


Figure 7. Photograph of the deflection beams.

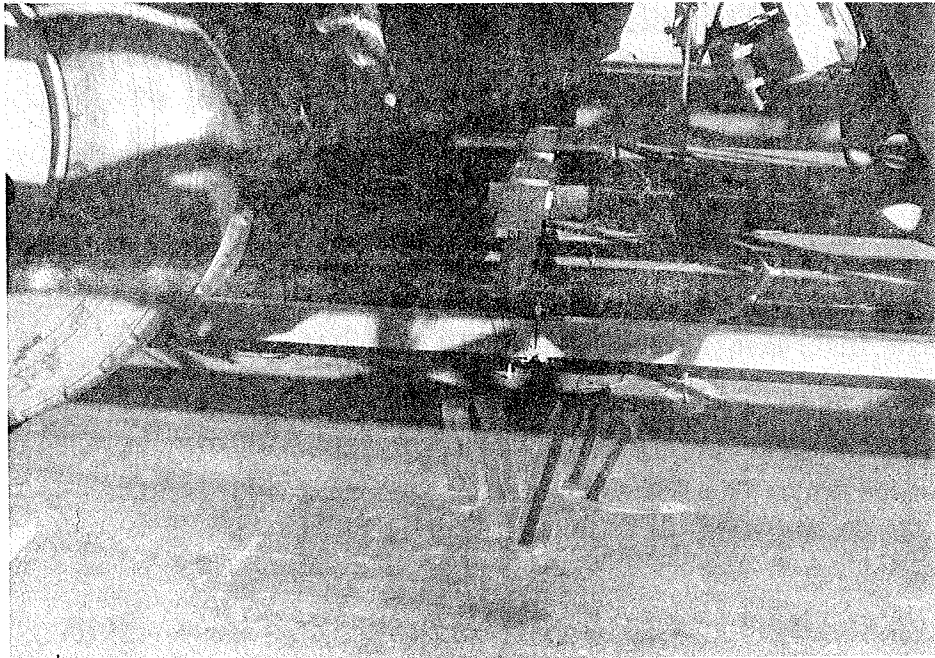


Figure 8. Photograph of surface strain gauge installation.

Strain at the Bottom of the Asphalt Layer

Strain gauges were installed at the interface between the asphalt binder and the crushed aggregate base during construction of the pavement in August, 1986. These gauges consist of a strain gauge encapsulated in a plastic strip (KYOWA KM-120-H2-1K 100-3). The plastic strip is in turn fastened to two anchors forming the letter "H".⁽⁸⁾ A photograph of one of these gauges is shown in figure 9. As with the surface strain gauges, each gauge was connected in a quarter bridge configuration with one of the channels of the computer data acquisition system and no temperature compensating gauges were installed.

Six strain gauges were installed at the bottom of the asphalt layer in each test section. Only two gauges in each lane were operational during the pavement response experiment. Figures 5 and 6 show the location of the operational gauges relative to the centerline of the test section. Several gauges were recovered from the pavement during post-failure investigations. Observations during these investigations indicated the gauges failed due to moisture and cabling problems.⁽⁷⁾

Pavement Temperatures

For each pavement response measurement, the temperature of the asphalt concrete was measured with thermocouples installed in the pavement adjacent to the response instrumentation. Figure 10 shows the depths where the thermocouples were installed in Lanes 1 and 2. The temperature measurements provide a thermal profile for the asphalt layer which can be used for temperature adjustment of the pavement response measurements.

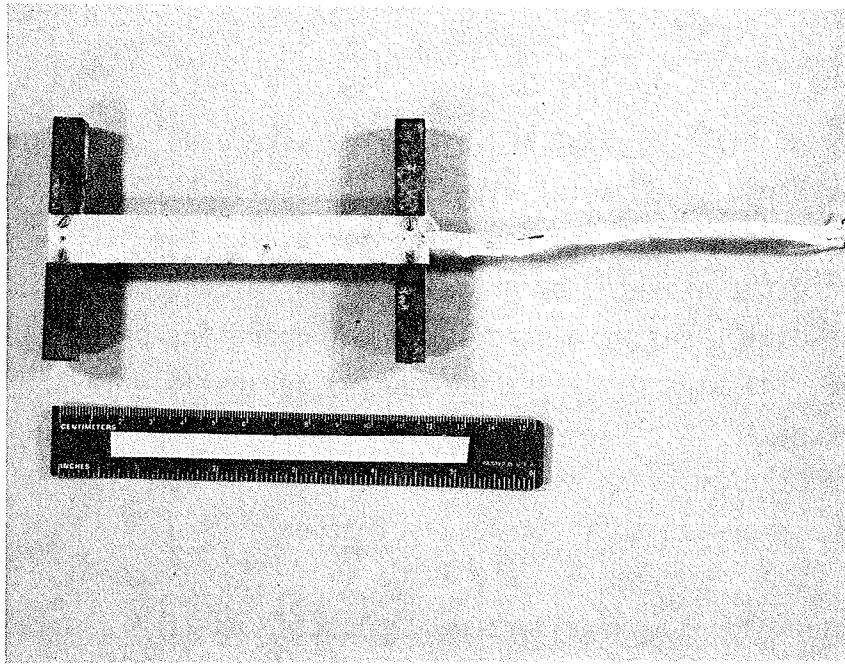


Figure 9. Photograph of a strain gauge installed at the bottom of the binder.

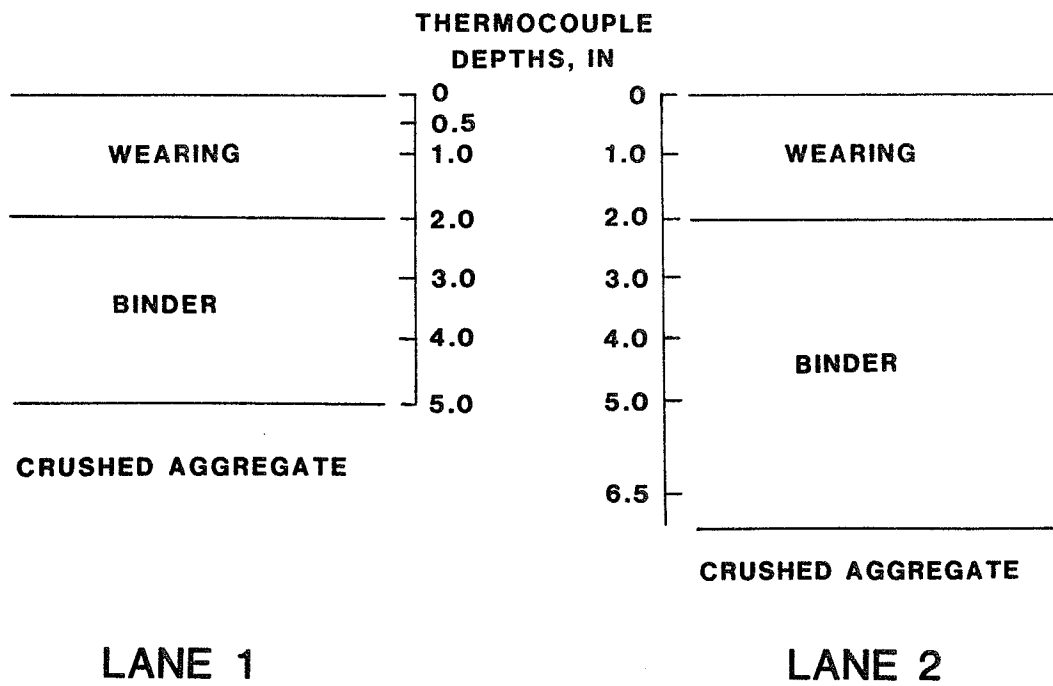


Figure 10. Thermocouple depths.

TIRES

Two types of tires, radial and bias ply, were used in the pavement response experiment. The radial tires were Michelin 11-R22.5. As purchased, the diameter of these tires was too large for use on the ALF. The tire supplier reduced the diameter by grinding which removed most of the tread rubber. The radial tires were used in normal operation of the ALF since October, 1986. The bias ply tires were Kelly Springfield 10-22.5. These tires were purchased in a size compatible with the ground Michelins, and were new at the time the response experiments were conducted. Manufacturer's data for the tires are presented in table 21 of appendix A.

Before the response experiment was conducted on Lane 2, tire contact areas were measured for each combination of load, tire pressure, and tire type used in the experiment. The contact areas were obtained by placing a sheet of posterboard on the pavement surface. The dual wheel assembly of the ALF was either lowered vertically or slowly rolled onto the posterboard. Paint was then sprayed around the tires to outline the contact areas. Finally, the dual wheel assembly was either raised vertically or slowly rolled off the posterboard. Rolling was used only with the 19,000-lb load because this load exceeded the capacity of the device used to raise and lower the wheel assembly vertically.

The contact areas were obtained from the posterboard outlines using a digitizing board connected to a personal microcomputer. Each print was digitized at least three, and up to five times to minimize deviation due to operator error. The contact areas were computed for the individual tires in each pair; no correction was made for the tread area. Figure 11 shows typical traces for radial and bias ply tires. The measured contact areas are summarized in table 22 of appendix A.

Most pavement response models assume a uniform circular tire, with the contact area computed as the ratio of load to inflation pressure. Figure 12 presents a comparison of contact areas calculated in this manner with those

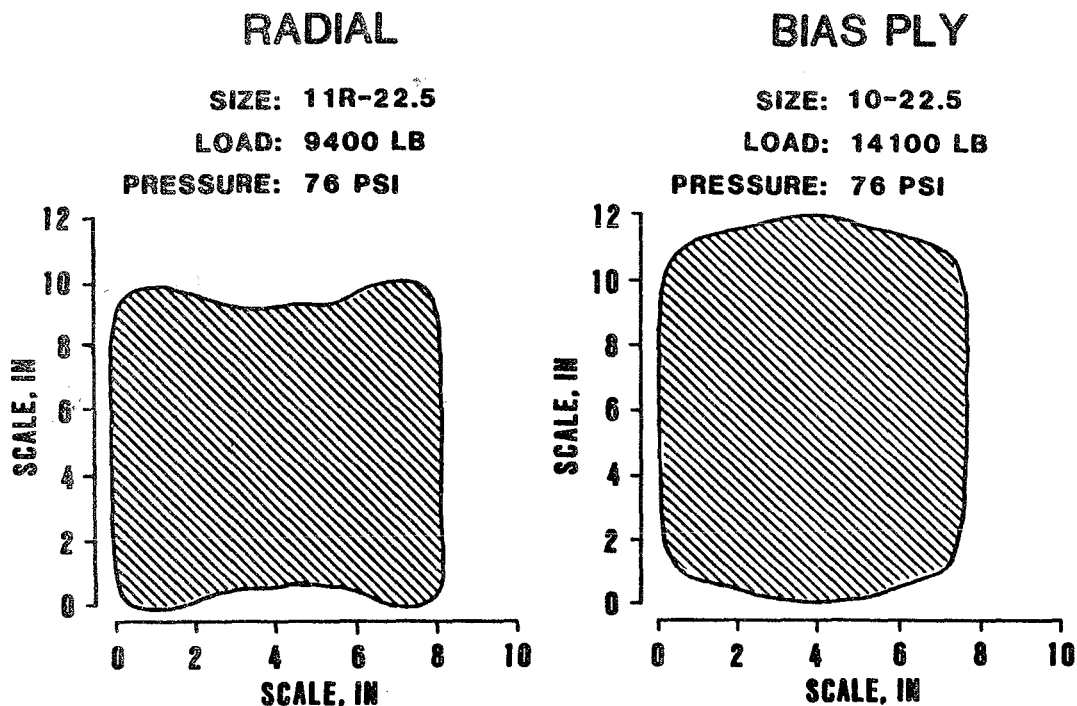


Figure 11. Typical contact areas for radial and bias ply tires.

measured during the response experiment. The measured area for the bias ply tires at 14,100 lb, 108 psi appears to be in error and probably is a repeat of the 140 psi test. Differences in measured versus computed areas varied from 12 to 58 in². Measured areas were larger than calculated areas except at the 19,000-lb load, 76-psi tire pressure. Differences increased with increasing tire pressure across all load ranges for both radial and bias ply tires.

The measured contact areas were not equal for the two tires in the ALF dual wheel assembly. Except at the 19,000-lb load, 140-psi tire pressure, the area for the left tire was smaller than the right tire. This difference ranged from 1 to 6 in² and can be attributed to the pavement cross slope.

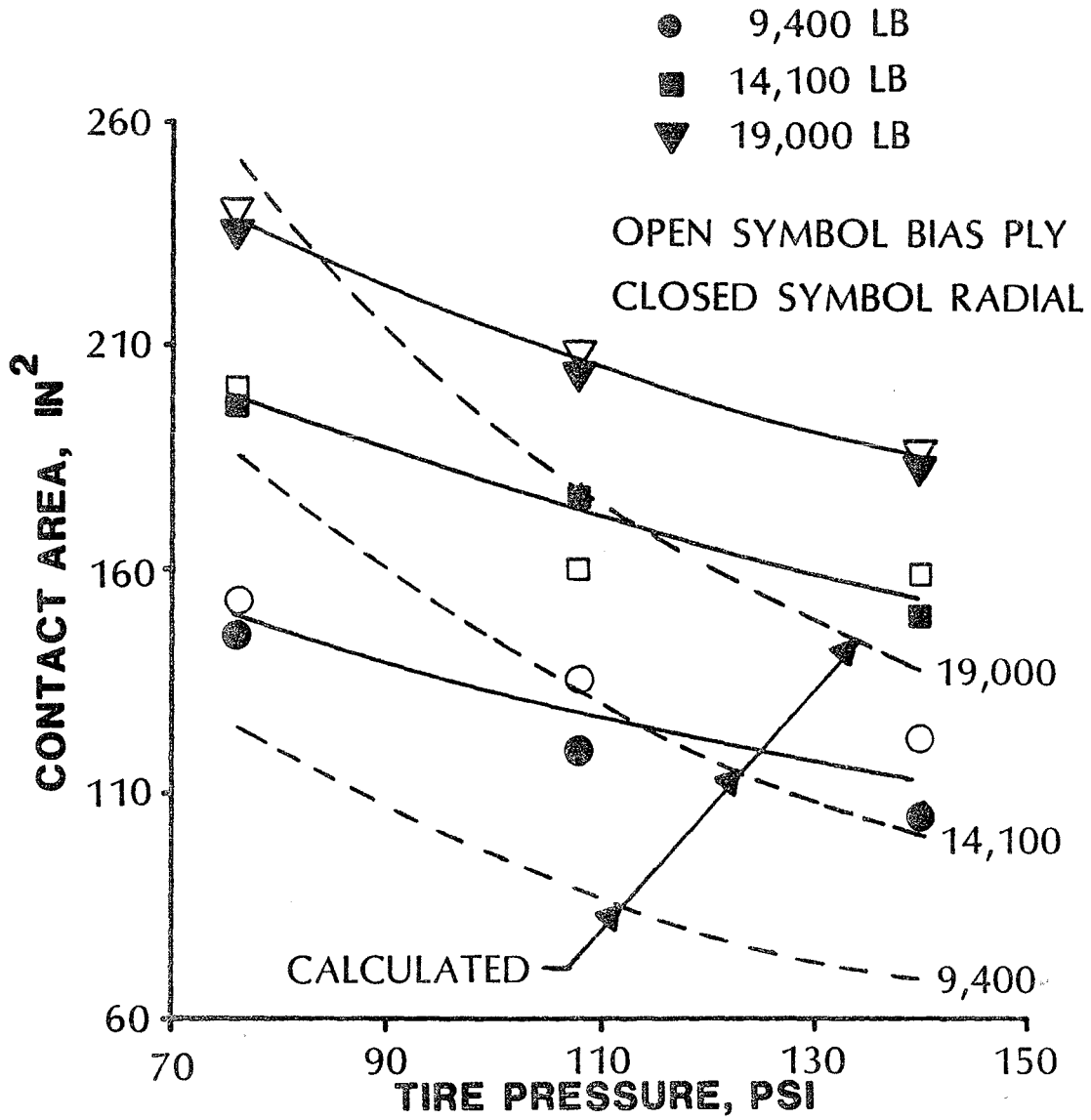


Figure 12. Comparison of calculated and measured contact areas.

LOADING

Figure 13 shows the ALF dual tire trolley assembly. The load on the test wheels was applied by the addition or subtraction of the ballast weights. Each weight was approximately 2,200 lb, and the minimum weight of 9,400 lb was obtained by removing all the weights and lifting the swinging arm. At the minimum weight, there was no suspension system, thus the entire mass of the trolley was unsprung. With the addition of the first ballast weight, an air bag and shock absorber system was incorporated into the trolley assembly. At 19,000 lb, approximately 50 percent of the load was sprung.

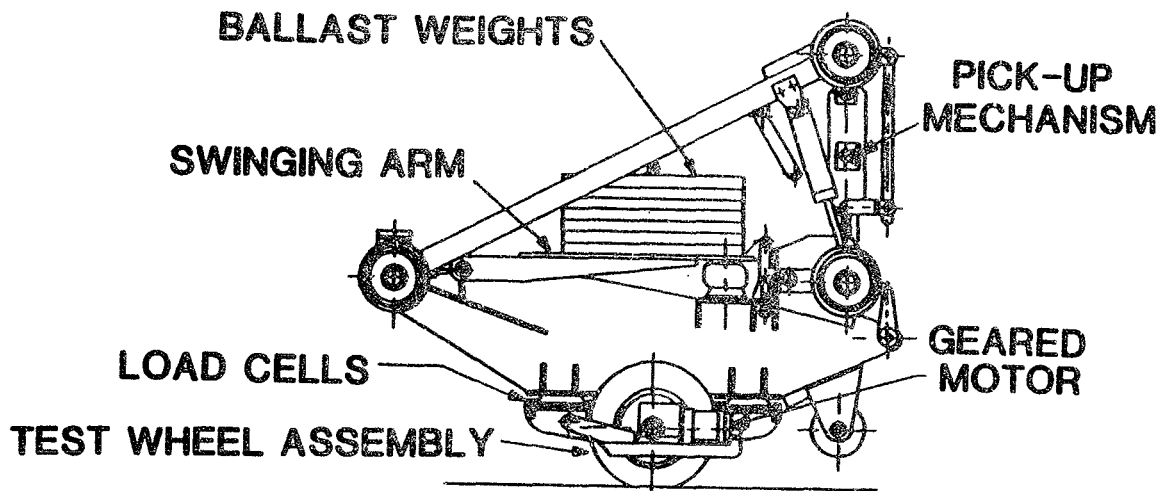


Figure 13. ALF dual tire trolley assembly.

The loading characteristics of the ALF changed as the sprung load increased from approximately 0 to 9,000 lb. Figure 14 shows the variation of load with longitudinal distance for the three loads used in the pavement response experiment. The loads were measured with load cells mounted in the trolley assembly. As can be seen in figure 14, the ALF applied a significant dynamic load component. This dynamic load was largest at the lighter loads when most of the load was unsprung.

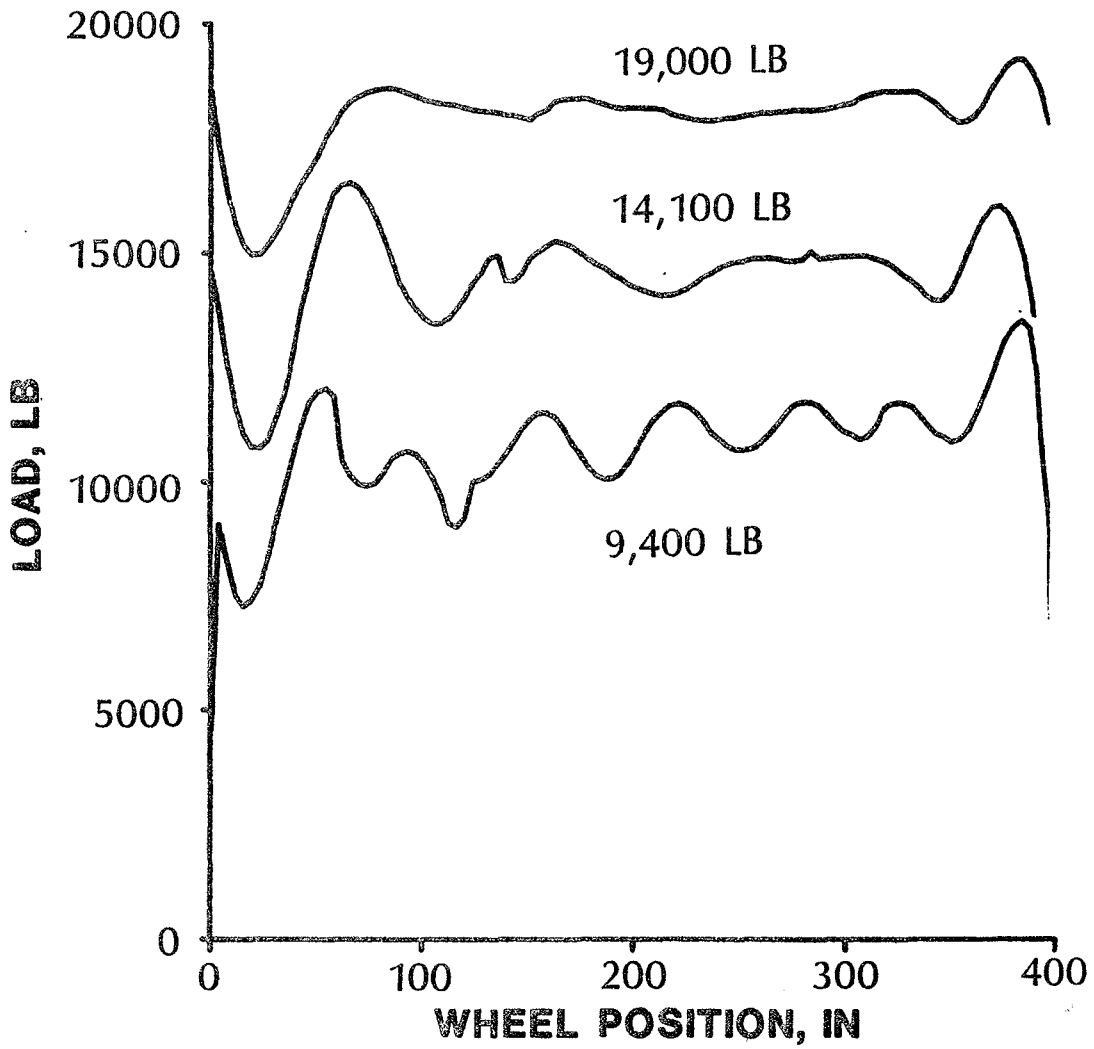


Figure 14. Typical ALF loading.

RESULTS AND COMPARISONS

Layered Elastic Analysis

Layered elastic theory was used to verify the pavement responses measured with the instrumentation. The ELSYM5 computer program was used to calculate pavement responses at the locations of the instrumentation. Responses were calculated for each load and tire pressure used in the experiment, and are summarized in tables 23 to 28 of appendix B.

For the analysis, the pavements were characterized as three-layer elastic systems as shown in table 3. The asphalt concrete and crushed aggregate base thicknesses represent average values measured by differential leveling during construction of the pavement sections. The elastic moduli were selected to represent average conditions during the response experiments, and were obtained from laboratory tests. The Poisson's ratios are typical assumed values.

Surface Deflection

Typical response curves for the parallel and cantilever LVDT beams are shown in figures 15 and 16. The first and third peaks for the parallel beam were the result of the beam supports being in the deflection basin for the ALF loading. A comparison of peak deflections measured with the two devices showed good agreement. The cantilever device, however, provided more information because both peak deflection and basin width may be obtained. The basins obtained from the parallel beam were distorted because the beam supports were within the deflection basin. Peak deflections measured with both devices are summarized in tables 29 to 34 of appendix B.

The peak deflections measured during these tests were not the maximum surface deflection. The instrumentation measured deflections 27 in from the center of the dual wheels. The maximum deflection occurs under one of the dual wheels, and could not be measured with the available instrumentation.

Table 3. Layered elastic representation of the PTF pavements.

LANE 1			
Layer	Thickness (in)	Modulus (psi)	Poisson's ratio
Asphalt Concrete	5.0	1,500,000	0.35
Crushed Aggregate Base	4.8	20,000	0.37
Subgrade	*	8,000	0.40

LANE 2			
Layer	Thickness (in)	Modulus (psi)	Poisson's ratio
Asphalt Concrete	6.8	180,000	0.35
Crushed Aggregate Base	11.2	20,000	0.37
Subgrade	*	8,000	0.40

* Subgrade assumed semi-infinite.

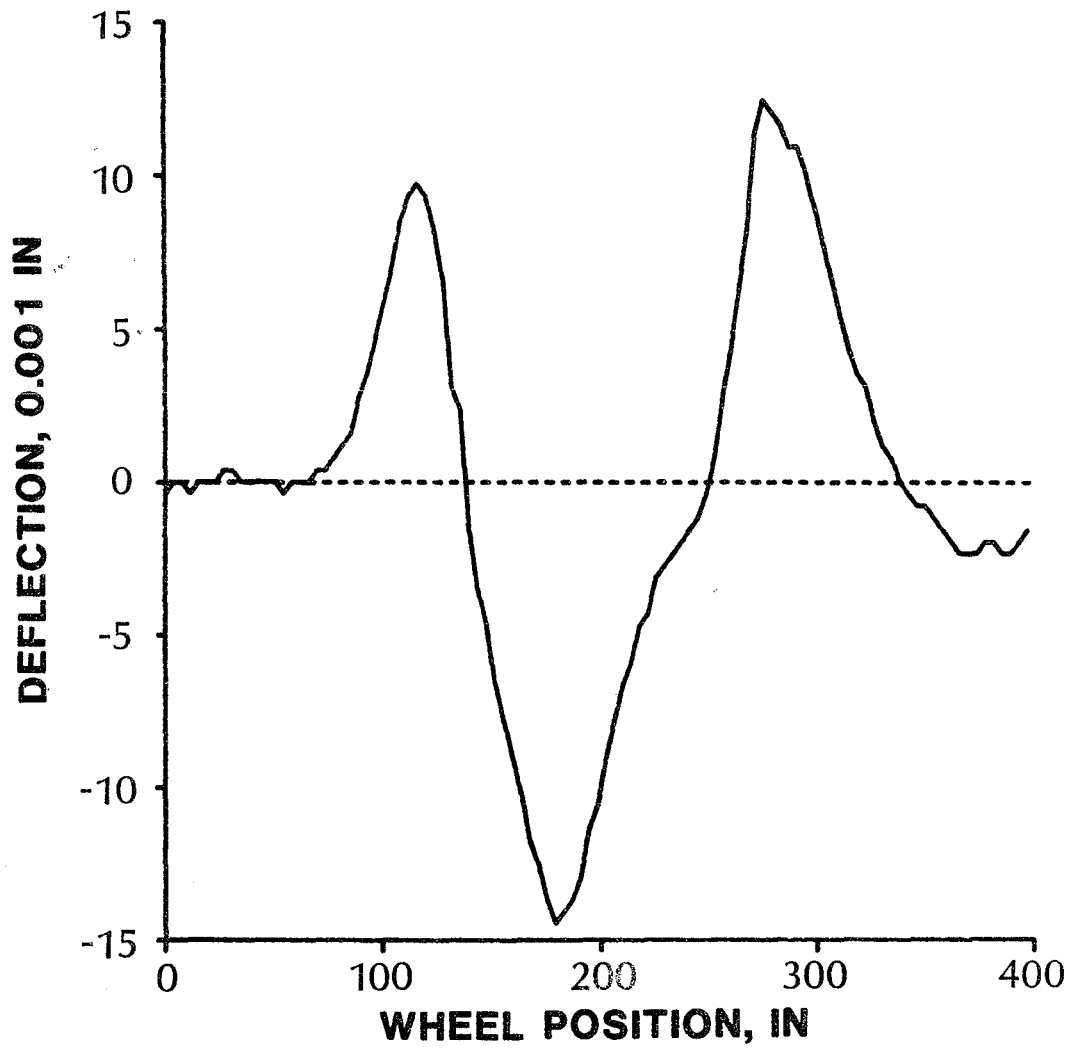


Figure 15. Typical response curve for the parallel deflection beam.

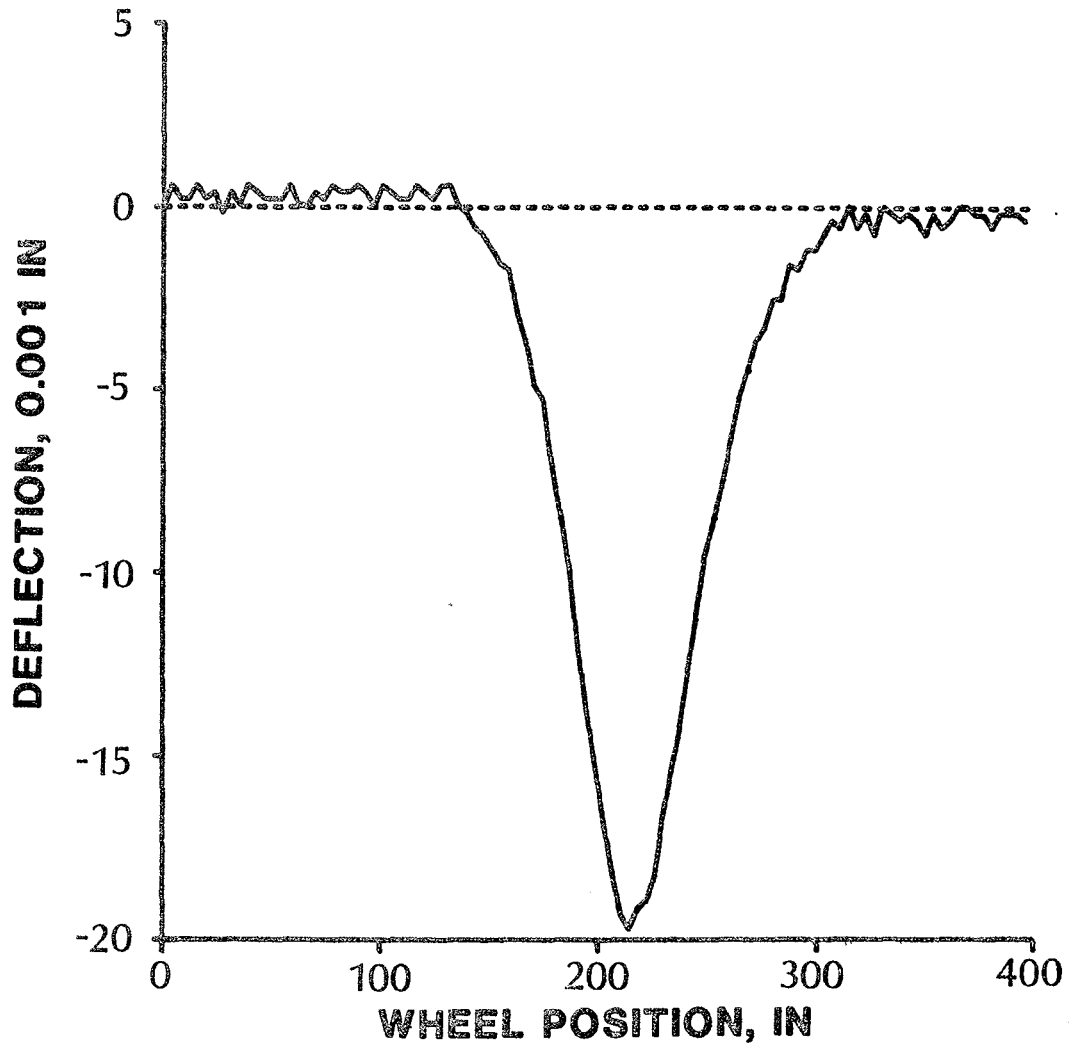


Figure 16. Typical response curve for the cantilever deflection beam.

The effects of load and tire pressure on the measured surface deflection are shown in figures 17 and 18 for Lanes 1 and 2, respectively. Each data point represents the average of five or six tests. No adjustments were made for differences in dynamic load or pavement temperature. Theoretical surface deflections from the layered elastic analysis are also presented. These figures show data for the +14.75 in offset position; similar effects were obtained for the other offset positions.

The effects of load and tire pressure on surface deflection generally agree with those predicted by layer theory. Both show the surface deflection 27 in from the center of the dual wheels to be highly sensitive to load and insensitive to tire pressure. There was no apparent trend in the data with respect to tire type. The tests on Lane 1 suggested bias ply tires produce higher deflections, while on Lane 2, the radial tires produced higher deflections.

Surface Strain

Typical response curves for surface strain gauges mounted in the longitudinal and transverse directions are shown in figures 19 and 20. Based on these figures, the following general observations concerning surface strain response were made. First, a strain reversal occurred in the longitudinal direction when the load passed by the gauges. As the load approached the gauges, tensile strains were induced at the pavement surface. When the load was over the gauges compressive strains occurred, and finally, tensile strains were once again induced as the load moved away from the gauges. This reversal did not occur in the transverse direction. Second, approximately 2 ft away from the center of the dual wheels, the surface strains in the transverse direction were in tension, while in the longitudinal direction the strains were in compression.

Many of the surface gauges failed during the response evaluation experiments. Peak strains from the operating gauges are summarized in tables 29 to 34 of appendix B. Only Gauge 5 for Lane 1 and Gauge 4 for Lane 2 were

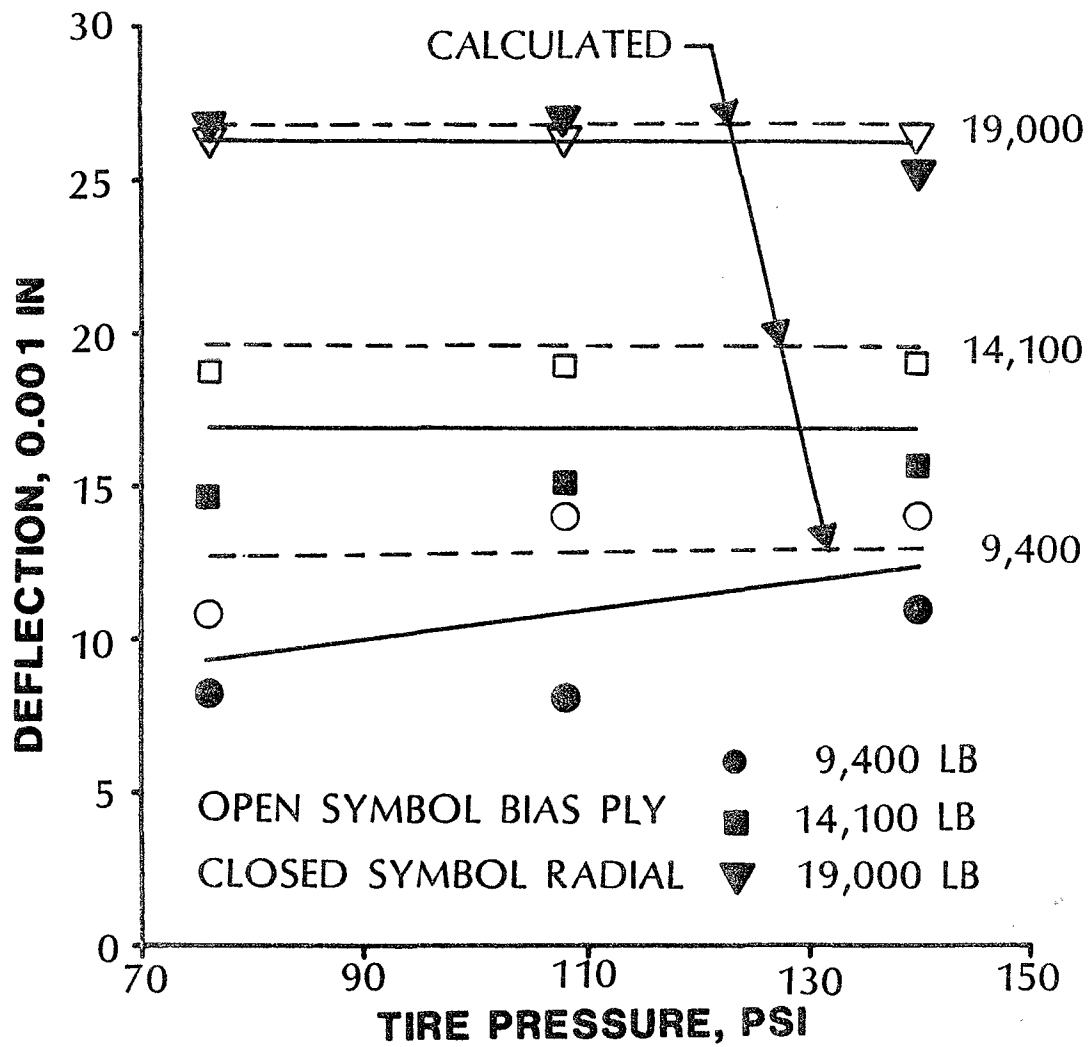


Figure 17. Effects of load and tire pressure on surface deflection for Lane 1.

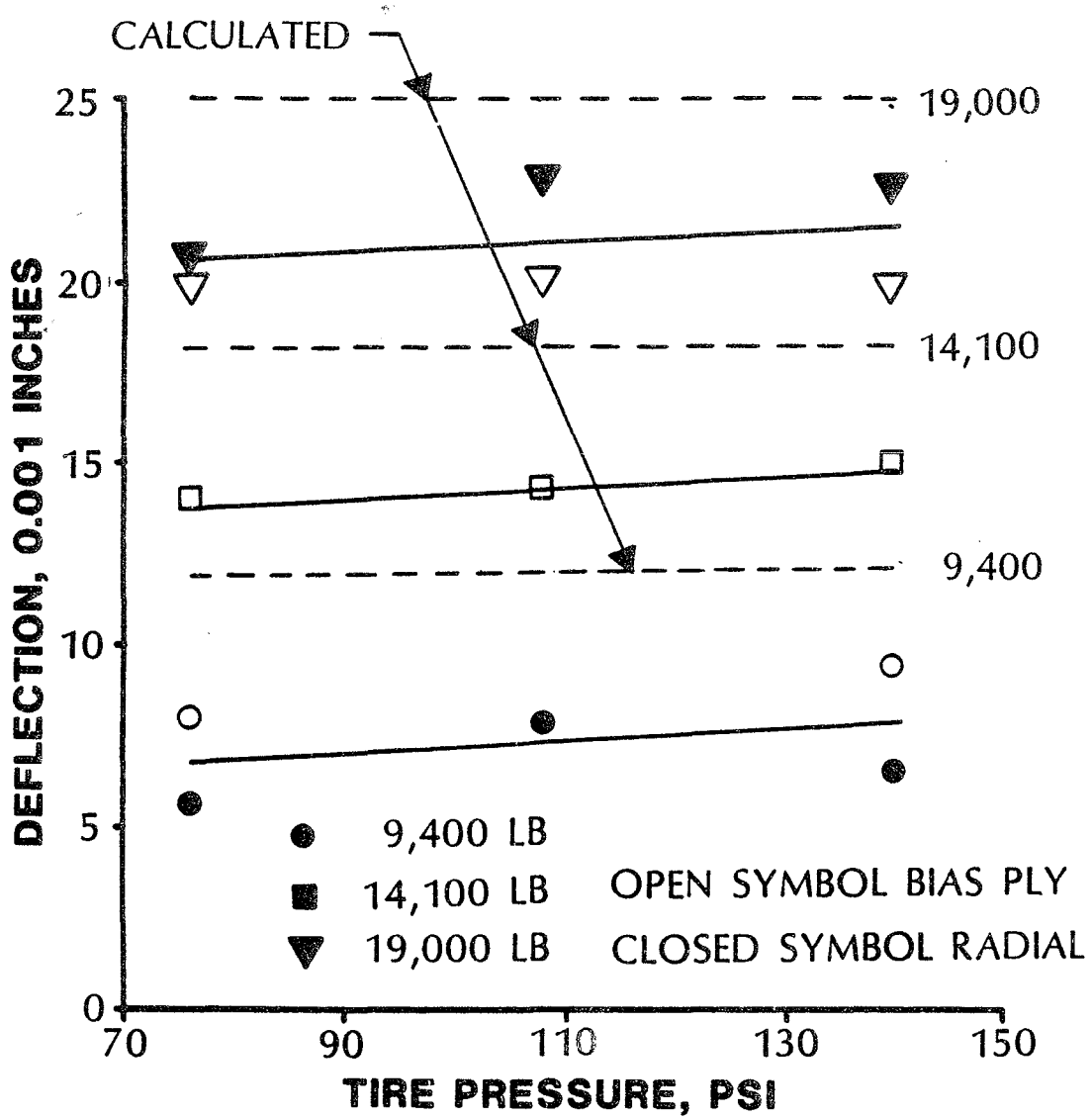


Figure 18. Effects of load and tire pressure on surface deflection for Lane 2.

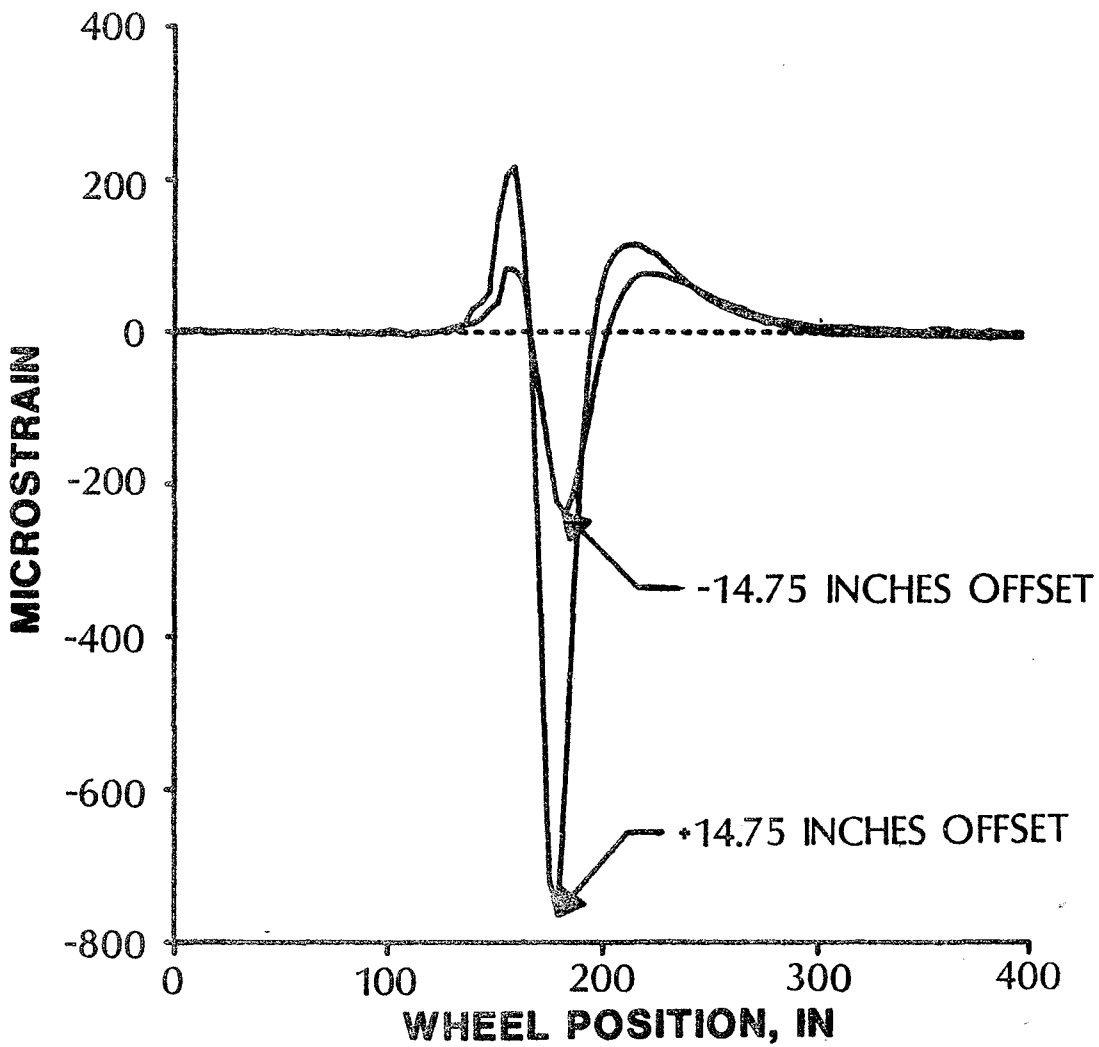


Figure 19. Typical response curve for longitudinal surface strain.

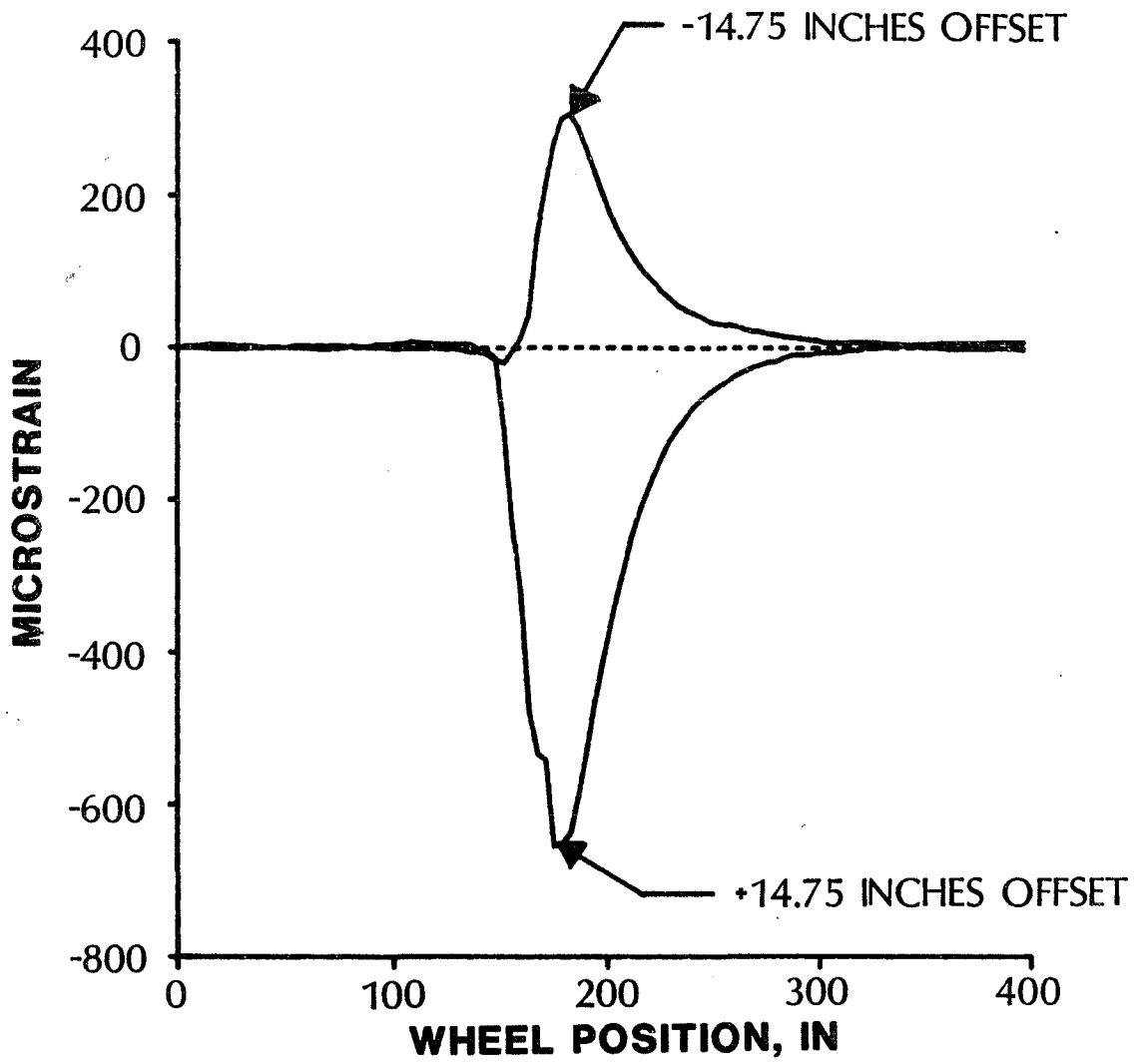


Figure 20. Typical response curve for transverse surface strain.

operational for all loads and tire pressures. Figures 21 and 22 present the effects of load and tire pressure on the surface strain measured by these gauges. Each data point represents the average of five or six tests. No adjustments were made for dynamic load or temperature variations. Theoretical strains from the layered-elastic analysis are also shown. These figures present data for the +14.75 in offset position; similar effects were obtained for the other offset positions.

At the instrumentation locations, the theoretical surface strains were insensitive to tire pressure and were affected only slightly by load. The measured strains, however, showed a different pattern. They were relatively insensitive to tire pressure, but highly sensitive to load. For Lane 2 at the 14,100 and 19,000-lb load levels, the bias ply tires produced much higher surface strains than the radial tires. This effect was probably due to temperature, not tire type. The average pavement temperatures during these tests were 6-10 °F higher than those during the corresponding tests for the radial tires. Based on laboratory resilient modulus data, this temperature difference would result in a 100,000 psi decrease in the modulus for the asphalt layer.

At all loads and tire pressures, the measured surface strains were significantly higher than those predicted by layer theory. This may be the result of horizontal tire forces induced at the pavement surface which were not accounted for in the layered-elastic analysis.

Strain at the Bottom of the Asphalt Layer

Typical response curves for longitudinal strain at the bottom of the asphalt layer are shown in figure 23. No transverse gauges were installed at the bottom of the asphalt layer. These response curves show a reversal similar to that described for the longitudinal surface strains. As the load approached the gauges, compressive strains were induced at the bottom of the asphalt layer. When the load was over the gauges, tensile strains occurred, and finally, compressive strains were once again induced as the load moved away from the gauges.

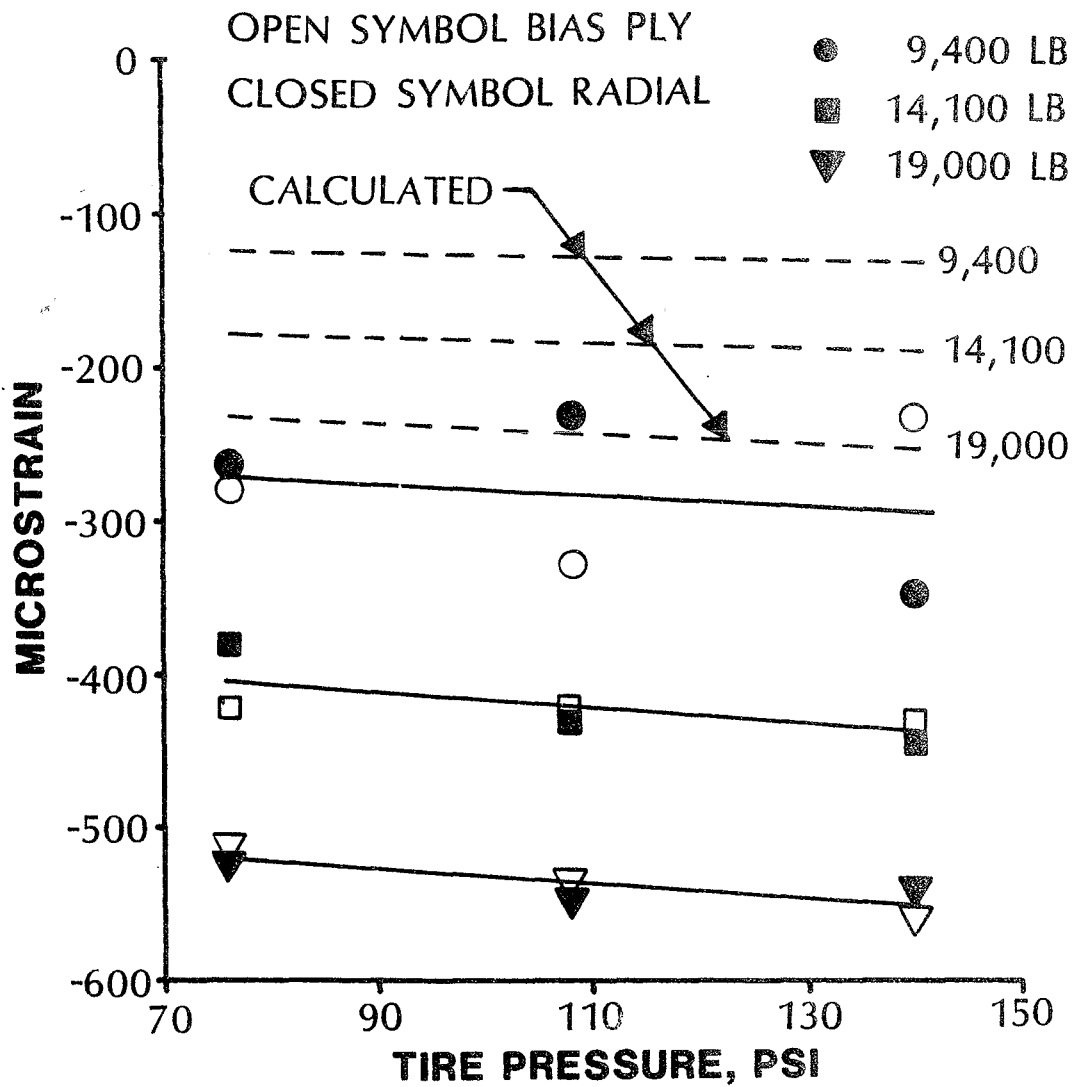


Figure 21. Effects of load and tire pressure on surface strain for Lane 1.

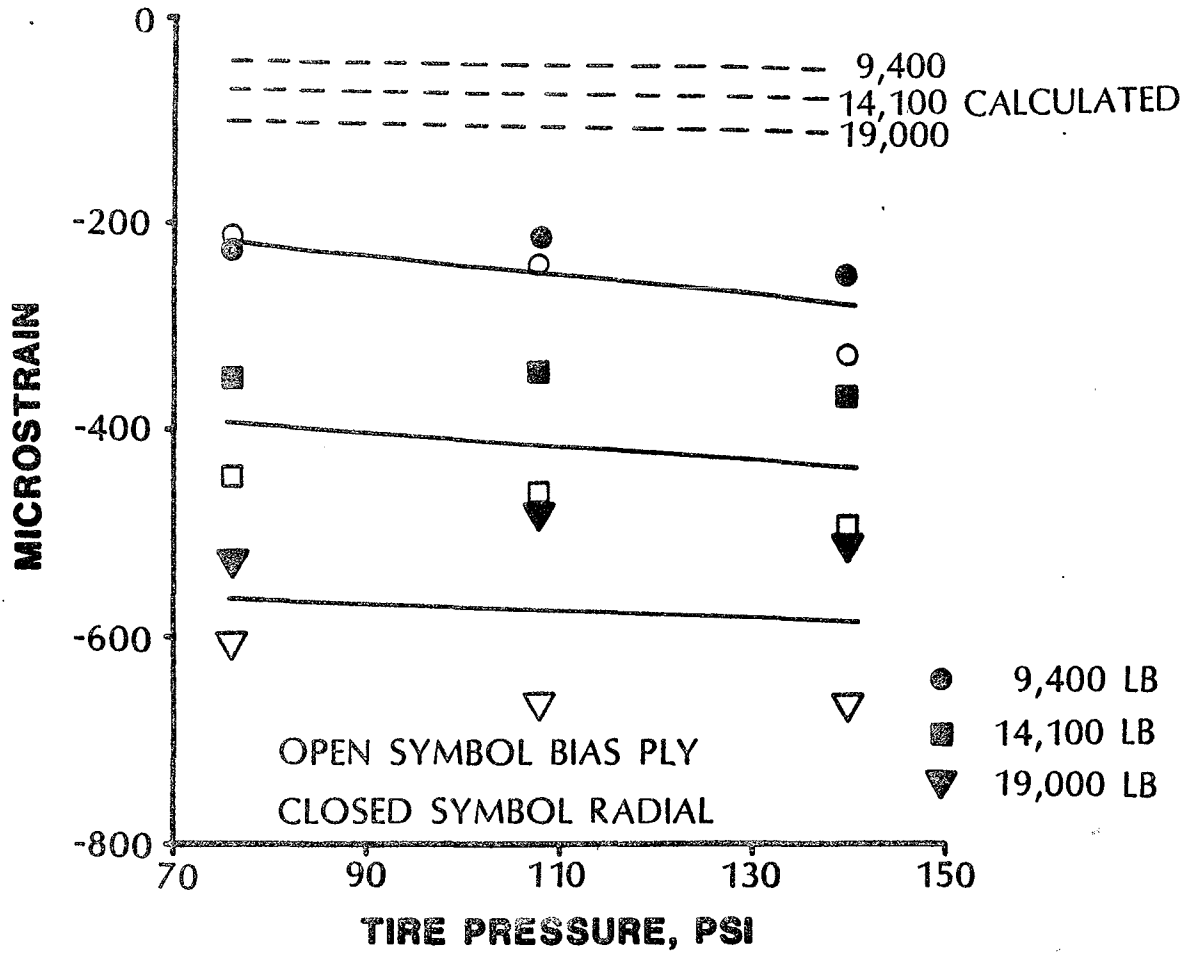


Figure 22. Effects of load and tire pressure on surface strain for Lane 2.

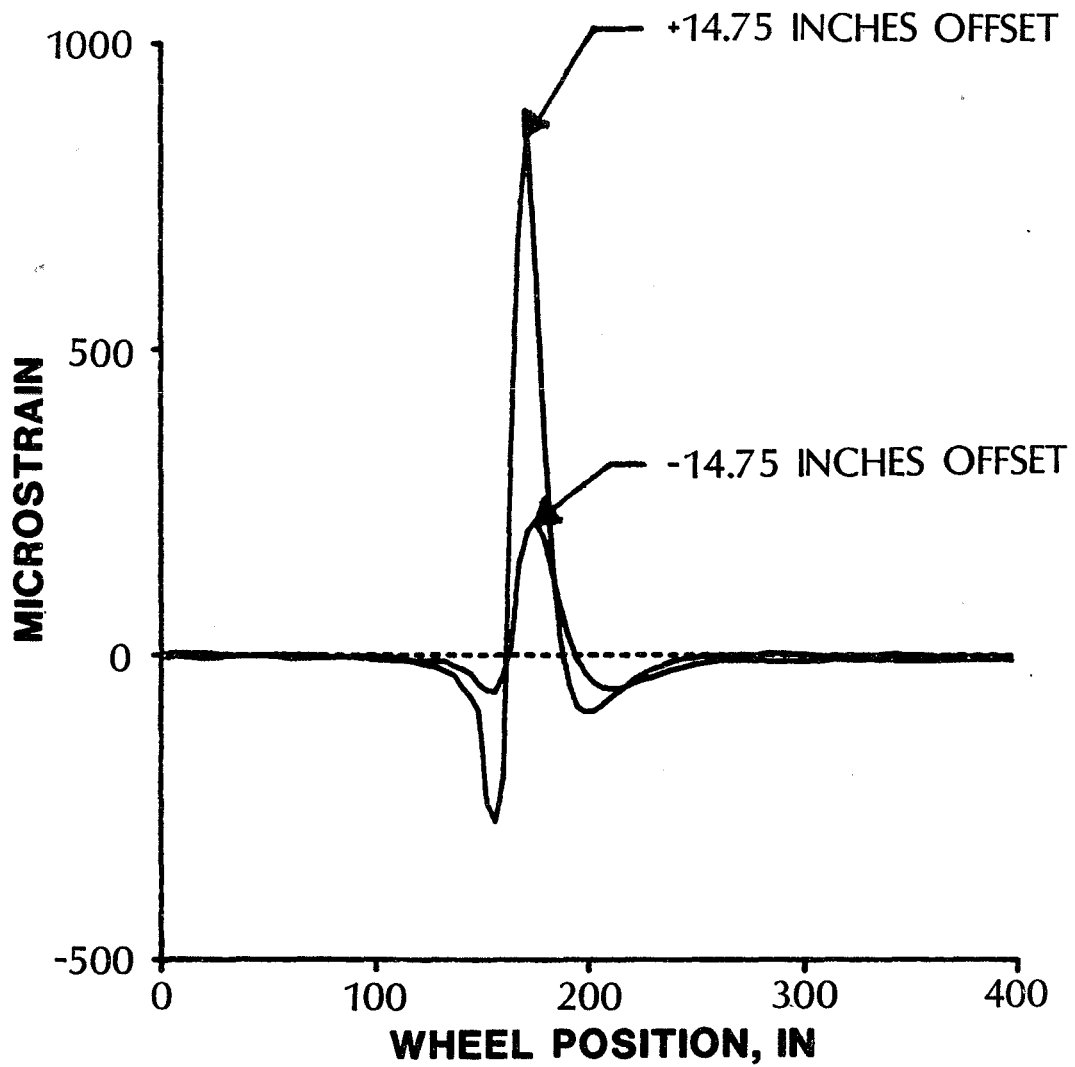


Figure 23. Typical response curve for longitudinal strain at the bottom of the asphalt layer.

Peak tensile strains for the gauges at the bottom of the asphalt layer are summarized in tables 29 to 34 of appendix B. Only one gauge in each lane was operational for all loads and tire pressures. Figures 24 and 25 show the effects of load and tire pressure on the strains measured by these gauges. Each data point in these figures represents the average of five or six tests. No corrections were made for dynamic load or temperature variations. Theoretical strains from the layered-elastic analysis are also shown. These figures present data for the +14.75 in offset position. Similar effects were obtained for the other offset positions.

Although the measured strains are somewhat higher than the calculated strains, the effects of load and tire pressure on the measured strains generally agree with those predicted by layer theory. Both show the strain at the bottom of the asphalt layer to be highly sensitive to load and less sensitive to tire pressure. For Lane 2 at the 14,100 and the 19,000-lb load levels, the bias ply tires produced much higher strains at the bottom of the asphalt layer. This effect was probably due to temperature as described in the previous section for surface strains.

The tests using the radial tires and the 14,100-lb load for Lane 1 and the 19,000-lb load for Lane 2 were repeated to assess the effect of accumulated damage during the response experiments. Figure 26 presents comparisons of strain at the bottom of the asphalt layer for these tests. The repeat tests show good agreement with the original tests indicating significant pavement damage did not occur during the experiment.

EVALUATION

Strain at the bottom of the asphalt layer can be used to assess the relative effects of load, tire pressure, and tire type on fatigue cracking. Fatigue equivalency factors may be developed for each combination used in the response experiment. By definition, an equivalency factor is the damage caused by one pass of any load configuration divided by the damage caused by one pass of a standard load configuration. Using Miner's Law, the damage

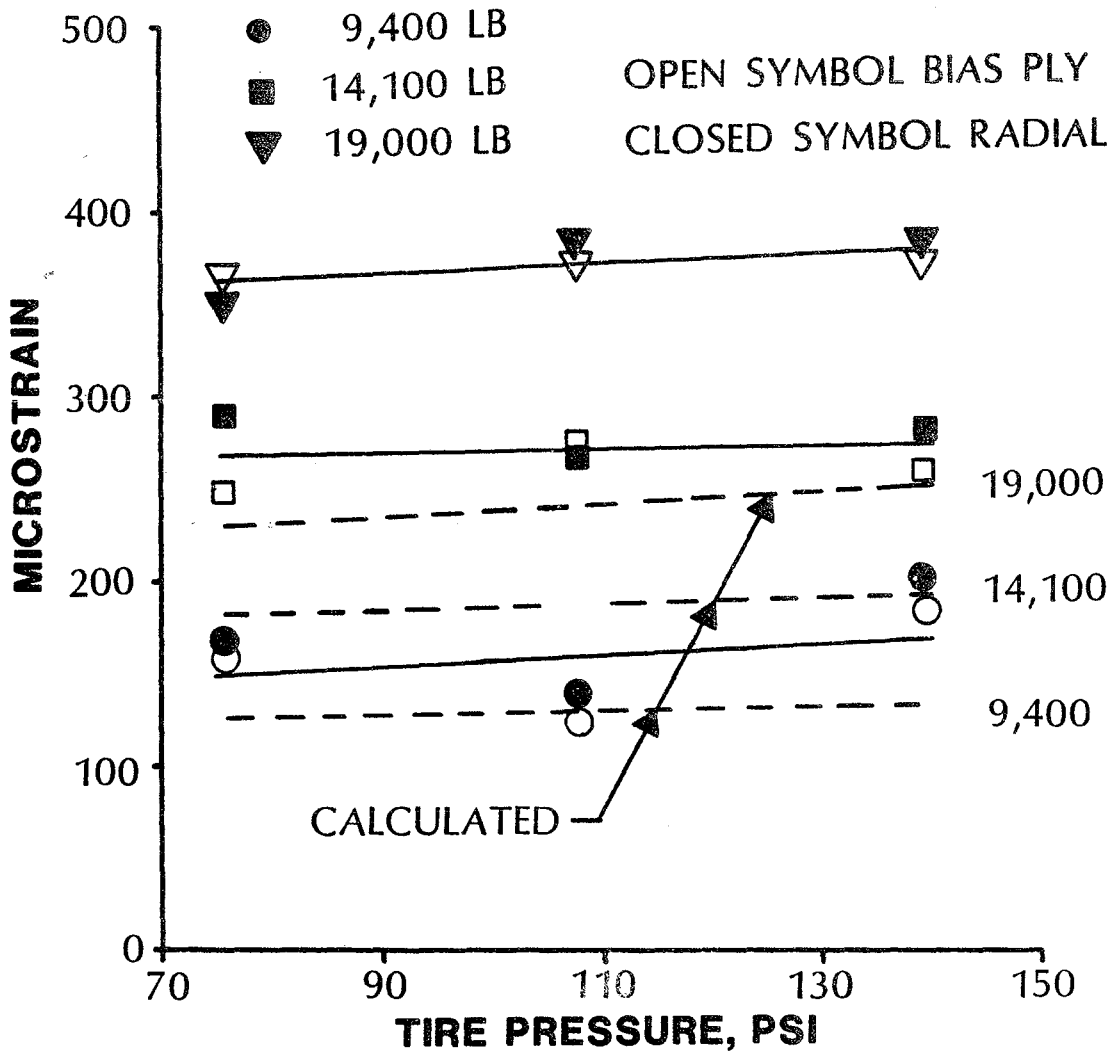


Figure 24. Effects of load and tire pressure on strain at the bottom of the asphalt layer for Lane 1.

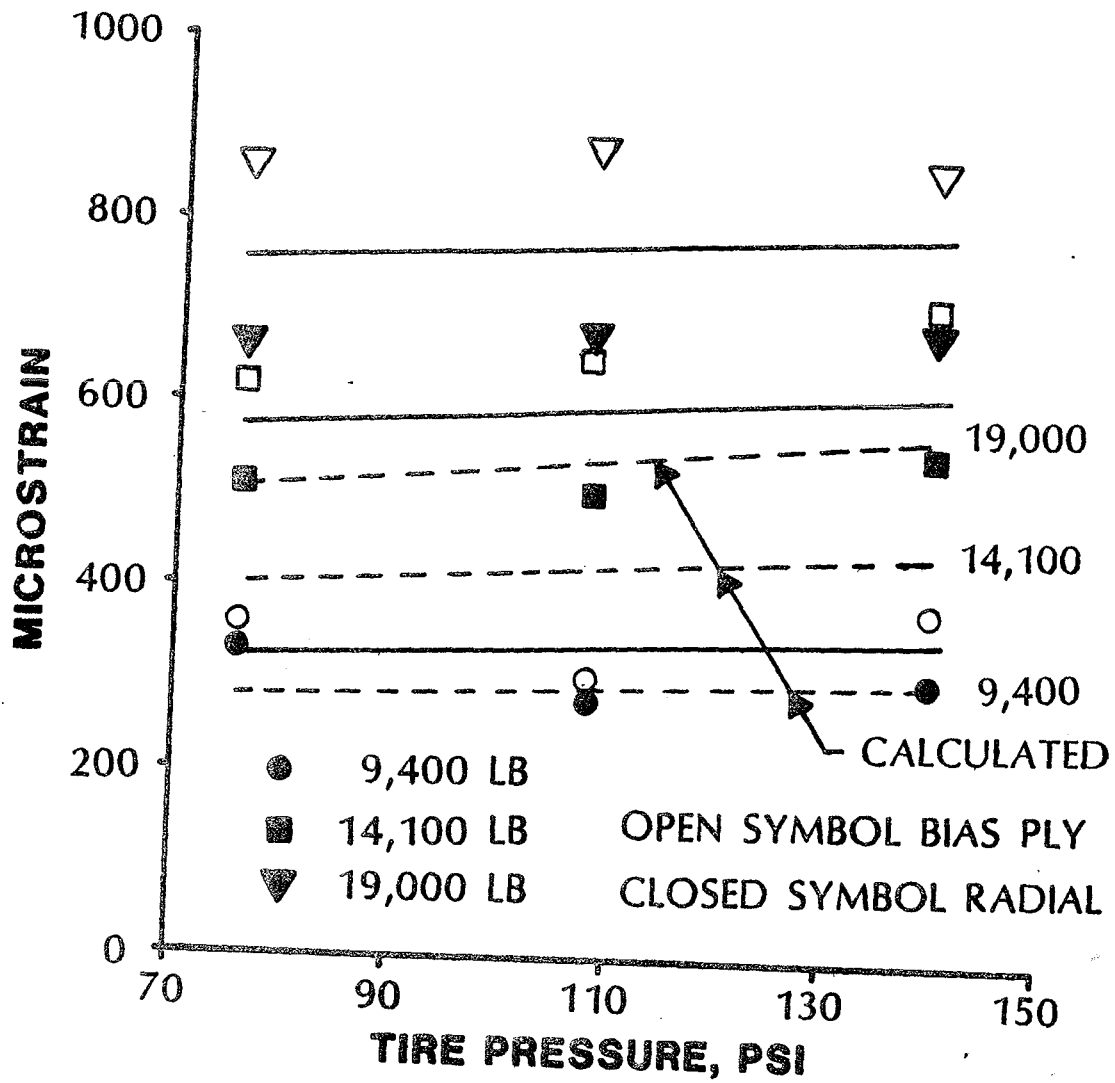


Figure 25. Effects of load and tire pressure on strain at the bottom of the asphalt layer for Lane 2.

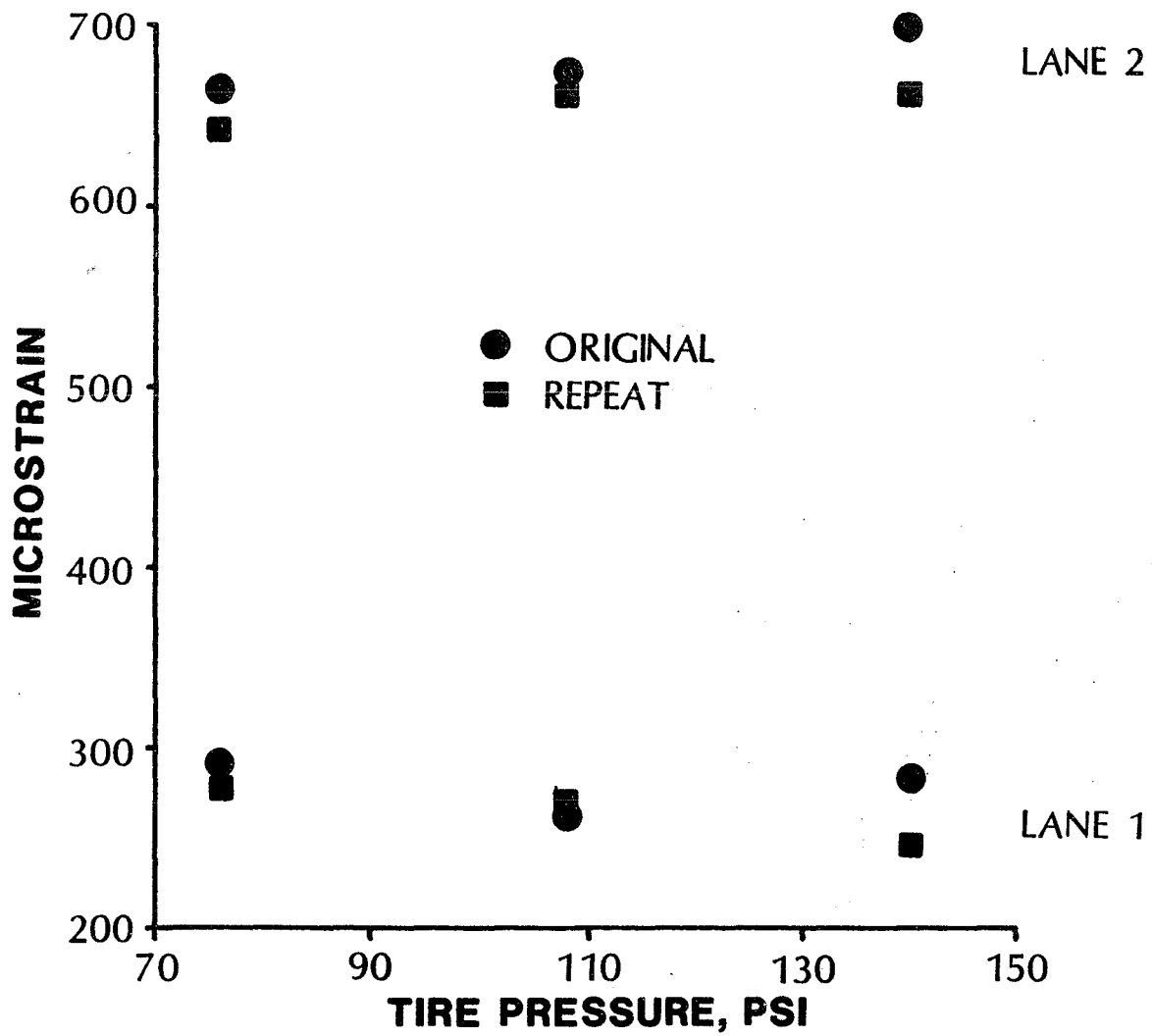


Figure 26. Comparison of strain at the bottom of the asphalt layer for original and repeat tests.

caused by one pass is the reciprocal of the fatigue life. Equation 1 is a mathematical expression for the fatigue equivalency factor:

$$F = \frac{N_f(\text{Std})}{N_f(\text{Any})} \quad (1)$$

where

F = Fatigue equivalency factor.

$N_f(\text{Any})$ = Fatigue life for any load configuration.

$N_f(\text{Std})$ = Fatigue life for the standard load configuration.

Reference 9 presents the following distress prediction model for fatigue cracking:

$$N_f = K_1 (e_t)^{3.29} (E^*)^{0.85} \quad (2)$$

where

N_f = Fatigue life.

e_t = Tensile strain at the bottom of the asphalt layer.

E^* = Dynamic modulus.

K_1 = Constant.

This model is based on laboratory fatigue curves and may be adjusted to correlate with field observations by changing K_1 . Using the above model, the fatigue equivalency factor may be expressed as:

$$F = \left[\frac{e_t(\text{Any})}{e_t(\text{Std})} \right]^{3.29} \left[\frac{E^*(\text{Any})}{E^*(\text{Std})} \right]^{0.85} \quad (3)$$

where

$e_t(\text{Any})$ = Strain for any load configuration.

$e_t(\text{Std})$ = Strain for the standard load configuration.

$E^*(\text{Any})$ = Dynamic modulus at the temperature for $e_t(\text{Any})$.

$E^*(\text{Std})$ = Dynamic modulus at the temperature for $e_t(\text{Std})$.

Table 4 and figure 27 present fatigue equivalency factors developed from the trends shown in the measured strain data using equation 3. The 9,400-lb load and 76-psi tire pressure combination was used as the standard configuration. The standard temperature was 40 °F for Lane 1 and 85 °F for Lane 2. These factors show a large effect due to load and a smaller effect due to tire pressure. Increasing the load from 9,400 to 14,100 lb increased the expected fatigue damage 350 percent for Lane 1 and 650 percent for Lane 2. On the other hand, increasing the tire pressure from 76 to 140 psi increased the expected fatigue damage less than 30 percent.

The fatigue equivalency factors cannot be compared between Lane 1 and Lane 2 due to the difference in the standard temperature used to develop the factors. The Lane 1 factors were developed using low temperature data (40 °F), while the Lane 2 factors were developed using high temperature data (85 °F).

It should be noted that the fatigue equivalency factors presented here are specific to the ALF loading, the pavement sections studied, the environmental conditions during the field testing, and the assumed fatigue model. More general factors, however, could be developed and used to assess the effects of changing truck characteristics on pavement fatigue life.

Table 4. Fatigue equivalency factors.

Load (lb)	LANE 1			LANE 2		
	76 (psi)	108 (psi)	140 (psi)	76 (psi)	108 (psi)	140 (psi)
9,400	1.0	1.1	1.4	1.0	1.1	1.3
14,100	3.5	3.6	3.8	6.6	7.4	8.5
19,000	9.2	10.0	11.0	16.2	17.5	19.0

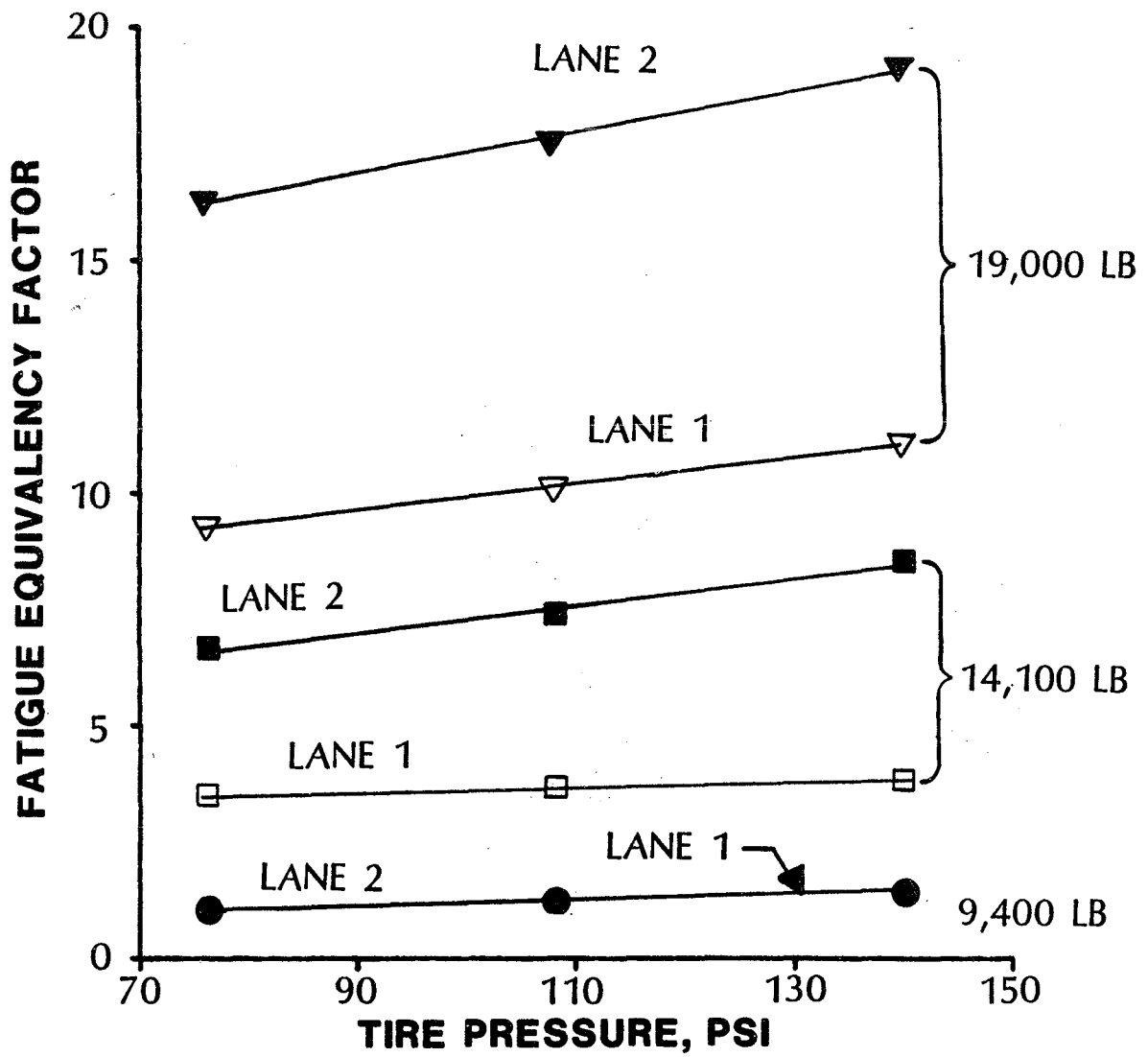


Figure 27. Equivalency between load and tire pressure based on measured strains.

III. PAVEMENT PERFORMANCE EVALUATION

INTRODUCTION

During the first phase of research at the PTF, two test sections, Lane 2, Section 3 (Test 2-3), and Lane 2, Section 2 (Test 2-2), were trafficked with the same load but different tire pressures. The wheel load was 19,000 lb and the tire pressures were 100 psi and 140 psi for Test 2-3 and Test 2-2, respectively. This chapter describes an evaluation of the effects of tire pressure on rutting and cracking for these two test sections.

TEST CONDITIONS

Load and tire pressure were carefully controlled during the tests used in this evaluation. Pavement performance, however, may be significantly affected by other test conditions including environment and construction variability which could not be controlled. These test conditions were quantified as outlined below to aid in the interpretation of the rutting and cracking data.

Environment

Temperature and moisture conditions have a significant impact on flexible pavement performance. The stiffness of asphalt concrete is affected by temperature, and the stiffness of subgrade soils and granular base materials is affected by moisture. Test 2-3 was conducted from January 8 to June 6, 1987, and Test 2-2 was conducted from June 18 to November 24, 1987. To quantify the thermal conditions during testing, daily maximum and minimum air temperatures were obtained from the National Oceanic and Atmospheric Administration weather station at Dulles International Airport, which is located 25 miles west of the PTF. Average air temperatures calculated from this data are shown in figure 28. The average air temperature for the first one-half of Test 2-2 was approximately 80 °F compared to only 40 °F for the first one-half of Test 2-3.

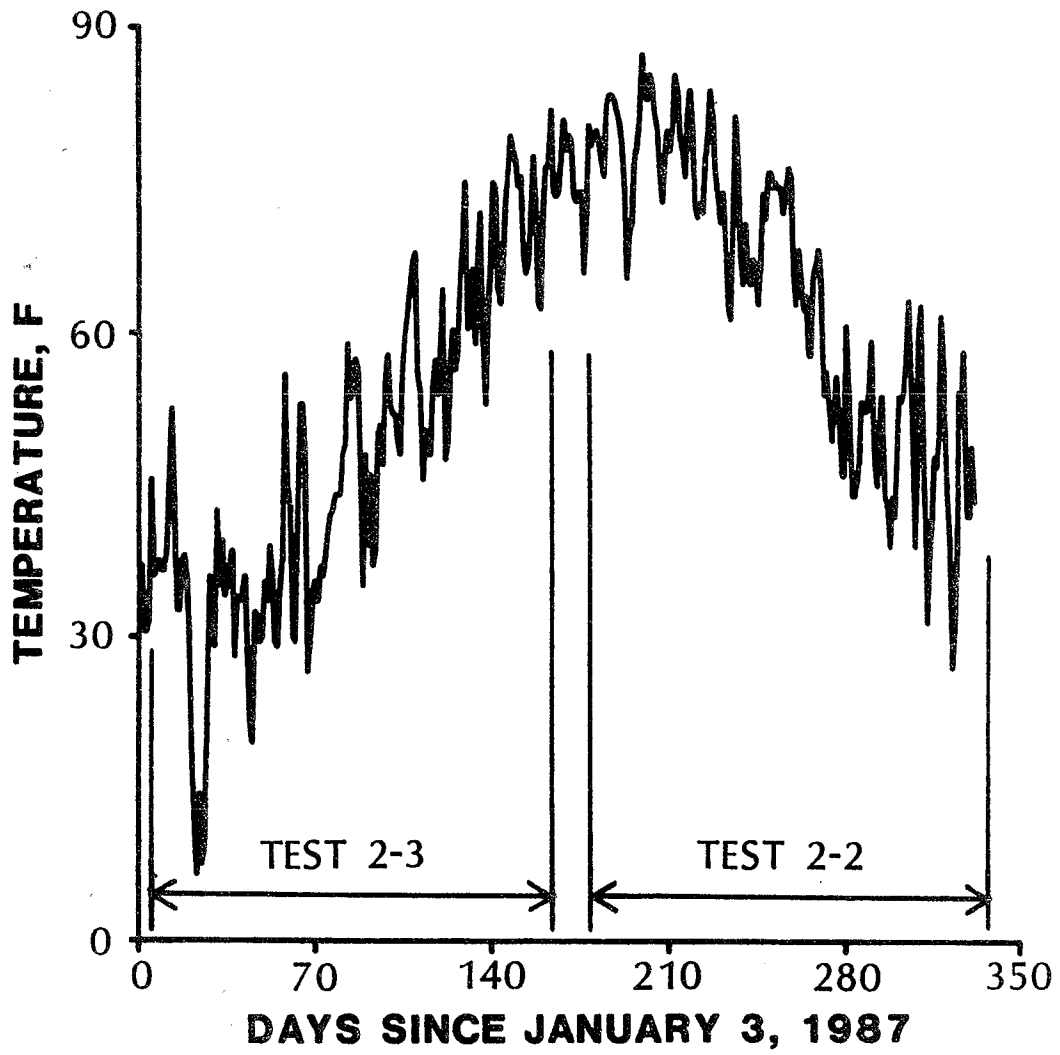


Figure 28. Daily average air temperatures.

Moisture cells, oven dried samples, and backcalculated moduli from periodic falling weight deflectometer (FWD) tests were used to track moisture content changes. These three methods indicated that moisture equilibrium was reached before trafficking of Test 2-3, and moisture conditions remained constant throughout Tests 2-3 and 2-2.⁽⁷⁾

Construction Variability

Thickness and density are two construction variables which have a significant impact on flexible pavement performance. The structural capacity of a pavement is influenced directly by the thickness of the component layers, and density affects the stiffness of paving materials. Pavement layer thicknesses were obtained by differential leveling during construction. Table 5 presents average layer thicknesses for Tests 2-2 and 2-3. Both the asphalt concrete and the crushed aggregate base were approximately 0.5 in thinner in Test 2-2 than Test 2-3.

Table 5. Average pavement thicknesses.

Layer	Thickness (in)	
	Test 2-2	Test 2-3
Asphalt Concrete	6.8	7.3
Crushed Aggregate Base	11.2	11.8
Total	18.0	19.1

In-place densities of the subgrade soil and crushed aggregate base were measured with a nuclear density gauge during construction. The asphalt concrete wearing and binder densities were obtained using cores from untrafficked areas of each section. Table 6 presents average layer densities for Tests 2-2 and 2-3. These data indicate the materials in both test sections

Table 6. Average layer densities.

	Test 2-2	Test 2-3
Subgrade		
Average Dry Density, pcf	125.0	119.5
AASHTO T180 Max. Dry Density, pcf	121.7	121.7
Crushed Aggregate Base		
Average Dry Density, pcf	149.3	146.2
AASHTO T180 Max. Dry Density, pcf	152.4	152.4
Lower Lift Binder		
Average Density, pcf	158.3	158.0
Average Air Voids, %	4.3	4.4
Upper Lift Binder		
Average Density, pcf	155.9	161.1
Average Air Voids, %	5.7	2.6
Wearing		
Average Density, pcf	153.8	154.9
Average Air Voids, %	5.4	4.7

were well compacted. The air void content of the asphalt layers and the density of the crushed aggregate base and subgrade were slightly higher in Test 2-2 than in Test 2-3.

The overall effect of the construction variability was evaluated using nondestructive testing. Deflections for each layer were measured with a falling weight deflectometer. The deflection at the middle of the loading

plate was used in conjunction with layer theory to calculate a composite modulus. This composite modulus is a measure of the structural capacity of the pavement. Table 7 presents average composite moduli for FWD tests conducted at the surface of each layer. These data show Test 2-2 initially had a lower structural capacity than Test 2-3.

Table 7. Average composite moduli.

Layer	Composite Modulus (ksi)	
	Test 2-2	Test 2-3
Subgrade	7.0	8.4
Base	12.0	15.4
Wearing	41.5	49.4

In summary, Test 2-2 represents a worst case condition. In addition to the higher tire pressure, the pavement temperature was also higher, and the initial structural capacity was lower than Test 2-3.

RUTTING

Rutting for Tests 2-2 and 2-3 was obtained by differential leveling conducted on a regular basis during each test. Rut depths were obtained at 8 locations along the test section. At each location, the elevation of the surface of the pavement was measured every 6 in across the pavement to produce a transverse profile. To eliminate initial surface irregularities from the rut depth data, profiles obtained before trafficking were used as references. Subsequent profiles were subtracted from the appropriate reference to calculate rut depths. Rut depths for Tests 2-2 and 2-3 are presented in tables 8 and 9.

Table 8. Rut depths for Tests 2-2.

Passes	Rut Depth, Inches							
	Sta. 62	Sta. 66	Sta. 70	Sta. 74	Sta. 78	Sta. 82	Sta. 86	Sta. 88
0	0	0	0	0	0	0	0	0
37,292	.08	.23	.25	.21	.23	.22	.23	.25
130,082	.16	.33	.34	.30	.34	.44	.40	.29
450,895	.39	.50	.68	.68	.80	.68	.50	.45
578,142	.83	.74	.79	.85	1.16	1.18	.78	.66

Table 9. Rut depths for Test 2-3.

Passes	Rut Depth, Inches							
	Sta. 99	Sta. 103	Sta. 107	Sta. 111	Sta. 115	Sta. 119	Sta. 123	Sta. 127
0	0	0	0	0	0	0	0	0
77,475	.10	0	.06	.03	0	.06	.04	.12
146,896	.10	0	.16	.13	0	.10	.11	.29
276,949	.14	.08	.28	.17	.12	.27	.52	.82
416,812	.43	.39	.53	.50	.38	.91	1.14	1.50

CRACKING

A manual procedure was used to measure cracking for Tests 2-2 and 2-3. On a regular schedule, a clear plastic sheet was placed over the test section and the cracks were traced onto the plastic. Different color markers were used each time a crack survey was performed. The test section was then divided into eight 4-ft long by 6-ft wide subsections. The total length of cracking in each subsection was measured using a map wheel, and the surface area of AASHTO Class 2 and Class 3 cracking was estimated. An analysis of the cracking data showed the total crack length method to be more sensitive to small amounts of cracking and changes in cracking than the AASHTO procedure.⁽¹⁰⁾ The accumulation of total crack length is presented in tables 10 and 11 for Tests 2-2 and 2-3.

Table 10. Cracking for Tests 2-2.

Passes	Cracking, Inches							
	Sta. 62	Sta. 66	Sta. 70	Sta. 74	Sta. 78	Sta. 82	Sta. 86	Sta. 88
0	0	0	0	0	0	0	0	0
248,200	0	0	0	0	0	0	0	26
314,847	21	37	99	79	154	87	46	246
375,023	21	39	112	79	207	116	56	318
430,766	21	39	119	79	288	132	74	460
462,920	39	46	149	88	456	251	108	608
511,765	40	46	192	93	540	332	163	637
538,963	60	56	262	148	809	531	240	805
578,142	122	70	499	270	1061	918	495	1130

Table 11. Cracking for Test 2-3.

Passes	Cracking, Inches							
	Sta. 99	Sta. 103	Sta. 107	Sta. 111	Sta. 115	Sta. 119	Sta. 123	Sta. 127
0	0	0	0	0	0	0	0	0
266,858	0	0	0	0	0	0	0	51
279,518	0	0	0	0	0	0	0	82
329,156	0	0	0	0	0	0	0	392
370,234	0	0	0	0	0	0	63	538
411,088	33	10	22	10	0	46	225	721
488,285	79	10	22	61	44	154	466	935
502,662	112	50	115	121	62	258	597	1051

EVALUATION

When evaluating rutting and cracking data from test sections at the PTF, three factors must be considered. First, the ALF applies a dynamic load. Figure 29 shows the dynamic loading for the ALF at the load and tire pressures used in Tests 2-2 and 2-3. The load near the beginning of the test section is approximately 20 percent lower than the average load. This decrease in load is reflected in the rutting and cracking data which show less damage in the area of low load. Second, the rutting and cracking near the end of Test 2-2 were influenced by previous trafficking of Test 2-3. At the PTF, there are only 5 ft between test sections in a given lane. Thus, pavement performance near station 92 of Test 2-2 was influenced by damage caused earlier near station 97 of Test 2-3. Finally, the high rutting and cracking near the end of Test 2-3 were the result of a core hole near the centerline of the section at station 128.

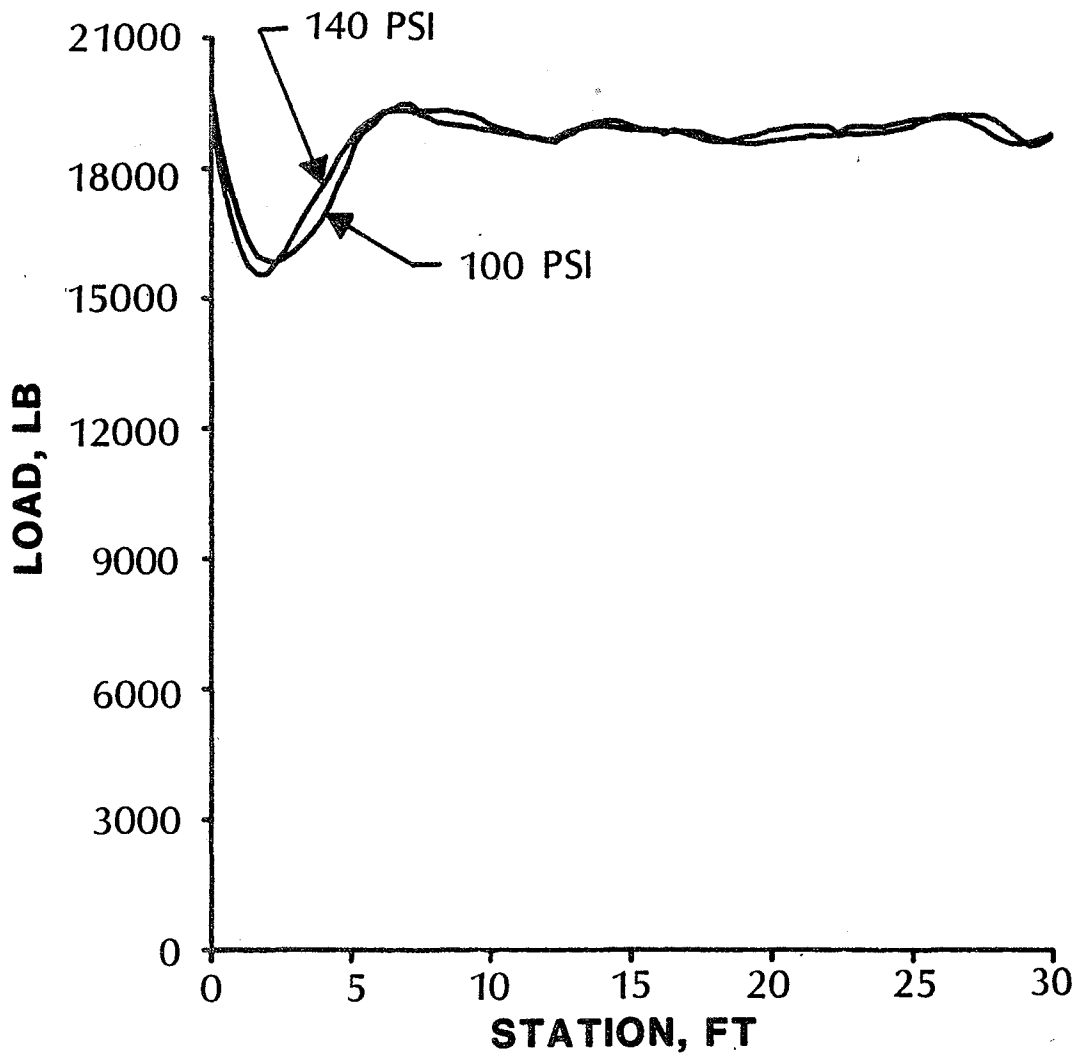


Figure 29. ALF dynamic loading at 19,000 lbs, 100 and 140 psi tire pressures.

Considering these three factors, the ends of the test sections were not representative. The evaluation of pavement performance was, therefore, based on data from station 66 to 86 for Test 2-2, and from station 103 to 115 for Test 2-3.

Comparisons of average rutting and cracking for these portions of Tests 2-3 and 2-2 are presented in figures 30 and 31. The comparisons show Test 2-2 had significantly higher rutting than Test 2-3, and cracking began much sooner in Test 2-2. These effects were the result of the higher tire pressure, higher temperature, and thinner pavement structure in Test 2-2.

After each test section failed, a postmortem evaluation was conducted in an area of the test section exhibiting average rutting and cracking. This evaluation consisted of excavating each layer of the pavement, and obtaining profiles, density measurements, and samples for laboratory testing. Table 12 summarizes the laboratory tests which were performed as part of the postmortem evaluations. The findings of these evaluations were used in conjunction with layer theory to estimate the relative influence of tire pressure, temperature, and thickness on the observed rutting and cracking.

Table 12. Laboratory tests for postmortem evaluations.

	Test 2-2	Test 2-3
Asphalt Concrete		
Density	X	X
Air Void Content	X	X
Extraction/Gradation	X	X
Crushed Aggregate Base		
Moisture Content	X	X
Gradation	X	X
Subgrade		
Moisture Content	X	X
Gradation	X	X

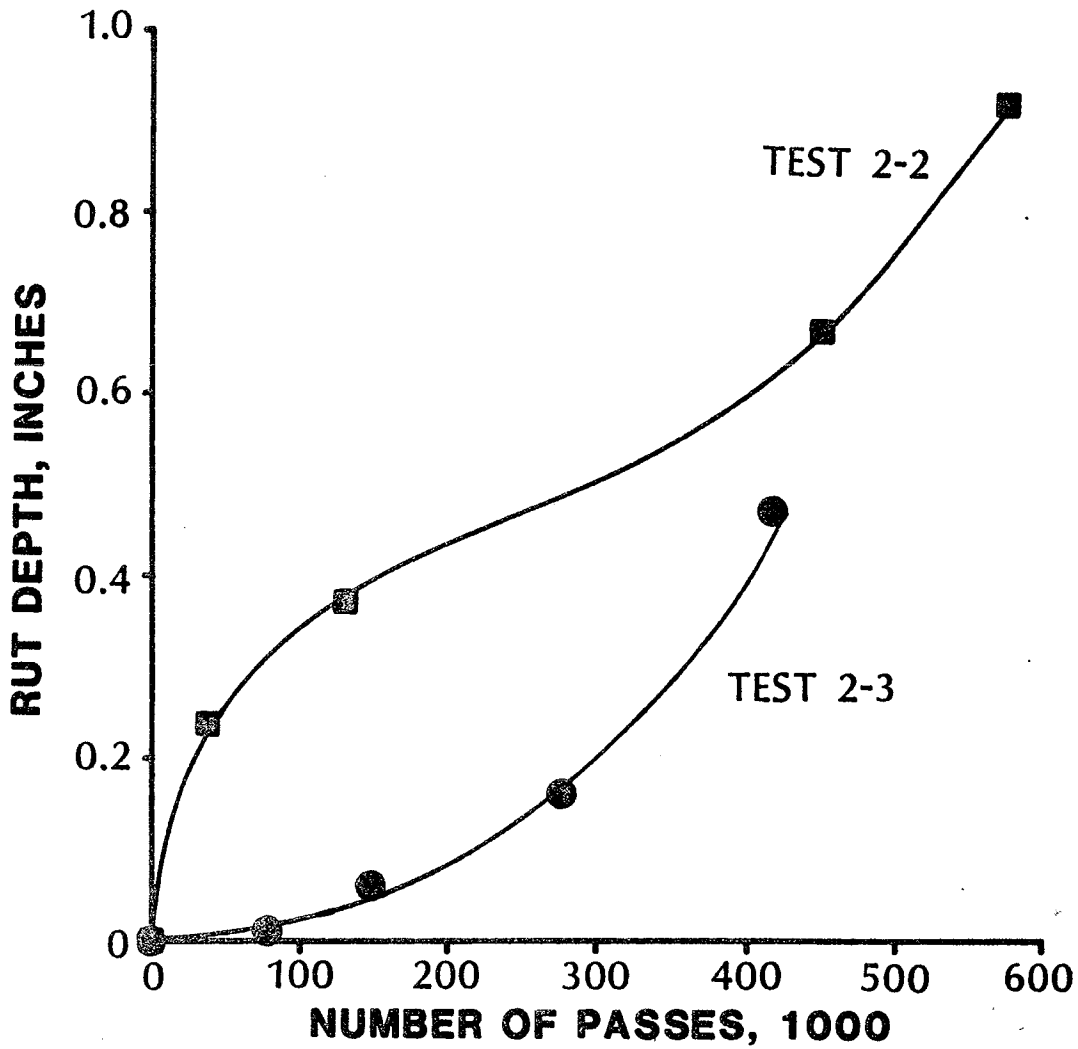


Figure 30. Comparison of average rutting for Tests 2-2 and 2-3.

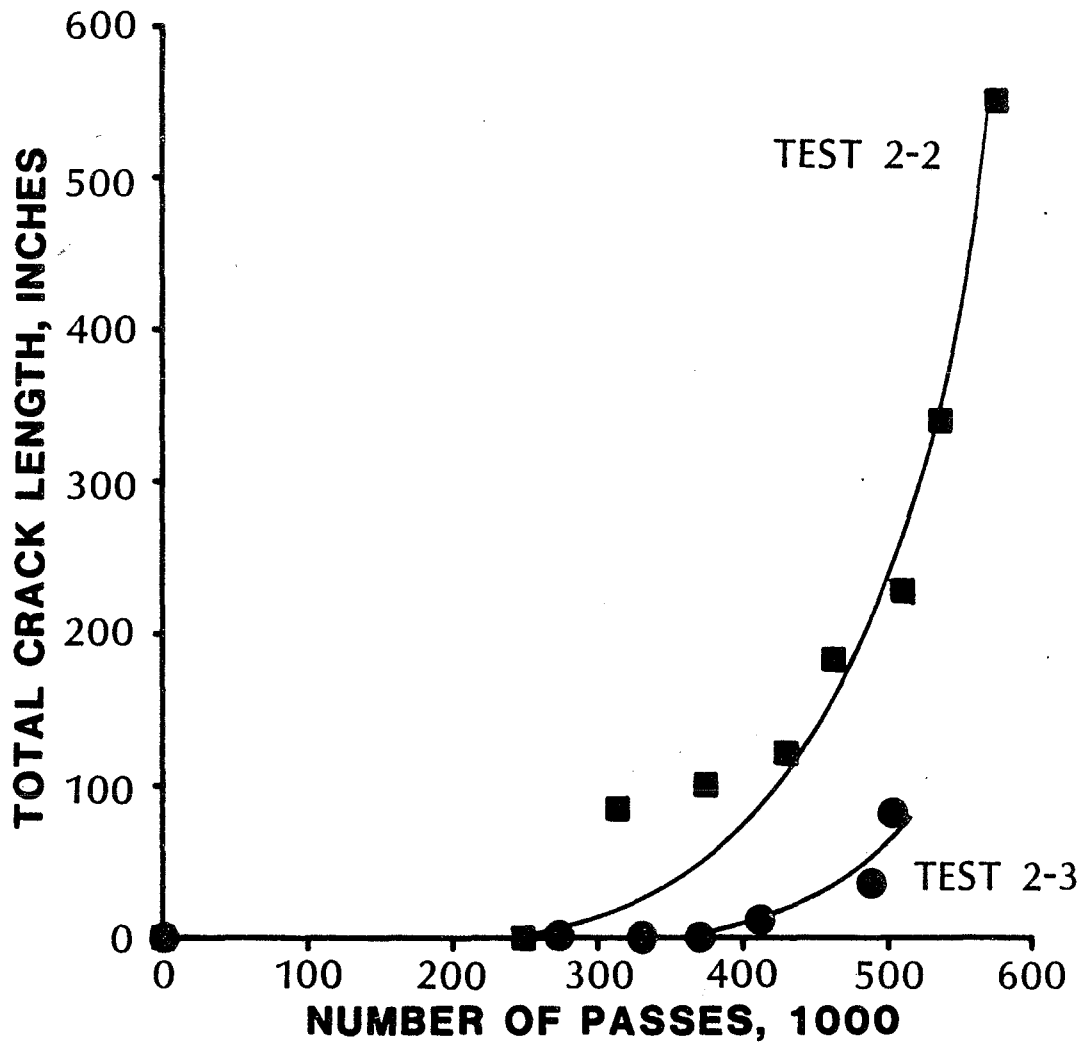


Figure 31. Comparison of average cracking for Tests 2-2 and 2-3.

The profiles obtained from the postmortem evaluations indicated that the majority of the rutting in Tests 2-3 and 2-2 occurred in the crushed aggregate base. Many pavement engineers attribute this rutting to the vertical compressive stress or strain at the top of the crushed aggregate base. The ELSYM5 computer program was used to calculate this strain for various temperatures using the load, pavement thicknesses and tire pressures from the PTF tests. Moduli for the asphalt concrete at different temperatures were obtained from figure 32 which shows the modulus versus temperature relationship for the PTF asphalt concrete, based on indirect tension tests on cores removed from the pavement shortly after construction. The moduli of the crushed aggregate base and subgrade were assumed constant at 20,000 psi and 8,000 psi, respectively. Figure 33 presents the calculated vertical compressive strains at the top of the crushed aggregate base. These data show temperature has the greatest effect on this strain. Assuming average pavement temperatures of 40 and 80 °F for the first one-half of Test 2-3 and 2-2, respectively, temperature accounted for 66 percent of the increase in the calculated strain at the top of the crushed aggregate base. Tire pressure accounted for 18 percent of the increase, and the 0.5 in difference in asphalt thickness accounted for the other 12 percent.

Thus, the difference in rutting between Tests 2-3 and 2-2 was due mainly to the higher temperature during Test 2-2. Test 2-2 was trafficked in the summer and fall under relatively high pavement temperatures, while Test 2-3 was trafficked in the winter and spring under much lower pavement temperatures. The vertical compressive strain at the top of the crushed aggregate base increases with increasing temperatures. At high temperatures, this strain is further increased by higher tire pressure.

The failure mode for Tests 2-3 and 2-2 was fatigue of the asphalt concrete. Many pavement engineers agree that this type of failure is governed by the tensile strain at the bottom of the asphalt layer. The ELSYM5 computer program was used to calculate this strain for various temperatures using the load, thicknesses, and tire pressures from the PTF tests. The moduli described in the rutting analysis were also used in this analysis. The calculated

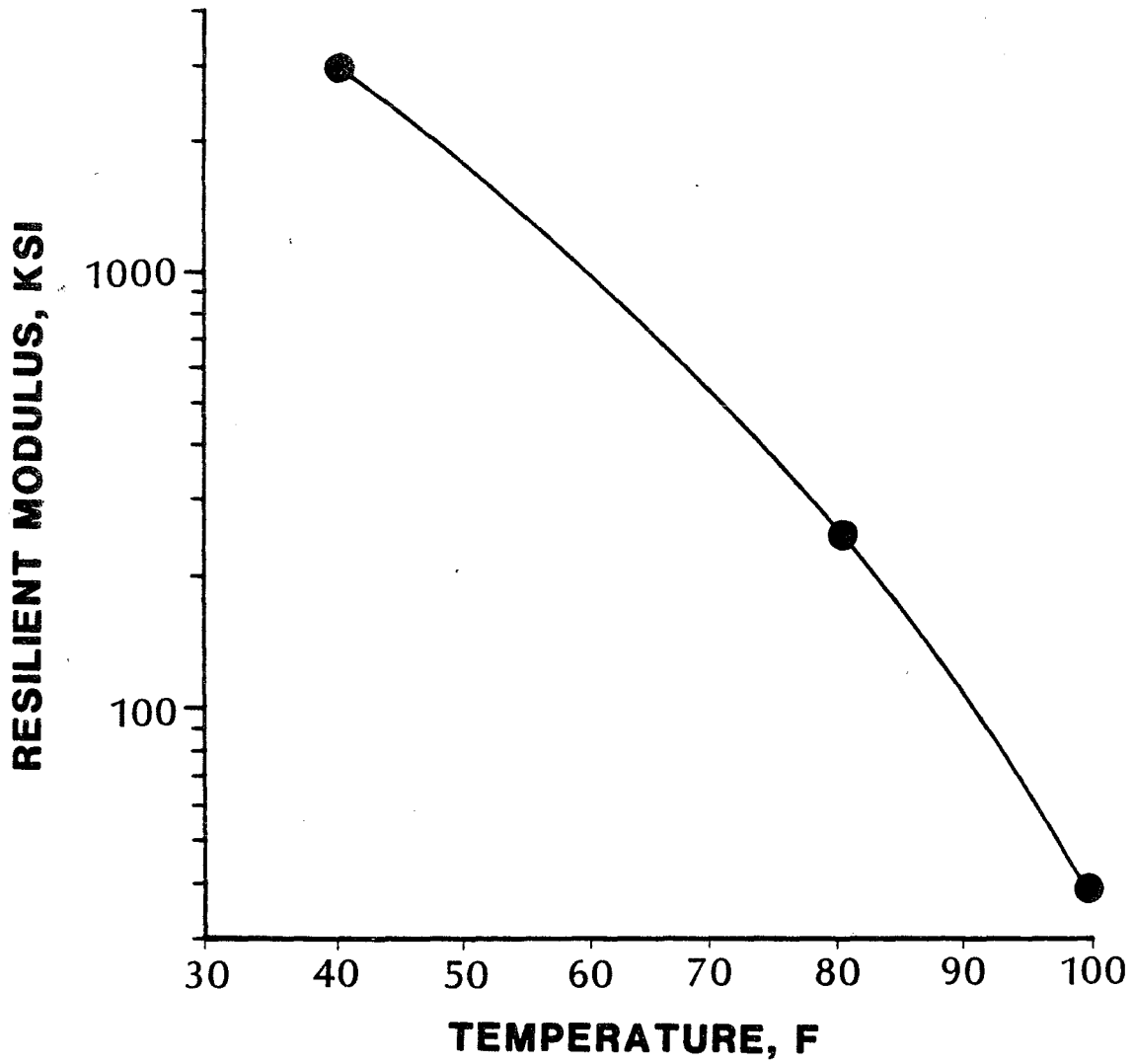


Figure 32. Resilient modulus versus temperature relationship for the PTF asphalt concrete.

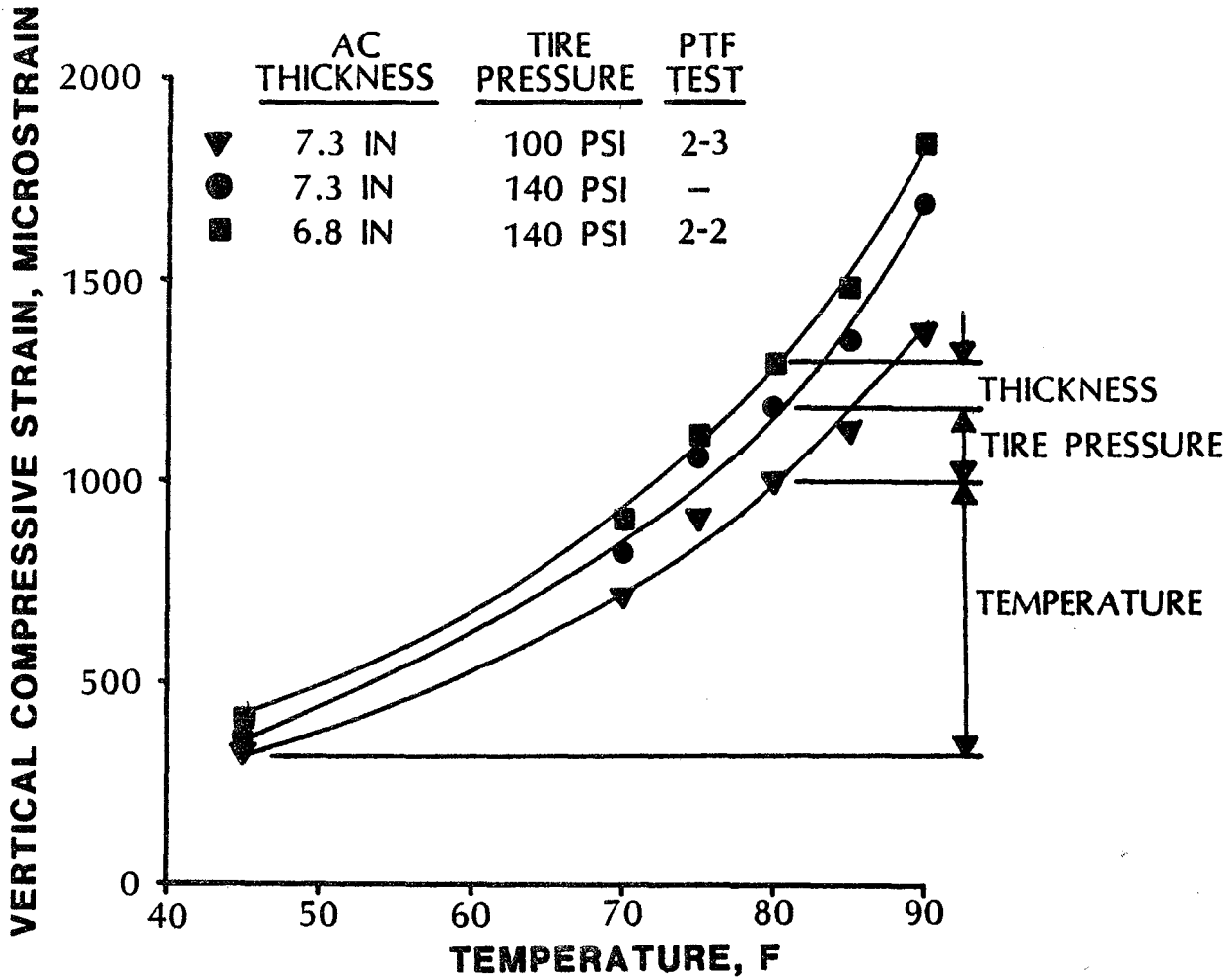


Figure 33. Vertical compressive strains at the top of the crushed aggregate base based on ELSYM5.

strains were then used in the fatigue model previously described in chapter II to predict the damage caused by one repetition of the load for each test condition. Figure 34 presents this damage normalized with respect to 70 °F, 100-psi tire pressure, and the thickness for Test 2-3. These data show the combined effects of temperature and difference in pavement thickness had the greatest effect on fatigue damage. Assuming average pavement temperatures of 40 and 80 °F for Tests 2-3 and 2-2, respectively, temperature accounted for only 14 percent of the difference in expected fatigue damage. At the higher temperature, however, the 0.5 in difference in asphalt thickness accounted for 53 percent of the difference in expected fatigue damage while the increased tire pressure accounted for 33 percent of the difference.

Thus, the difference in cracking between Tests 2-2 and 2-3 was due mainly to the combined effects of high temperature and thinner pavement structure. This combination accounted for 67 percent of the difference in expected fatigue damage.

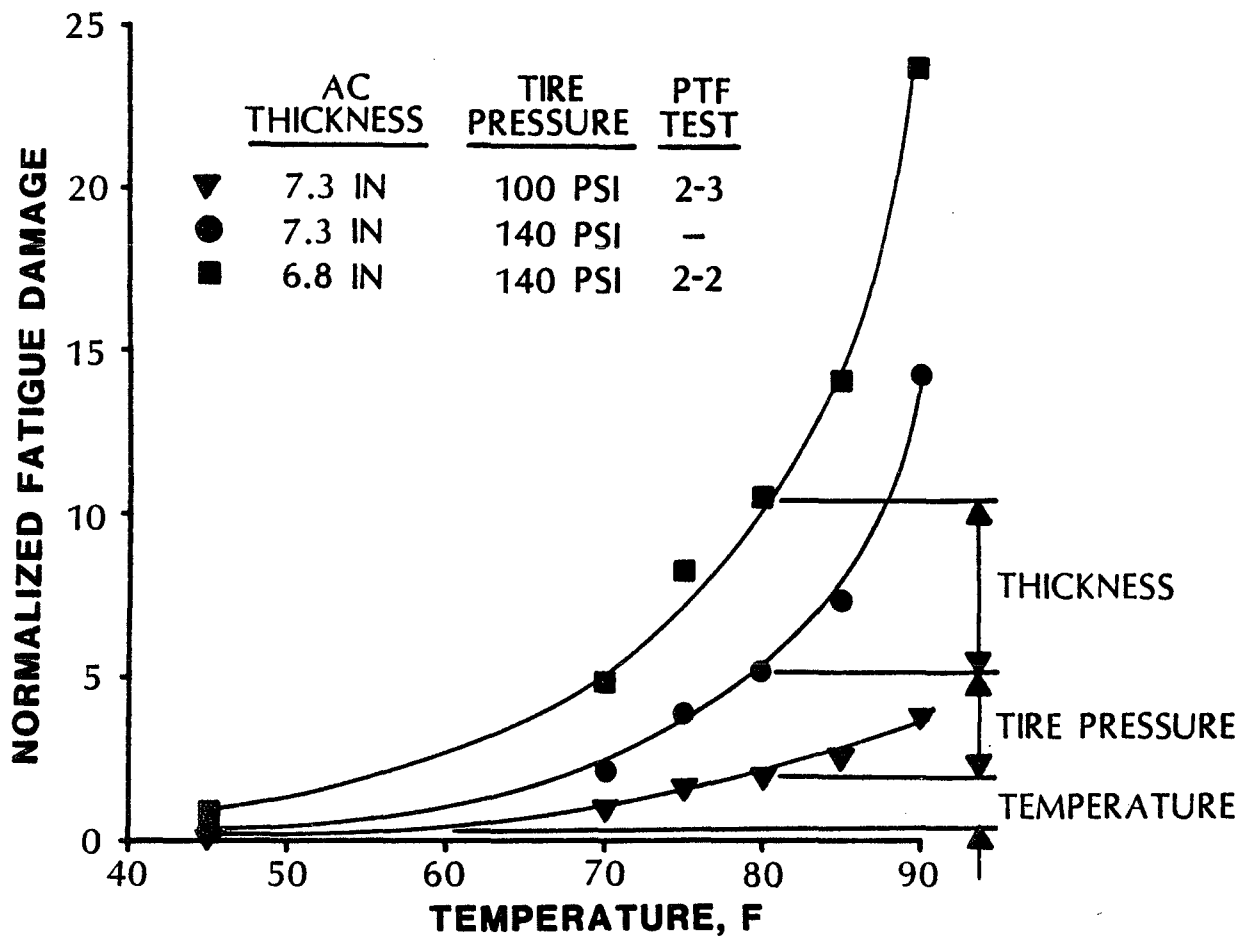


Figure 34. Predicted fatigue damage.

IV. MATERIALS EVALUATION

INTRODUCTION

This chapter presents an evaluation of the effects of tire pressure on the materials used in the PTF test sections. The evaluation is based on tests performed during the postmortem investigations conducted on Tests 2-2 and 2-3. After trafficking each test section to failure, trenches were excavated across the test section as shown in figure 35. Transverse profiles were obtained at the top of the wearing course, the top of the crushed aggregate base course, and the top of the subgrade. The asphalt concrete was cored and air void contents and resilient moduli were measured in the laboratory. In-situ density and moisture content measurements were obtained in the base and the subgrade, and samples of these materials were removed for grain size analyses.

PROFILES

Transverse profiles obtained during the postmortem investigations are shown in figures 36 and 37 for Tests 2-2 and 2-3, respectively. Rut depths at the pavement surface were approximately 0.5 in for both profiles. During construction, grade control for the subgrade and crushed aggregate base was not as precise as that for the asphalt concrete. Some of the variability shown in figures 36 and 37 may, therefore, be the result of initial construction irregularities. With this consideration in mind, it is difficult to discern a rut in the profile for either subgrade. Rutting is evident in both base courses, and for Test 2-3, it appears that all of the rutting occurred in the crushed aggregate base. The profile for Test 2-2 shows rutting occurred in both the asphalt concrete and the crushed aggregate base, with the majority being in the base course.

ASPHALT CONCRETE

The asphalt concrete for Lane 2 was placed in three lifts: two 2.5-in lifts of binder, and one 2-in lift of wearing course. Both the binder and

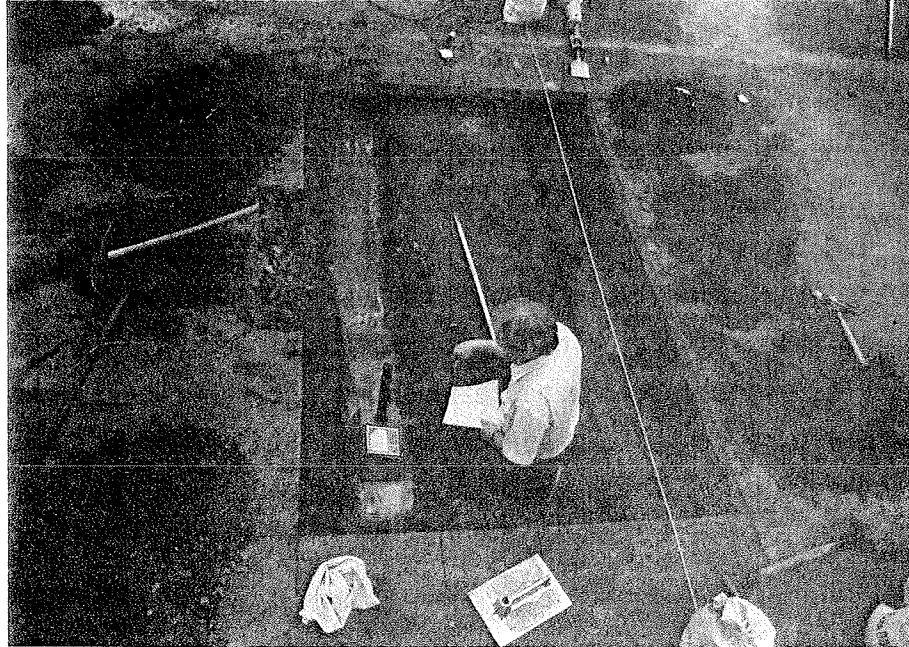


Figure 35. Photograph of postmortem trenching.

wearing course consist of crushed aggregate and AC-20 asphalt cement. Marshall mix design parameters for the two materials are presented in table 13.

During the postmortem investigation, cores were cut from each section at the locations shown in figures 38 and 39. The cores were returned to the laboratory and split into their component layers. The air void content of each core was determined in accordance with ASTM D3203.⁽¹¹⁾ Resilient moduli for selected cores were measured at 41, 77, and 104 °F in accordance with ASTM D4123. The data are presented in tables 35 and 36 of appendix C.

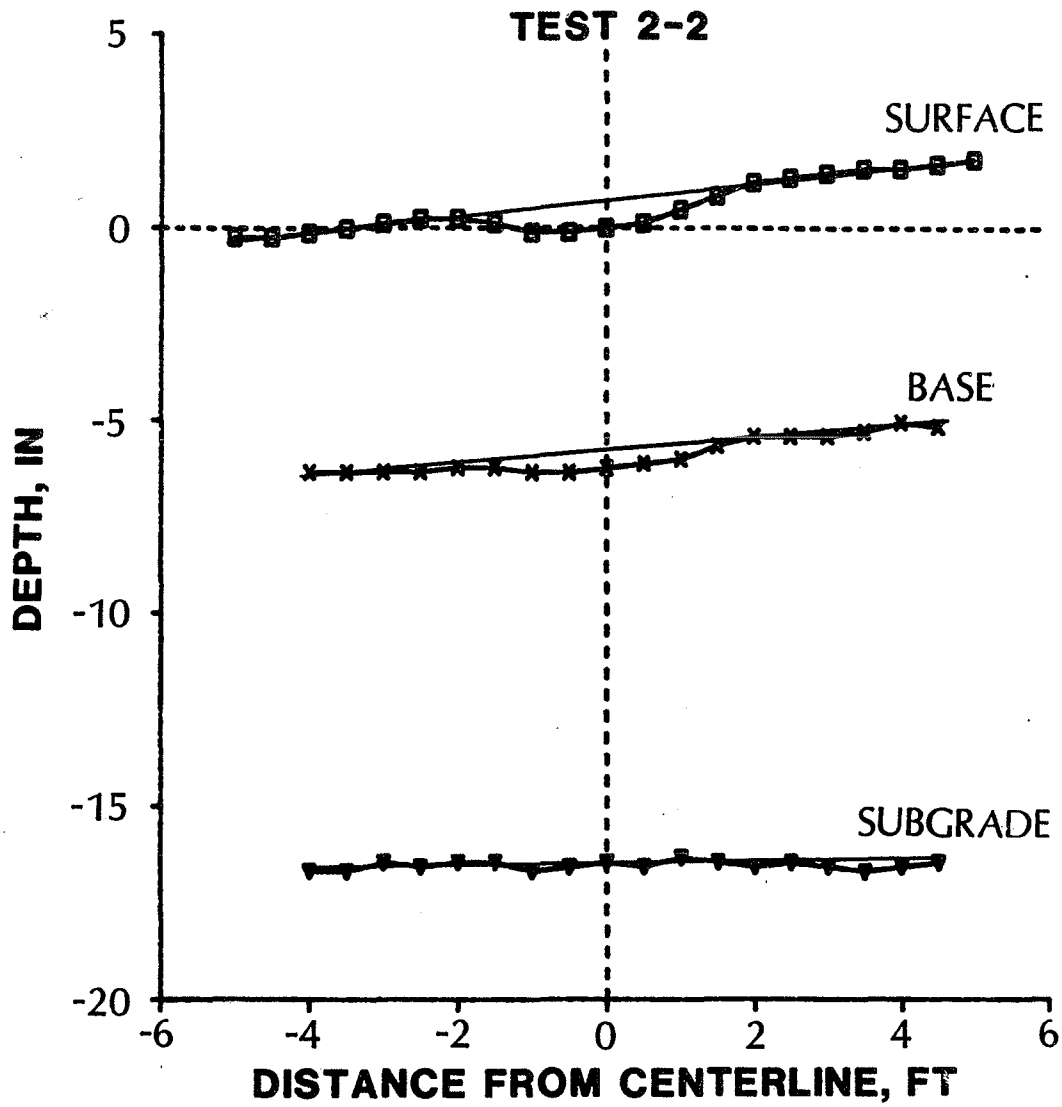


Figure 36. Transverse profile for Test 2-2.

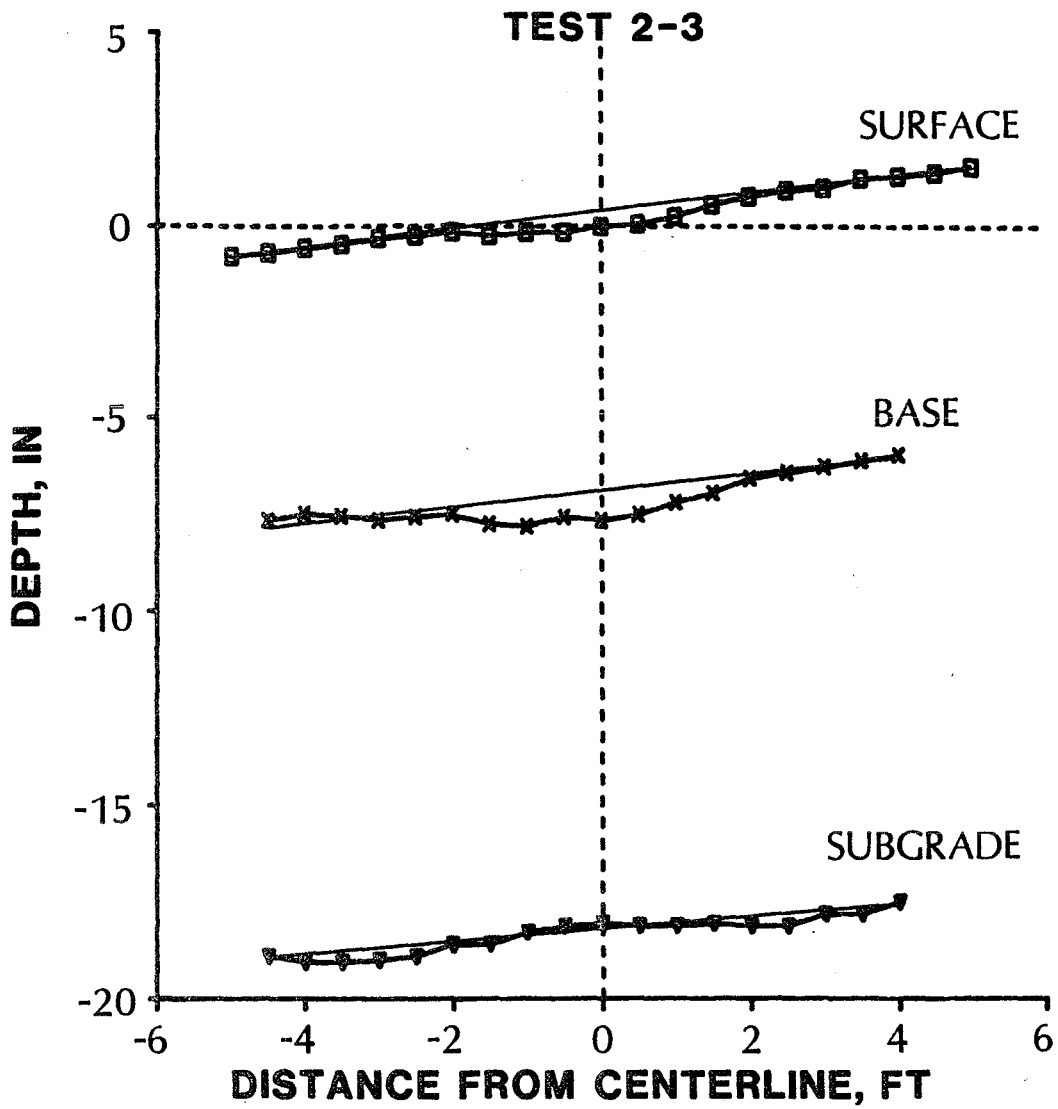


Figure 37. Transverse profile for Test 2-3.

Table 13. Marshall mix design parameters for the PTF asphalt concrete.

Parameter	Wearing Course	Binder Course
Asphalt Content, percent	5.6	4.5
Density, pcf	160	161
Air Voids, percent	1.9	2.6
Stability, lb	3330	4880
Flow, 0.01 in	14	--
Gradation, percent passing		
1.5-in		100.0
1.0		94.8
3/4	100.0	79.0
1/2	99.9	53.9
3/8	94.5	46.7
No. 4	61.6	40.6
8	44.0	34.2
16	33.4	27.1
30	24.6	20.0
50	15.9	12.4
100	11.0	8.3
200	8.5	6.2

Note: Based on samples taken from the paver, and compacted in the laboratory using 75 blows per side at a compaction temperature of 250 °F.

TEST 2-2

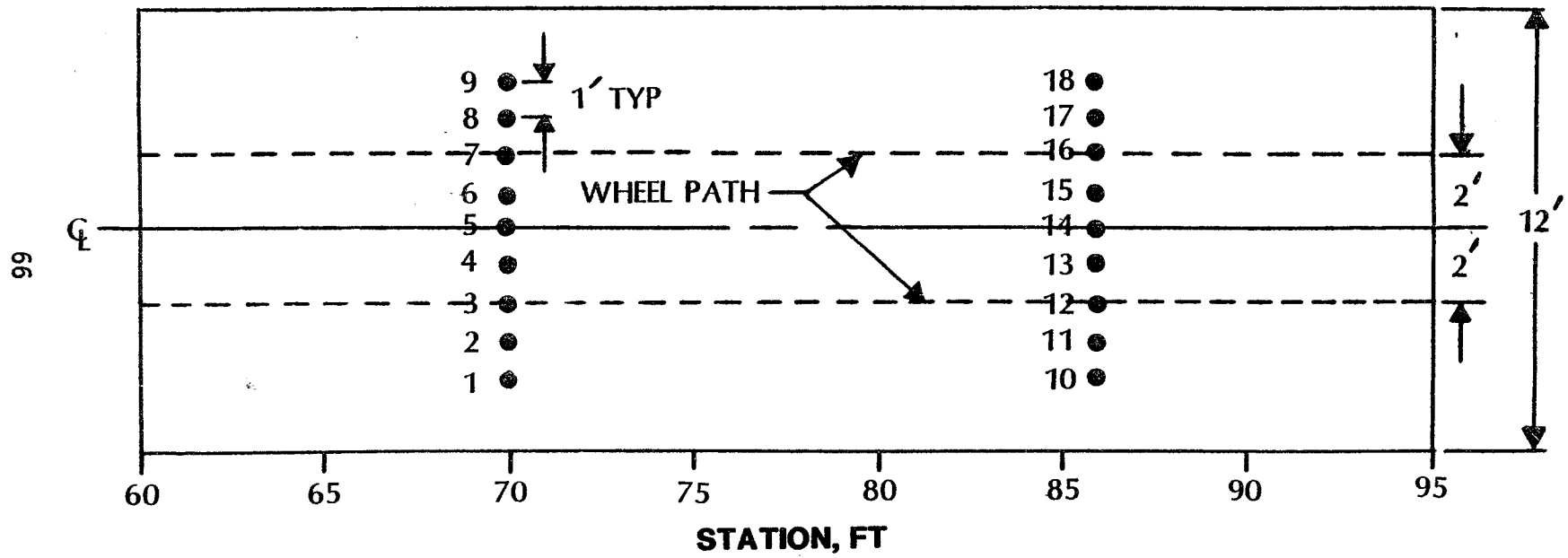


Figure 38. Core locations for Test 2-2.

TEST 2-3

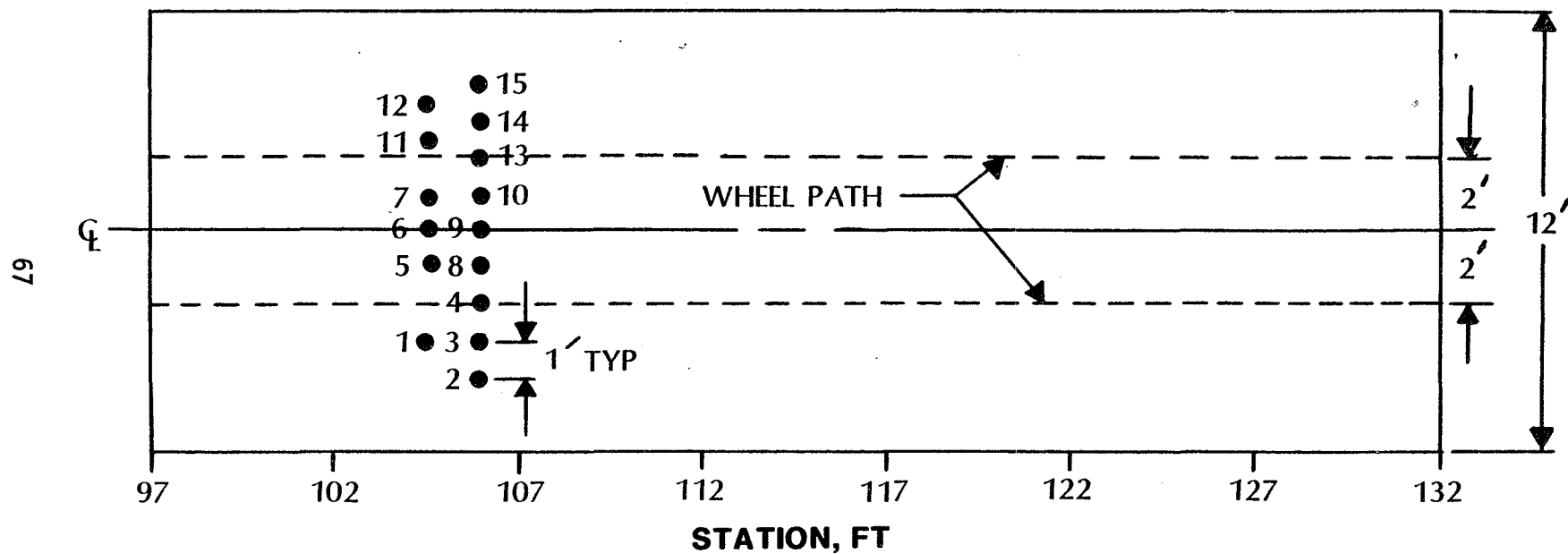


Figure 39. Core locations for Test 2-3.

Average air void contents and resilient moduli for trafficked and untrafficked areas of Tests 2-2 and 2-3 are presented in table 14. Analyses of variance were conducted to determine the significance of the differences shown in table 14. The resilient modulus data, did not show consistent significant differences at the 95 percent confidence level when comparing cores from trafficked versus untrafficked areas or Test 2-2 versus Test 2-3. For air voids, the analyses of variance showed at the 95-percent confidence level that the air void content of the cores in the wheelpath was significantly lower than those out of the wheelpath for all lifts in both sections except the upper binder lift in Test 2-3. For this lift, the air void content in the wheelpath was higher than out of the wheelpath. Additionally, at the 95-percent confidence level, the air void content for surface course and upper binder lift cores from untrafficked areas were significantly higher for Test 2-2 than Test 2-3. The air void content of the lower binder lift was the same for both test sections.

To determine whether densification was greater for the 140 psi test, an analysis of variance was performed on the change in air voids. The change in air voids was obtained by subtracting the corresponding average out of wheelpath air void content from the air void content of each wheelpath core. This analysis indicated at the 95 percent confidence level that the densification in the surface course was the same for both tests, and the densification in the lower binder course was significantly higher for Test 2-2. The analysis could not be conducted for the upper binder layer since the data for Test 2-3 showed an increase in air voids for trafficked areas.

Thus the higher tire pressure did not result in greater densification of the wearing course for Test 2-2 in spite of the higher pavement temperatures and lower initial density. The increased densification in the lower lift of the binder was probably the result of the higher pavement temperatures in Test 2-2. Figure 40 shows the effect of temperature and tire pressure on the vertical compressive stresses within the asphalt layers under the center of one of the dual wheels based on ELSYM5. This figure shows that the effect of temperature on the vertical compressive stresses within the lower lift of

Table 14. Average air void contents and resilient moduli for cores from Tests 2-2 and 2-3.

TEST 2-2

	Surface		Upper Binder		Lower Binder	
	<u>In</u>	<u>Out</u>	<u>In</u>	<u>Out</u>	<u>In</u>	<u>Out</u>
Air Voids, percent	3.95	5.11	4.36	6.23	3.24	4.38
Mr 41 °F, ksi	1600	1700	1780	1760	1970	1810
Mr 77 °F, ksi	216	270	251	295	243	230
Mr 100 °F, ksi	44	54	56	62	43	48

TEST 2-3

	Surface		Upper Binder		Lower Binder	
	<u>In</u>	<u>Out</u>	<u>In</u>	<u>Out</u>	<u>In</u>	<u>Out</u>
Air Voids, percent	3.47	4.47	4.36	2.57	3.95	4.43
Mr 41 °F, ksi	1730	1500	1530	1830	1470	1770
Mr 77 °F, ksi	232	209	186	216	164	208
Mr 100 °F, ksi	45	41	41	42	38	44

binder is greater than the effect of tire pressure. Additionally, asphalt concrete tends to densify more at higher temperatures when the stiffness of the asphalt binder is low.

CRUSHED AGGREGATE BASE

The base course consists of dense graded crushed aggregate with a high amount of fines, approximately 50 percent passing the #8 sieve. The transverse profiles showed the majority of the rutting for Tests 2-2 and 2-3 occurred in the crushed aggregate base course. The results of density tests

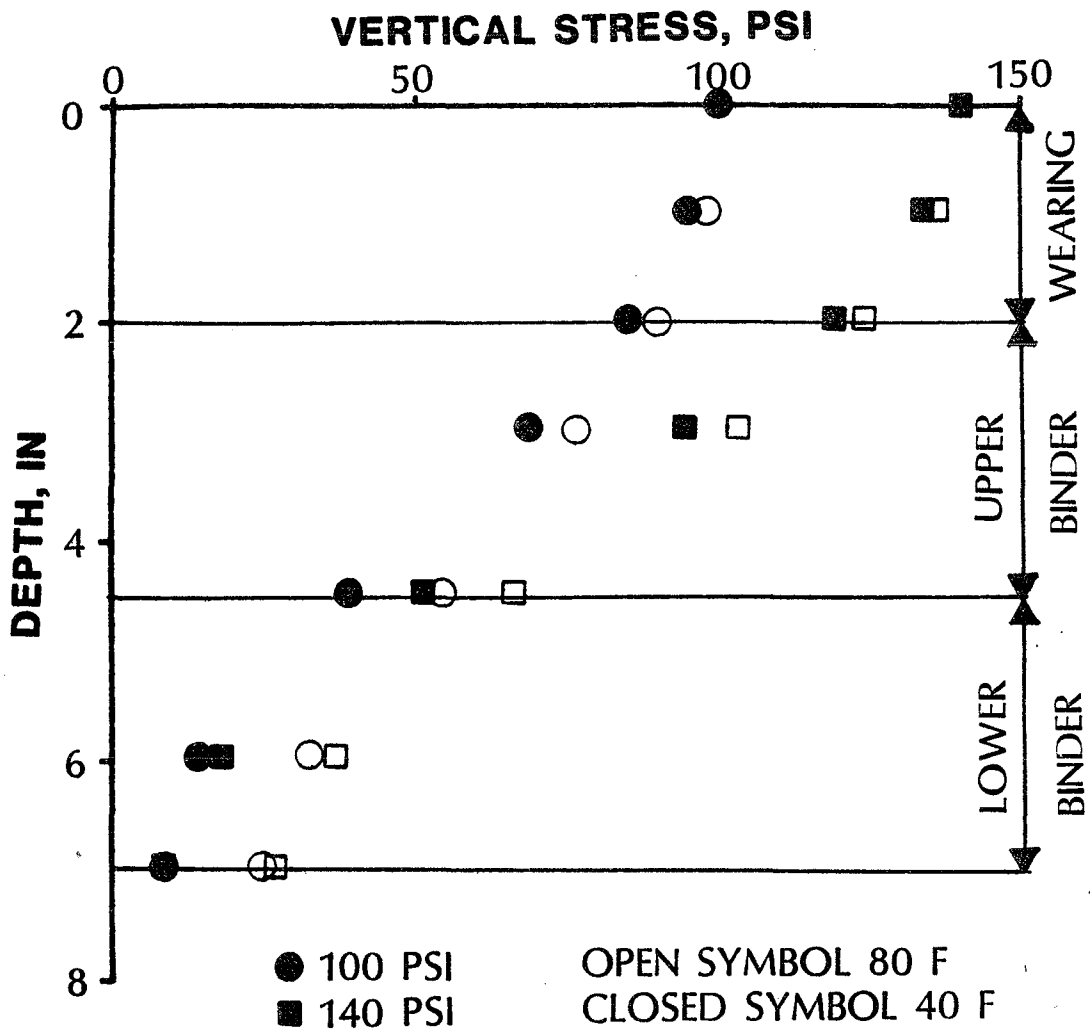


Figure 40. Effects of temperature and tire pressure on vertical compressive stresses based on ELSYM5.

obtained with a nuclear gauge during construction are presented in table 15. The data range from 87 to 102 percent of AASHTO T180 maximum dry density averaging 98 and 96 percent for Tests 2-2 and 2-3, respectively. The nuclear gauge was inoperative during the postmortem investigations; therefore, only a limited number of sand cone density tests were performed in the crushed aggregate base. These data are presented in table 16. Although there are insufficient data for a statistical analysis, it does not appear that excessive densification under traffic occurred in the crushed aggregate base during either test.

The moisture content of the crushed aggregate base was similar for both tests. The moisture content increased from the as-constructed value of 3.1 percent to 5.5 and 4.5 percent for Tests 2-2 and 2-3, respectively.

The gradation of the crushed aggregate base from samples taken in and out of the wheelpath are compared with data obtained during construction in table 17. Although there are differences in the gradation data, these differences are readily attributable to the variability of the material. The data do not support degradation of the base course as a cause of the rutting in either section.

Rutting in dense graded crushed aggregate bases is not uncommon. Pavement engineers have attributed this rutting to a number of factors including increased compaction, saturation, and migration of fines. The results of the tests conducted during the postmortem investigations are inconclusive concerning the cause of the rutting. They do, however, show no difference in the material characteristics of the base course between the 140 and the 100 psi tests.

SUBGRADE

The subgrade classifies as an AASHTO A-4(0) soil. The transverse profiles did not show any rutting in the subgrade for either test. The results of density tests obtained with a nuclear gauge during construction are

Table 15. As-constructed crushed aggregate base course density.

Test Section	Station	Percent of AASHTO T-180 Maximum Dry Density		
		2 ft left	CL	2 ft right
2-2	70	98	98	98
2-2	77	89	99	98
2-2	84	99	102	101
2-3	105	96	96	94
2-3	112	95	87	98
2-3	119	99	97	102

Table 16. Crushed aggregate base course density from postmortem testing.

Test Section	Station	Percent of AASHTO T-180 Maximum Dry Density	
		In Wheelpath	Out of Wheelpath
2-2	79	95	100
2-3	112	93	98

Table 17. Gradation of crushed aggregate base course before and after trafficking.

Sieve	As-Constructed	Test 2-2		Test 2-3	
		In Wheelpath	Out of Wheelpath	In Wheelpath	Out of Wheelpath
1-1/2-in	100	100	100	100	100
1-in	95	95	95	94	96
3/4-in	85	87	85	86	84
1/2-in	75	76	74	73	72
3/8-in	70	70	68	67	66
No. 4	63	59	59	56	56
No. 8	49	47	47	44	44
No. 16	37	38	36	34	34
No. 30	28	28	28	26	26
No. 50	21	21	21	19	19
No. 100	16	16	15	14	14
No. 200	11	11	11	10	10

presented in table 18. The data range from 96 to 105 percent of AASHTO T180 maximum dry density averaging 103 and 98 percent for Tests 2-2 and 2-3, respectively. The results of a limited number of sand cone density tests performed during the postmortem investigations are shown in table 19. As expected, the data do not show densification in either test as a result of trafficking.

Table 18. As-constructed subgrade density.

Test Section	Station	Percent of AASHTO T-180 Maximum Dry Density		
		2 ft left	CL	2 ft right
2-2	70	103	102	103
2-2	77	101	105	102
2-2	84	103	103	104
2-3	105	97	97	100
2-3	112	96	98	98
2-3	119	99	99	99

Table 19. Subgrade density from postmortem testing.

Test Section	Station	Percent of AASHTO T-180 Maximum Dry Density	
		In Wheelpath	Out of Wheelpath
2-2	79	97	97
2-3	112	95	100

The moisture content of the subgrade was similar for both tests. The moisture content increased from the as-constructed value of 10.5 percent to 15.5 and 16.9 percent for Tests 2-2 and 2-3, respectively.

The gradation of subgrade samples taken from the wheelpath are compared with data obtained during construction in table 20. Like the crushed aggregate base, the subgrade did not degrade as a result of trafficking.

It appears that the subgrade was well protected from the effects of traffic loading. The cross-section of Lane 2 provided sufficient protection for the subgrade even under the 19,000-lb dual tire wheel load used in both tests.

Table 20. Gradation of subgrade before and after trafficking.

Sieve	As-Constructed	Test 2-2		Test 2-3	
		In Wheelpath	Out of Wheelpath	In Wheelpath	Out of Wheelpath
3/4-in	98	100	--	100	--
3/8-in	97	98	--	99	--
No. 10	92	96	--	97	--
No. 40	79	85	--	92	--
No. 200	45	48	--	52	--

V. SUMMARY AND CONCLUSIONS

The effects of tire pressure on flexible pavements were evaluated in three ways. First, deflections and strains for various combinations of load and tire pressure were measured and compared. Second, rutting and cracking for two test sections trafficked with the same load but different tire pressures were evaluated. Finally, changes in the pavement materials resulting from traffic were compared for the two sections trafficked with different tire pressures.

The response evaluation showed the measured pavement responses were affected by both load and tire pressure. For the loads and tire pressures used in the evaluation, the effect of load was greater than the effect of tire pressure. The measured responses doubled for an increase in load from 9,400 to 19,000 lb, while increasing tire pressure from 76 psi to 140 psi resulted in less than a 10-percent increase in the measured responses.

Fatigue equivalency factors were developed to evaluate the effects of load and tire pressure on fatigue cracking. The factors were based on an exponential relationship between the number of cycles to failure and the magnitude of the tensile strain at the bottom of the asphalt layer. For the pavement sections and environmental conditions studied, increasing tire pressure from 76 to 140 psi, increased the expected fatigue damage less than 30 percent. However, increasing the load from 9,400 to 14,100 lb increased the expected fatigue damage 350 to 650 percent.

The performance evaluation showed increased rutting and cracking for the test section trafficked with the 140 psi tire pressure. This section was, however, thinner and was trafficked at a higher temperature than the 100 psi test section. An analysis of pavement strains using layer theory showed the increased rutting resulted mainly from the higher temperature during the 140 psi test. A similar analysis showed the increased cracking resulted mainly from the combined effects of higher temperature and thinner pavement structure for the 140 psi test.

For the pavement sections studied, the strains associated with rutting increased with increasing temperature. At high temperatures, these strains were further increased by high tire pressure. Also, damage predicted by classical fatigue models increased with increasing temperature, increasing tire pressure, and decreasing thickness.

The materials evaluation showed little difference in the characteristics of the subgrade, crushed aggregate base, and asphalt concrete between the sections trafficked with 100 psi and 140 psi tire pressure. The results of trenching after trafficking the sections to failure showed the pavement structure of Lane 2 provided sufficient protection for the subgrade even under the 19,000-lb dual tire wheel load used in both tests. The majority of the rutting in both test sections occurred in the crushed aggregate base layer. The asphalt concrete in both tests showed densification in the wheelpaths as a result of the traffic loading. The higher tire pressure did not result in greater densification of the wearing course in spite of the higher pavement temperatures and lower initial density for the 140 psi test. Both test sections showed an air void content decrease of 1.0 percent for the wearing course. The binder course in the 140 psi test showed an air void content decrease of 1 percent while the 100 psi test showed a decrease of only 0.5 percent. Based on stresses from a layered elastic analysis, this increased densification in the lower part of the asphalt pavement was attributed to the higher pavement temperatures for the 140 psi test.

Thus the data concerning the effects of tire pressure on flexible pavements collected during the first phase of research at the PTF show tire pressure to be a second order effect. The effect of tire pressure on flexible pavement response and performance is less significant than the effects of load and temperature. During the response experiment, when temperature and load were constant, the effects of tire pressure could be observed. However, during the performance and materials evaluations, the effects of increased tire pressure were masked by differences in temperature.

VI. REFERENCES

1. K. M. Marshek, H. H. Chen, R. B. Connell, and C. L. Saraf, "Effects of Truck Tire Inflation Pressure and Axle Loads on Flexible and Rigid Pavement Performance," Transportation Research Record 1070, 1986.
2. H. F. Southgate and R. L. Dean, Effects of Load Distributions and Axle and Tire Configurations on Pavement Fatigue, Research Report UKTRP-85-13, Kentucky Transportation Research Program, University of Kentucky, 1985.
3. F. L. Roberts, J. T. Tielking, D. Middleton, R. L. Lytton, and K. Tseng, Effects of Tire Pressure in Flexible Pavements, Research Report 372-1F, Texas Transportation Institute, Texas A&M University, 1986.
4. Road and Bridge Specifications, July 1, 1982, Virginia Department of Highways and Transportation, Richmond, VA, 1982.
5. D. A. Anderson, W. P. Kilareski, and Z. Siddiqui, Pavement Testing Facility - Design and Construction, Report No. FHWA-RD-88-059, Federal Highway Administration, Washington, D. C., 1987.
6. H. K. Berry, and R. C. Panuska, Manufacture of an Accelerated Loading Facility (Alf), Executive Summary, Report No. FHWA/RD-87/071, Federal Highway Administration, Washington, D.C., 1987.
7. D. A. Anderson, P. Sebaaly, N. Tabatabae, R. Bonaquist, and C. Churilla, Pavement Testing Facility -Performance of the Initial Two Test Sections, Report No. FHWA-RD-88-060, Federal Highway Administration, Washington, D. C., 1987.
8. Organization for Economic Cooperation and Development, Strain Measurements in Bituminous layers, Paris, 1985.

9. F. Finn, C. L. Saraf, R. Kulkarni, K. Nair, W. Smith, and A. Abdullah, "Development of Pavement Structural Subsystems, National Cooperative Highway Research Program Report 291, National Research Council, Washington, D. C., 1986.
10. P. Sebaaly, N. Tabatatbaee, R. Bonaquist, and D. Anderson, Evaluating Structural Damage of Flexible Pavements Using Cracking and FWD Data, Paper presented at the Transportation Research Board Annual Meeting, January, 1989.
11. Annual Book of ASTM Standards, Volume 4.03, Road and Paving Materials; Traveled Surface Characteristics, American Society for Testing Materials, Philadelphia, PA, 1987.

Table 21. Manufacturer tire data.

TIRE	PLY	OVERALL DIA. (in)	OVERALL WIDTH (in)	LOADED RADIUS (in)	DUAL WHEEL RATED LOAD (lbs)						
					70 (psi)	75 (psi)	80 (psi)	85 (psi)	90 (psi)	95 (psi)	100 (psi)
MICHELIN 11-R22.5	16	41.4	10.7	19.3	3990	4225	4455	4690	4920	5180	5440
KELLY SPRINGFIELD 10-22.5	10	40.4	10.0	18.9	4040	---	---	---	---	---	---

Table 22. Tire contact areas.

TIRE TYPE	LOAD (kips)	TIRE PRESSURE (psi.)	LEFT AVERAGE AREA (sq. in.)	RIGHT AVERAGE AREA (sq. in.)	TOTAL AVERAGE AREA (sq. in.)	CALCULATED AREA (sq. in.)
RADIAL	9.4	76	69.25	75.01	144.26	123.68
RADIAL	9.4	108	56.29	62.91	119.20	87.04
RADIAL	9.4	140	49.04	55.44	104.48	67.14
RADIAL	14.1	76	96.14	100.64	196.78	185.53
RADIAL	14.1	108	84.91	90.68	175.59	130.56
RADIAL	14.1	140	72.91	76.21	149.12	100.71
RADIAL	19.0	76	116.43	119.18	235.61	250.00
RADIAL	19.0	108	101.27	102.65	203.92	175.93
RADIAL	19.0	140	91.44	90.51	181.95	135.71
BIAS PLY	9.4	76	74.62	77.27	151.89	123.68
BIAS PLY	9.4	108	64.24	68.95	133.19	87.04
BIAS PLY	9.4	140	58.98	63.41	122.39	67.14
BIAS PLY	14.1	76	96.37	102.05	198.42	185.53
BIAS PLY	14.1	108	77.95	81.72	159.67	130.56
BIAS PLY	14.1	140	76.81	81.68	158.49	100.71
BIAS PLY	19.0	76	117.52	120.38	237.90	250.00
BIAS PLY	19.0	108	100.94	105.1	206.04	175.93
BIAS PLY	19.0	140	93.60	92.38	185.98	135.71

Table 23. Calculated pavement responses at the instrument locations for Lane 1 with the wheels in the -14.75-in offset position.

LOAD (lb)	TIRE PRESSURE (psi)	DEFLECTION (0.001 in)	STRAIN, MICROINCHES						
			SURFACE					BINDER	
			GAUGE 1	GAUGE 2	GAUGE 3	GAUGE 4	GAUGE 5	GAUGE 22	GAUGE 19
9,400	76	6.2	17.3	14.2	8.6	18.8	-36.6	34.1	34.1
9,400	108	6.2	17.5	14.4	8.8	19.2	-36.7	34.2	34.2
9,400	140	6.2	17.9	14.5	9.3	19.4	-36.8	34.4	34.4
14,100	76	9.2	25.4	20.5	11.2	28.1	-54.6	50.9	50.9
14,100	108	9.2	26.0	21.1	12.7	28.2	-54.8	51.1	51.1
14,100	140	9.2	26.0	21.6	12.9	28.6	-55.0	51.3	51.3
19,000	76	12.5	33.4	25.8	12.9	37.1	-73.2	68.2	68.2
19,000	108	12.5	34.5	27.7	15.2	37.9	-73.6	68.7	68.7
19,000	140	12.5	35.0	28.3	16.9	37.9	-73.9	68.9	68.9

Note: "-" denotes compression.

Table 24. Calculated pavement responses at the instrument locations for Lane 1 with the wheels in the 0-in offset position.

			STRAIN, MICROINCHES						
			SURFACE				BINDER		
LOAD (lb)	TIRE PRESSURE (psi)	DEFLECTION (0.001 in)	GAUGE 1	GAUGE 2	GAUGE 3	GAUGE 4	GAUGE 5	GAUGE 22	GAUGE 19
			9,400	76	8.7	-40.0	-79.5	-85.0	-16.4
9,400	108	8.7	-36.6	-85.6	-61.0	-15.2	-105.8	106.3	106.3
9,400	140	8.7	-36.1	-90.5	-95.6	-14.4	-107.1	108.5	108.5
14,100	76	13.1	-78.3	-108.2	-116.9	-27.2	-145.3	145.4	145.4
14,100	108	13.1	-76.4	-117.7	-125.8	-24.7	-154.1	152.8	152.8
14,100	140	13.1	-54.0	-124.0	-132.5	-23.4	-157.2	157.2	157.2
19,000	76	17.6	-101.1	-135.5	-147.8	-39.5	-185.6	185.5	185.5
19,000	108	17.6	-107.5	-147.8	-159.6	-35.7	-197.9	197.9	197.9
19,000	140	17.6	-113.2	-157.4	-168.3	-33.9	-206.7	205.2	205.2

Note: "-" denotes compression.

Table 25. Calculated pavement responses at the instrument locations for Lane 1 with the wheels in the +14.75-in offset position.

			STRAIN, MICROINCHES						
			SURFACE				BINDER		
LOAD (lb)	TIRE PRESSURE (psi)	DEFLECTION (0.001 in)	GAUGE 1	GAUGE 2	GAUGE 3	GAUGE 4	GAUGE 5	GAUGE 22	GAUGE 19
9,400	76	12.8	-53.5	-84.2	-80.6	-51.2	-125.1	125.4	125.4
9,400	108	12.8	-52.6	-90.2	-87.2	-49.4	-127.7	129.3	129.3
9,400	140	12.8	-52.1	-95.0	-92.0	-48.1	-129.1	131.4	131.4
14,100	76	19.2	-106.5	-116.8	-109.9	-81.0	-178.3	179.1	179.1
14,100	108	19.2	-78.4	-125.0	-120.0	-77.4	-186.9	187.1	187.1
14,100	140	19.2	-80.6	-132.2	-126.3	-75.2	-190.0	192.0	192.0
19,000	76	25.9	-139.7	-144.8	-137.3	-113.4	-228.5	229.7	229.7
19,000	108	25.9	-142.3	-159.3	-150.1	-108.5	-242.3	243.2	243.2
19,000	140	25.9	-112.0	-167.3	-159.9	-104.9	-251.2	251.0	251.0

Note: "-" denotes compression.

Table 26. Calculated pavement responses at the instrument locations for Lane 2 with the wheels in the -14.75-in offset position.

			STRAIN, MICROINCHES						
			SURFACE				BINDER		
LOAD	TIRE PRESSURE	DEFLECTION	GAUGE 1	GAUGE 2	GAUGE 3	GAUGE 4	GAUGE 5	GAUGE 16	GAUGE 14
(lb)	(psi)	(0.001 in)							
9,400	76	6.0	46.0	47.0	43.5	42.4	-65.8	288.0	43.2
9,400	108	6.0	46.0	47.0	42.5	44.7	-65.9	300.4	43.3
9,400	140	6.0	48.5	46.8	44.9	45.0	-66.0	307.5	43.4
14,100	76	9.0	68.4	69.4	59.1	65.3	-98.2	403.3	64.6
14,100	108	9.0	69.5	69.8	64.9	63.5	-98.6	428.7	64.8
14,100	140	9.0	67.8	71.7	62.9	65.6	-98.8	443.6	64.9
19,000	76	12.1	90.7	86.6	72.5	85.8	-131.8	507.4	86.8
19,000	108	12.1	92.9	93.6	79.6	87.6	-132.5	549.2	87.2
19,000	140	12.1	94.0	93.4	86.5	85.5	-132.8	574.3	87.4

Note: "-" denotes compression.

Table 27. Calculated pavement responses at the instrument locations for Lane 2 with the wheels in the 0-in offset position.

			STRAIN, MICROINCHES						
			SURFACE				BINDER		
LOAD	TIRE PRESSURE	DEFLECTION	GAUGE 1	GAUGE 2	GAUGE 3	GAUGE 4	GAUGE 5	GAUGE 16	GAUGE 14
(lb)	(psi)	(0.001 in)							
9,400	76	8.3	-31.3	-211.9	-218.1	4.9	-271.9	228.2	228.2
9,400	108	8.3	-45.6	-252.0	-257.8	7.6	-276.7	240.3	240.3
9,400	140	8.3	-1.6	-289.9	-293.5	9.9	-279.6	247.2	247.2
14,100	76	12.4	-200.2	-261.7	-274.0	.3	-357.3	314.9	314.9
14,100	108	12.4	-187.8	-310.0	-318.4	7.4	-403.3	339.0	339.0
14,100	140	12.4	.7	-347.9	-360.0	10.0	-412.5	353.4	353.4
19,000	76	16.7	-240.7	-311.1	-328.5	-4.9	-437.0	391.3	391.3
19,000	108	16.7	-284.3	-361.4	-377.9	5.5	-489.9	429.7	429.7
19,000	140	16.7	-332.7	-410.0	-421.0	7.5	-536.4	453.6	453.6

Note: "-" denotes compression.

Table 28. Calculated pavement responses at the instrument locations for Lane 2 with the wheels in the +14.75-in offset position.

			STRAIN, MICROINCHES						
			SURFACE				BINDER		
LOAD (lb)	TIRE PRESSURE (psi)	DEFLECTION (0.001 in)	GAUGE 1	GAUGE 2	GAUGE 3	GAUGE 4	GAUGE 5	GAUGE 16	GAUGE 14
9,400	76	12.5	-24.2	-214.7	-212.9	-44.9	-323.5	43.2	288.0
9,400	108	12.5	-21.4	-254.9	-255.9	-41.2	-329.6	43.3	300.4
9,400	140	12.5	-21.0	-293.2	-292.2	-37.5	-332.9	43.4	307.5
14,100	76	18.7	-245.0	-272.5	-264.6	-75.8	-445.2	64.6	403.3
14,100	108	18.7	-19.5	-313.9	-312.6	-68.6	-484.1	64.8	428.7
14,100	140	18.7	-43.1	-360.8	-352.2	-64.4	-490.9	64.9	443.6
19,000	76	25.2	-294.6	-327.0	-313.7	-108.9	-551.5	86.8	507.4
19,000	108	25.2	-321.7	-377.3	-366.3	-102.0	-609.0	87.2	549.2
19,000	140	25.2	-78.0	-416.5	-414.7	-94.2	-650.8	87.4	574.3

Note: "-" denotes compression.

Table 29. Measured pavement responses for Lane 1 with the wheels in the -14.75-in offset position.

TIRE TYPE	LOAD (lb)	TIRE PRESSURE (psi)	AVERAGE TIRE PAVEMENT TEMP (F)	PARALLEL LVDT (0.001 in)	CANTILEVER LVDT (0.001 in)	STRAIN, MICROINCHES						
						SURFACE			BINDER			
						GAUGE 1	GAUGE 2	GAUGE 3	GAUGE 4	GAUGE 5	GAUGE 22	GAUGE 19
RADIAL	9,400	76	41.9	2.6	2.8					-97.2	83.8	92.7
RADIAL	9,400	108	42.0	2.0	2.4					-79.7	50.9	86.6
RADIAL	9,400	140	42.0	2.6	3.1					-127.3	79.4	45.5
RADIAL	14,100	76	40.9	4.1	4.4					-152.2	111.6	130.5
RADIAL	14,100	108	40.4	4.4	4.6					-163.8	120.4	117.1
RADIAL	14,100	140	40.6	4.3	5.1					-166.2	127.4	120.3
RADIAL	19,000	76	39.6	6.0	7.1	104.4			138.1	-220.8	158.0	166.7
RADIAL	19,000	108	39.2	6.1	7.0	104.9			134.2	-214.6	158.6	172.5
RADIAL	19,000	140	39.3	5.9	6.8	103.7			133.4	-214.0	161.6	170.3
BIAS PLY	9,400	76	39.7	1.9	2.6		39.4		65.4	-92.4		79.4
BIAS PLY	9,400	108	39.0	2.6	3.4		52.0		81.9	-117.8		47.5
BIAS PLY	9,400	140	38.7	2.3	4.0		44.3		71.0	-92.2		69.8
BIAS PLY	14,100	76	39.0	4.4	4.9				106.4	-161.6		119.5
BIAS PLY	14,100	108	38.8	3.6	4.9				100.9	-157.0		128.2
BIAS PLY	14,100	140	38.8	2.5	4.8				95.1	-152.4		119.4
BIAS PLY	19,000	76	38.0	5.9	7.0				133.4	-208.2	139.0	141.5
BIAS PLY	19,000	108	38.3	5.7	7.0				132.8	-210.6	142.7	170.5
BIAS PLY	19,000	140	38.6	5.6	6.8				128.7	-210.6		167.1
RADIAL *	14,100	76	37.9	3.9	4.7				99.4	-200.2		132.3
RADIAL *	14,100	108	38.2	4.2	5.1				107.4	-168.1		122.6
RADIAL *	14,100	140	38.6	4.1	5.0				106.6	-166.5	106.0	133.3

Note: "*" denotes repeat tests.

"-" denotes compression.

Table 30. Measured pavement responses for Lane 1 with the wheels in the 0-in offset position.

TIRE TYPE	LOAD (lb)	TIRE PRESSURE (psi)	AVERAGE PAVEMENT TEMP (F)	PARALLEL LVDT (0.001 in)	CANTILEVER LVDT (0.001 in)	STRAIN, MICROINCHES						
						SURFACE			BINDER			
						GAUGE 1	GAUGE 2	GAUGE 3	GAUGE 4	GAUGE 5	GAUGE 22	GAUGE 19
RADIAL	9,400	76	41.8	5.5	5.7	-230.0			-167.0		154.0	180.0
RADIAL	9,400	108	41.8	4.0	4.4	-170.2			-213.9		109.7	166.9
RADIAL	9,400	140	42.0	5.9	5.6	-305.6			-312.3		174.0	90.2
RADIAL	14,100	76	40.6	8.4	8.2	-396.6			-332.2		200.2	250.2
RADIAL	14,100	108	40.6	9.0	8.6	-480.6			-384.0		229.9	233.9
RADIAL	14,100	140	40.8	8.8	8.2	-306.8			-398.6		247.4	240.2
RADIAL	19,000	76	39.3	12.4	14.8	-238.7	-461.4		-454.9		255.6	302.7
RADIAL	19,000	108	39.2	16.7	14.2	-216.6	-441.8		-467.4		285.3	322.3
RADIAL	19,000	140	39.2	11.1	13.1	-175.7	-433.8		-449.6		312.5	320.0
BIAS PLY	9,400	76	39.5	4.1	5.4	-67.2	-193.8		-38.2	-92.4		141.2
BIAS PLY	9,400	108	38.9	4.9	7.4	-90.4	-292.2		-33.8	-117.8		105.6
BIAS PLY	9,400	140	38.8	5.0	7.6	-111.5	-289.1		-38.6	-92.2		151.4
BIAS PLY	14,100	76	39.1	8.1	10.3	-135.0	-366.8		-64.8	-161.6		214.4
BIAS PLY	14,100	108	38.7	6.8	10.3	-128.9	-376.5		-55.9	-157.0		237.8
BIAS PLY	14,100	140	38.8	4.6	9.7	-115.6	-335.6		-54.0	-152.4		218.4
BIAS PLY	19,000	76	37.8	12.0	14.8	-183.4	-496.5		-83.0	-208.2		309.6
BIAS PLY	19,000	108	38.5	11.8	14.6	-185.4	-505.1		-83.8	-210.6		320.8
BIAS PLY	19,000	140	38.7	11.2	13.8	-170.8	-482.7		-79.7	-210.6		321.3
RADIAL *	14,100	76	37.8	8.1	9.4	-151.0	-296.7		-64.2	-325.2		239.0
RADIAL *	14,100	108	38.3	8.7	10.6	-160.6	-334.0		-65.0	-375.9		230.4
RADIAL *	14,100	140	39.0	8.6	10.6	-164.8	-353.4		-65.1	-370.0		257.5

Note: "*" denotes repeat tests.

"-" denotes compression.

Table 31. Measured pavement responses for Lane 1 with the wheels in the +14.75-in offset position.

TIRE TYPE	LOAD (lb)	TIRE PRESSURE (psi)	AVERAGE PAVEMENT TEMP (F)	PARALLEL LVDT (0.001 in)	CANTILEVER LVDT (0.001 in)	STRAIN, MICROINCHES						
						SURFACE			BINDER			
						GAUGE 1	GAUGE 2	GAUGE 3	GAUGE 4	GAUGE 5	GAUGE 22	GAUGE 19
RADIAL	9,400	76	41.8	11.3	8.2	-230.6			-264.8	169.0	212.0	
RADIAL	9,400	108	42.0	8.7	8.1	-152.0			-233.0	129.2	194.2	
RADIAL	9,400	140	42.1	12.4	10.9	-200.6			-348.0	195.0	110.6	
RADIAL	14,100	76	40.7	16.0	14.6	-233.0			-380.8	213.5	291.5	
RADIAL	14,100	108	40.4	16.9	15.1	-348.8			-429.8	250.2	267.4	
RADIAL	14,100	140	40.8	17.4	15.7	-293.8			-447.0	270.2	283.6	
RADIAL	19,000	76	39.4	22.2	26.8	-313.9	-513.9		-349.7	-528.0	271.2	351.4
RADIAL	19,000	108	39.4	21.7	26.6	-310.2	-509.6		-344.1	-542.7	309.9	377.3
RADIAL	19,000	140	39.3	20.7	25.3	-305.9	-513.7		-329.6	-542.1	339.4	381.2
BIAS PLY	9,400	76	39.5	8.3	10.8	-130.6	-209.5		-148.4	-277.4		159.0
BIAS PLY	9,400	108	38.9	10.2	14.1	-160.8	-279.2		-178.9	-329.3		122.8
BIAS PLY	9,400	140	38.7	9.6	14.1	-148.5	-275.9		-167.6	-232.8		184.8
BIAS PLY	14,100	76	39.0	14.8	18.7	-219.2	-374.3		-253.0	-423.2		249.4
BIAS PLY	14,100	108	38.8	13.6	18.9	-221.0	-380.1		-241.5	-428.1		276.8
BIAS PLY	14,100	140	38.8	9.3	19.0	-226.3	-371.6		-248.6	-433.6		256.8
BIAS PLY	19,000	76	38.0	22.1	26.4	-292.2	-506.0		-322.5	-519.4		362.7
BIAS PLY	19,000	108	38.6	21.6	26.3	-295.5	-486.8		-320.6	-547.4		373.5
BIAS PLY	19,000	140	38.5	21.1	26.3	-297.9	-519.0		-330.9	-563.8		375.1
RADIAL *	14,100	76	38.0	15.4	16.9	-215.5	-348.9		-235.6	-380.2		278.5
RADIAL *	14,100	108	38.3	16.5	18.1	-235.1	-388.3		-265.4	-435.6		269.0
RADIAL *	14,100	140	38.8	16.3	18.4	-237.6	-406.2		-265.7	-438.5		295.9

Note: "*" denotes repeat tests.

"-" denotes compression.

Table 32. Measured pavement responses for Lane 2 with the wheels in the -14.75-in offset position.

TIRE TYPE	LOAD (lb)	TIRE PRESSURE (psi)	AVERAGE PAVEMENT TEMP (F)	PARALLEL CANTILEVER LVDT (0.001 in)		STRAIN, MICROINCHES					
						SURFACE			BINDER		
						GAUGE 1	GAUGE 2	GAUGE 3	GAUGE 4	GAUGE 5	GAUGE 16
RADIAL	9,400	76	82.9				104.7			371.0	102.5
RADIAL	9,400	108	81.7				95.4			338.8	94.0
RADIAL	9,400	140	82.2				101.9			323.4	97.1
RADIAL	14,100	76	79.2				140.6			544.0	171.8
RADIAL	14,100	108	78.4				144.7			558.5	175.0
RADIAL	14,100	140	78.8				148.3			609.8	184.1
RADIAL	19,000	76	78.6				207.3			706.4	
RADIAL	19,000	108	78.3				185.5			731.2	232.6
RADIAL	19,000	140	78.4				197.8			765.5	231.3
BIAS PLY	9,400	76	85.6					153.8	138.2	-100.5	108.5
BIAS PLY	9,400	108	86.5					138.2	129.8	-96.6	90.5
BIAS PLY	9,400	140	82.9						128.9	-101.5	98.8
BIAS PLY	14,100	76	85.6						229.2	-221.8	183.9
BIAS PLY	14,100	108	84.9						237.0	-188.6	194.0
BIAS PLY	14,100	140	85.1						244.3	-187.3	212.6
BIAS PLY	19,000	76	88.5						350.7	-254.9	227.4
BIAS PLY	19,000	108	88.0						336.9	-334.5	238.7
BIAS PLY	19,000	140	89.4						337.8	-224.4	234.8
RADIAL *	19,000	76									
RADIAL *	19,000	108									
RADIAL *	19,000	140									

Note: "**" denotes repeat tests.

"-" denotes compression.

Table 33. Measured pavement responses for Lane 2 with the wheels in the 0-in offset position.

TIRE TYPE	LOAD (lb)	TIRE PRESSURE (psi)	AVERAGE PAVEMENT TEMP (F)	PARALLEL LVDT (0.001 in)	CANTILEVER LVDT (0.001 in)	STRAIN, MICROINCHES					
						SURFACE		BINDER			
						GAUGE 1	GAUGE 2	GAUGE 3	GAUGE 4	GAUGE 5	GAUGE 16
RADIAL	9,400	76	82.8			-346.5		-103.8		280.3	335.5
RADIAL	9,400	108	81.9			-319.1		-92.1		247.0	310.7
RADIAL	9,400	140	82.2			-317.2		-96.6		231.7	303.5
RADIAL	14,100	76	79.2			-483.8		-179.7		414.8	487.9
RADIAL	14,100	108	78.4					-132.8			475.3
RADIAL	14,100	140	79.0			-504.0		-138.4		498.8	532.5
RADIAL	19,000	76	78.6					-180.3		562.2	587.5
RADIAL	19,000	108	78.4					-176.3		580.5	611.1
RADIAL	19,000	140	78.3					-182.8		590.6	635.9
BIAS PLY	9,400	76	85.5			-576.2		-101.1			344.2
BIAS PLY	9,400	108	87.1			-463.4		-112.5			319.4
BIAS PLY	9,400	140	83.3					-104.3	-362.5		358.0
BIAS PLY	14,100	76	85.8					-171.4			552.0
BIAS PLY	14,100	108	84.7					-172.3	-533.5		587.2
BIAS PLY	14,100	140	85.5					-186.9			526.7
BIAS PLY	19,000	76	88.7					-276.3	-430.9		752.3
BIAS PLY	19,000	108	88.0					-236.7	-676.2		776.8
BIAS PLY	19,000	140	89.8						-507.4		797.3
RADIAL *	19,000	76									
RADIAL *	19,000	108									
RADIAL *	19,000	140									

Note: "*" denotes repeat tests.

"-" denotes compression.

Table 34. Measured pavement responses for Lane 2 with the wheels in the +14.75-in offset position.

TIRE TYPE	LOAD (lb)	TIRE PRESSURE (psi)	AVERAGE PAVEMENT TEMP (F)	PARALLEL LVDT (0.001 in)	CANTILEVER LVDT (0.001 in)	STRAIN, MICROINCHES					
						SURFACE			BINDER		
						GAUGE 1	GAUGE 2	GAUGE 3	GAUGE 4	GAUGE 5	GAUGE 16
RADIAL	9,400	76	82.9	5.6	-306.5	-224.3				99.2	330.8
RADIAL	9,400	108	81.7		-286.8	-213.8				93.4	286.9
RADIAL	9,400	140	82.2	6.6	-259.0	-248.8				92.7	306.9
RADIAL	14,100	76	79.2		-499.5	-351.1				174.5	507.9
RADIAL	14,100	108	78.4		-455.7	-343.2				166.8	503.5
RADIAL	14,100	140	78.8		-503.0	-367.1				185.7	553.0
RADIAL	19,000	76	78.6			-527.5				236.0	663.5
RADIAL	19,000	108	78.3			-479.2				227.8	673.4
RADIAL	19,000	140	78.4			-495.5					699.3
BIAS PLY	9,400	76	85.6	8.0	-286.8	-224.2	-316.2				357.0
BIAS PLY	9,400	108	86.5	7.9	-242.5	-238.2	-377.2				285.2
BIAS PLY	9,400	140	82.9	9.5		-323.4	-141.4				385.5
BIAS PLY	14,100	76	85.6	14.0		-447.4	-461.0				617.5
BIAS PLY	14,100	108	84.9	14.3		-474.5	-578.4				655.1
BIAS PLY	14,100	140	85.1	15.1		-503.4	-606.5				711.9
BIAS PLY	19,000	76	88.5	19.9		-609.0	-778.2				856.7
BIAS PLY	19,000	108	88.0	20.1		-662.2	-648.2				885.3
BIAS PLY	19,000	140	89.4	20.0		-663.3	-770.0				869.8
RADIAL *	19,000	76	81.3	20.3							642.0
RADIAL *	19,000	108	78.8	22.9							660.5
RADIAL *	19,000	140	79.2	22.8							662.4

Note: "*" denotes repeat tests.

"-" denotes compression.

Table 35. Air void contents and resilient moduli for cores from Test 2-2.

CORE NUMBER	SURFACE			UPPER BINDER			LOWER BINDER					
	AIR VOIDS Percent	Mr 41 ksi	Mr 77 ksi	Mr 104 ksi	AIR VOIDS Percent	Mr 41 ksi	Mr 77 ksi	Mr 104 ksi	AIR VOIDS Percent	Mr 41 ksi	Mr 77 ksi	Mr 104 ksi
1	5.08	1700	262	50	4.56	1960	306	65	3.24	2310	293	53
2	5.93	1660	244	49	5.66	1660	253	55	3.62	1990	310	51
3	5.55	1520	177	48	8.03	1260	206	46	3.42	2150	277	51
4	4.28	1580	194	37	4.83	1630	249	61	3.47	2420	330	50
5	4.12	1530	184	42	3.88	1990	246	49	3.09	2090	279	62
6	3.93	1560	187	40	3.39	1900	283	54	3.47	1950	282	55
7	4.93	1710	293	55	8.71	--	--	--	5.39	1340	165	36
8	5.2	1690	301	57	4.71	2190	376	68	5.66	1720	207	44
9	6.05	1750	302	61	5.09	1920	368	74	6.18	2030	256	48
10	4.51	1770	297	56	5.69	1820	259	52	3.58	2100	235	44
11	5.86	1560	247	48	7.77	1620	281	64	4.22	1950	236	43
12	4.24	1740	302	59	6.82	1780	278	57	3.96	1550	172	32
13	3.81	1640	250	48	6.01	1200	190	42	2.98	2000	197	49
14	3.74	1670	227	49	4.22	1880	238	53	2.83	1410	146	33
15	3.81	1600	254	51	3.85	2060	302	76	3.62	1940	225	36
16	4.35	1770	277	56	7.16	1470	222	60	4.83	1340	159	29
17	4.66	1830	283	58	5.58	2120	415	82	4.11	1860	278	50
18	5.01	1730	252	54	5.02	1600	286	64	4.41	1390	177	34

Table 36. Air void contents and resilient moduli for cores from Test 2-3.

CORE NUMBER	SURFACE			UPPER BINDER			LOWER BINDER					
	AIR VOIDS Percent	Mr 41 ksi	Mr 77 ksi	Mr 104 ksi	AIR VOIDS Percent	Mr 41 ksi	Mr 77 ksi	Mr 104 ksi	AIR VOIDS Percent	Mr 41 ksi	Mr 77 ksi	Mr 104 ksi
1	4.16	1620	214	41	2.98	1800	196	43	4.18			
2	4.01	1510	207	43	2.52	2010	239	44	4.07	1670	180	37
3	3.97				3.05				4.03			
4	3.62				2.75				4.03			
5	3.35	1690	247	46	3.62	1490	168	32	3.25	1550	155	33
6	3.35				5.50				3.92	1380	138	45
7	3.16	1750	227	46	4.30				4.75	1470	147	35
8	3.70				3.39	1700	204	54	3.54			
9	3.43				6.03	1400	186	38	3.92			
10	3.81	1740	223	45	3.32				4.34			
11	4.74				3.36				4.49			
12	4.97	1370	206	38	2.30				4.11	1880	243	56
13	4.89				2.71				5.47			
14	4.89				2.30	1680	212	40	5.16	1770	201	38
15	4.97				1.13				4.34			

